UNIVERSIDADE DE LISBOA
FACULDADE DE CIÊNCIAS
DEPARTAMENTO DE BIOLOGIA ANIMAL

Biologging an invader: habitat use and activity patterns of the European catfish in the lotic Tagus River (Portugal)

Beatriz Mendes Fernandes Ribeiro de Castro

Mestrado em Ecologia e Gestão Ambiental

Dissertação orientada por:
Doutor Bernardo Quintella
Doutor Filipe Ribeiro

2025

Acknowledgements

During the trials and tribulations of the making of this work I gathered a lot of people to whom I owe my gratitude to, so I would like to give thanks:

To my supervisors, Dr. Bernardo Quintella and Dr. Filipe Ribeiro, for their patience, kindness, and wisdom in guiding me through this thesis. Your encouragement and support not only shaped this work but also allowed me to enrich my academic experience with opportunities I would not have had otherwise. I'm forever grateful for this opportunity.

To Rita Almeida and Gil Santos, thank you for all your help and guidance, from long hours of fieldwork to long hours discussing life inside and outside of academia.

To Diogo Ribeiro, Diogo Dias and Dr. Rui Rivaes, for always finding a way to help me go and track my fish, even though it meant long tedious hours spent waiting for me inside the car.

To the *Fish Invasions Lab* team, you all truly lead by example, and I couldn't have asked for a better group to share this journey with. From the early on crash course in fish species, going through the ups and downs of fieldwork and ending in your encouragement and friendship during this process, you have never shied away from sharing your knowledge, joy and love for science and for that I'm beyond grateful. Mafalda, my day one girlie thank you for all the laughs.

To Prof. Dr. Tiago Marques, thank you for the all the R knowledge!

To all the fisherman who made this work possible and taught me the art of fishing and handling fish, especially to Carlos Serras, André and Rosita.

To EDP S.A., through Dr. Liliana Carvalho, thank you for generating and providing the river flow data.

To all my friends at EAWAG. Especially to Dr. Jelger Elings and Luis Habersetzer thank you for all the knowledge and patience during my internship and for all the help with my thesis. To Tara and Juliette for being the perfect flatmates and amazing friends.

To the "Ano Certo", [2019; +∞[.

To Carol and Tiago for all the group work during our masters, and for all the friendship that ensued.

To my ride or die 11, whose friendship I acquired long before I started talking about fish and fishing, I'm sorry, I guess this is now something you must deal with! Thanks especially to Margarida and Rita, for this journey of a lifetime, and everything else really…

To the people who give meaning to the word Home, from V.F.X to Madeira, especially Maria, Dinis, Vânia, Hugo, Carol, Maggie and Cau. Thank you for eating all my stress baking!

To my grandparents, uncles, aunts and my precious cousins, especially Bárbara for listening to my many struggles thought this time (and life in general) always with and encouraging word. You can't choose family, but even if I had, I couldn't have chosen any better.

Finally, to my mum Elisabete, my dad Paulo and my sister Leonor. I would like to dedicate this work to you. Words cannot describe how much I love and admire you.

This work was supported by:

Fundação para a Ciência e a Tecnologia (FCT) through the project: *MEGAPREDATOR: A giant on the water: from predation pressure to population control of the European catfish (Silurus glanis)* PTDC/ASP-PES/4181/2021 (https://doi.org/10.54499/PTDC/ASP-PES/4181/2021). MARE is supported by the strategic funding UIDP/04292/2020 (https://doi.org/10.54499/UIDP/04292/2020), and the FCT base funding UIDB/04292/2020 (https://doi.org/10.54499/UIDB/04292/2020). The Associated Laboratory ARNET is supported by the grant LA/P/0069/2020 (https://doi.org/10.54499/LA/P/0069/2020).

Abstract

The European catfish (*Silurus glanis*), an invasive species recently introduced to the Iberian Peninsula, presents a significant ecological threat due to its large size, high fecundity, and strong predatory potential. As a voracious apex predator, it can disrupt fish assemblages across the region. While biotelemetry studies have examined its habitat use and activity patterns in non-native areas, most focused on lentic systems using passive telemetry, leaving its lotic behaviour understudied. Since its first record in Portugal (2014) and subsequent establishment in the Tagus and Douro rivers, understanding its habitat use and activity patterns in these dynamic environments has become crucial for effective management. To address this, 12 adult catfish were tagged with radio telemetry archival tags equipped with temperature, pressure (depth), and 3D-accelerometer sensors to assess habitat use and activity patterns in a lotic stretch of the lower Tagus River. A controlled experiment with two individuals validated acceleration-derived activity thresholds, classifying behaviours as immobile (<0.03 g), mobile (0.03–0.78 g) or burst movement (>0.78 g). The remaining 10 fish were actively tracked for a year. Results showed that catfish occupied deeper habitats in winter (mean depth: 3 m) and moved to shallower areas in spring and summer (mean depth: 1.6 m). Activity persisted year-round but was lower in winter and autumn and higher in warmer seasons. Circadian depth use patterns remained stable, with fish preferring shallower depths during the day and deeper habitats at night. Activity peaked at dusk and was lowest during daylight hours. Individuals exhibited strong site fidelity, consistently occupying small areas near riverbanks. These patterns were strongly correlated with several environmental predictors, possibly linked to prey availability and reproduction cycles. Findings provide valuable insights for targeted management strategies, including optimizing timing and location of fishing efforts to improve mass removal actions aimed at controlling this invasive species.

Keywords: *Silurus glanis*; Biological invasions; Biotelemetry; GAMs; Hurdle models

Resumo

As invasões biológicas são, atualmente, uma das principais causas da diminuição da biodiversidade a nível global. Estas são particularmente prejudiciais para os ecossistemas dulçaquícolas cujos peixes são um dos grupos biológicos mais ameaçados do mundo, bem como um dos *taxa* mais introduzidos.

A Península Ibérica, situada na bacia do Mediterrâneo, um dos principais *hotspots* de biodiversidade do planeta, abriga uma comunidade de peixes dulçaquícolas com níveis excecionais de endemismo. No entanto, os rios ibéricos estão entre os ecossistemas mais invadidos da região, principalmente devido às alterações do ecossistema causadas pela atividade humana. Nos rios portugueses, cerca de 14 novas espécies de animais são introduzidas a cada década, um terço das quais corresponde a peixes de água doce, incluindo predadores piscívoros que representam uma séria ameaça para a ictiofauna nativa, pouco adaptada a uma intensa pressão predatória. O estudo da distribuição e dos padrões de atividade destas espécies é fundamental para avaliar o seu impacto nas comunidades nativas e melhorar estratégias de mitigação e controlo populacional, incluindo a remoção de indivíduos dos sistemas invadidos.

Detetado pela primeira vez em Portugal em 2014, o peixe-gato-europeu (*Silurus glanis*), tem demonstrado um impacto substancial nos ecossistemas onde se estabelece. Atualmente presente nos rios Tejo e Douro, este predador de topo, devido ao seu grande porte (>2,8 m), elevada fecundidade e extraordinário potencial predatório, ameaça as populações de peixes nativos. Estudos de dieta no baixo Tejo indicam um amplo espectro de presas, incluindo espécies nativas como tainhas (*Chelon* spp.), barbos (*Luciobarbus* spp.) e espécies ameaçadas, como a enguia-europeia (*Anguilla anguilla*), o sável e a savelha (*Alosa* spp.). Embora já existam estudos sobre a ecologia do peixe-gato-europeu, a maioria foca populações de lagos e albufeiras, recorrendo principalmente a telemetria acústica passiva. Comparativamente, estudos semelhantes em sistemas lóticos permanecem escassos. Dado o aumento da sua presença em rios sem barreiras ao movimento longitudinal, como o baixo Tejo, que alberga uma comunidade diversificada de presas, torna-se essencial estudar o seu comportamento nestes habitats.

Combinando a radiotelemetria com sensores que registam diferentes parâmetros ambientais e biológicos, foi possível monitorizar detalhadamente o comportamento do peixe-gato-europeu. Os dispositivos eletrónicos utilizados registaram temperatura, pressão (profundidade) e acelerometria tridimensional (*proxy* de atividade) a cada 40 segundos, emitindo, paralelamente, sinais de rádio a cada 2 segundos para localização dos indivíduos. Esta tecnologia permitiu avaliar a posição tridimensional dos peixes no rio e quantificar o seu comportamento predatório ao longo dos ciclos anual e circadiano. Os dados obtidos são fundamentais para compreender o impacto da espécie, particularmente em áreas de elevada diversidade piscícola, como o baixo Tejo, onde a sua atividade pode ser intensa. Esta análise é essencial para desenvolver estratégias de gestão e controlo, contribuindo para conter a sua expansão e mitigar os seus efeitos sobre as comunidades nativas.

Para esse fim, 12 exemplares adultos foram capturados com redes de pesca e palangres, tendo o transmissor sido implantado internamente na cavidade peritoneal. Realizaram-se duas experiências distintas. Numa experiência preliminar, dois indivíduos foram mantidos num tanque sob condições controladas e expostos a diferentes estímulos para desencadear respostas comportamentais distintas, permitindo validar os registos de atividade e posteriormente auxiliar na caracterização dos padrões de atividade da espécie. Os restantes 10 indivíduos foram

monitorizados ativamente durante um ano (novembro de 2022 a novembro de 2023) num troço lótico de 28 km do rio Tejo, entre o açude do Pego (Abrantes) e Almourol (Vila Nova da Barquinha), dividido em duas secções separadas pelo açude de Abrantes: montante (9,5 km) e jusante (18,5 km). Este estudo analisou quer o uso longitudinal do espaço a partir das localizações obtidas nas campanhas de *tracking* manual quer o uso vertical e os padrões de atividade, com base nos dados dos transmissores, relacionando-os com fatores abióticos. Além disso, a identificação de atividades predatórias, através dos registos de acelerometria 3D, utilizando como referência os valores da experiência preliminar, permitiu analisar o comportamento alimentar em função das condições ambientais locais.

Os resultados da experiência preliminar, analisados a partir dos registos de aceleração dos transmissores no software R, permitiram estabelecer valores limite para três categorias comportamentais distintas indivíduos: imóveis (<0,03 g), móveis (0,03-0,78 g) e com atividade explosiva (>0,78 g), esta última potencialmente associada a ataques a presas ou comportamentos agonísticos.

No total foram obtidas 113 localizações ao longo de 26 campanhas de *tracking* manual, abrangendo um ciclo anual. Recorrendo ao *software* de sistemas de informação geográfica QGIS, foram calculadas três métricas de utilização longitudinal do espaço: *Home* e *Core Range*, correspondendo à menor área onde há uma probabilidade de deteção do animal de 95% e 50%, respetivamente, ao longo do período de estudo, e o *Mid-Stream Linear Range* (MSLR), definido como a distância linear entre as localizações mais a montante e a jusante registadas por cada indivíduo. Resultados desta análise, representados em mapas, revelaram que o peixe-gato-europeu apresenta áreas vitais reduzidas (*Home Range* mediano de 0,292 km²) podendo utilizar um troço de rio com cerca de 3,34 km de extensão (valor mediano de MLSR). Além disso, a elevada percentagem de deteções junto às margens do rio (42,1%), especialmente em zonas com vegetação densa e raízes de árvores de grande porte, sugere uma forte preferência por habitats com estruturas que oferecem refúgio.

Para obter a informação recolhida pelos sensores, foi imprescindível recapturar os peixes marcados com os transmissores. No total, foram recuperados quatro transmissores, fornecendo 2 177 835 registos de atividade e profundidade, permitindo um estudo detalhado da ecologia do peixe-gato-europeu. Com base nos dados dos sensores de pressão e acelerometria, analisou-se, a uma escala temporal muito detalhada, tanto o uso vertical do habitat como os padrões de atividade. Recorrendo ao software R, a profundidade e a atividade foram estudadas para identificar padrões sazonais e circadianos, relacionando-os com fatores abióticos através de modelos aditivos generalizados (GAMs). Os resultados indicaram que o peixe-gato-europeu manteve atividade ao longo de todo o ano, apresentando níveis mais baixos no outono e inverno e mais elevados na primavera e verão. Também foram observadas variações sazonais na profundidade utilizada, com os indivíduos a ocuparem águas mais profundas no inverno (profundidade mediana de 3,1 m) e mais superficiais no verão (profundidade mediana de 1,6 m). Os padrões circadianos de utilização da profundidade mantiveram-se estáveis na maior parte do ano com os espécimes a ocuparem menores profundidades durante o dia e maiores durante a noite exceto no outono, quando o padrão se inverteu. A atividade dos peixes marcados variou ao longo do dia, sendo maior ao anoitecer e menor durante o dia. Os GAMs de atividade e profundidade mostraram-se relacionados com a temperatura e o caudal do rio, o Dia Juliano, a estação do ano, e com a profundidade dos indivíduos no caso da atividade e a atividade destes no caso da profundidade, geralmente seguindo tendências não lineares. Os resultados indicam que a atividade aumentou com a temperatura e o caudal do rio até um máximo de 1000 m³/s, assim como com o aumento da profundidade até cerca

de 8 m. Por outro lado, a profundidade utilizada pelos indivíduos mostrou uma relação inversa com a temperatura, enquanto o aumento do caudal resultou numa ligeira diminuição da profundidade ocupada até atingir o pico de 1000 m^3/s.

Para avaliar o comportamento predatório do peixe-gato-europeu, inferido a partir de registos de atividade intensa classificada com base na experiência em cativeiro, foi utilizado um modelo Hurdle permitindo identificar os principais preditores ambientais associados à ocorrência de atividade explosiva. Os resultados demonstraram uma variação sazonal e circadiana na ocorrência de atividade explosiva, observada principalmente na primavera e ao anoitecer. A temperatura da água, o caudal, a estação do ano e o período do dia influenciaram significativamente essa dinâmica. Além disso, fatores como a época de reprodução do peixe-gato-europeu e alterações nos padrões comportamentais das suas presas revelaram-se determinantes para compreender a variação na profundidade ocupada pelos indivíduos, os padrões de atividade e os episódios de atividade explosiva.

Os dados deste estudo poderão contribuir para melhorar a gestão do peixe-gato-europeu em sistemas invadidos, particularmente através de ações de controlo populacional baseadas na remoção de indivíduos. Propõe-se que os esforços de remoção na secção lótica do rio Tejo se concentrem na primavera e verão, especialmente entre abril e junho. Para maximizar a eficácia, os dispositivos de pesca devem ser posicionados durante o dia em áreas com vegetação densa, a profundidades entre 1,5 e 3 metros.

No futuro, os dados já recolhidos, bem como os que poderão ser obtidos com estes dispositivos eletrónicos, poderão ser substancialmente melhorados através de experiências laboratoriais que calibrem os registos de aceleração tridimensional em relação aos comportamentos observados ao longo do estudo. A utilização de um sistema de vídeo-monitorização permitiria uma correspondência mais precisa entre os valores do sensor de acelerometria e comportamentos específicos. Adicionalmente, o aumento da amostra na componente de *tracking* reforçaria a robustez das análises espaciais e comportamentais, proporcionando uma avaliação mais representativa dos padrões de movimento e uso do habitat. Por fim, dado o deslocamento sazonal para habitats estuarinos e a preferência por presas anádromas, será relevante investigar a atividade e o uso da profundidade em áreas influenciadas pela maré.

Palavras-chave: *Silurus glanis*; Invasões Biológicas; Biotelemetria; Modelos aditivos gerais; Modelos Hurdle

Index of contents

Index of figures

Index of tables

List of abbreviations, acronyms, and symbols

3D – Three-dimensional

AIC – Akaike Information Criterion

APA – Portuguese Environmental Agency

ASum – Activity as the vector sum of acceleration

BIC – Bayesian Information Iriterion

BPUE – Biomass per unit of effort

CPUE – Catch per unit of effort

CR – Core Range

CSV – Comma-separated value

df – Degrees of freedom

DLC – Data Logger Communication

Freq. – Transmitter frequency

GAM – Generalized Additive Model

GISD – Global Invasive Species Database

HR – Home Range

IAS – Invasive alien species

ICNF – Institute for Nature and Forests Conservation

ID – Identification

IPBES – Intergovernmental Science-policy Platform on Biodiversity and Ecosystem Services

KDE – Kernel Density Estimation

LRT – Likelihood ratio test

ML – Maximum Likelihood

MSLR – Mid-Stream Linear Range

PIT – Passive Integrated Transponder

QGIS – Quantum Geographic Information System

RAT– Recapturing attempt tracking

SDT– Single day tracking

TL – Total Length

V_{sum} – Activity as the rate of acceleration change in gravitational force

$\chi 2$ – Kruskal-Wallis statistic

1. Introduction

Invasive alien species (IAS) are deemed as one of the major direct drivers of global environmental change, as identified in the 2019 *Global Assessment Report on Biodiversity and Ecosystem Services* by the Intergovernmental Science-Policy Platform on Biodiversity and Ecosystem Services (IPBES). Alongside IAS, other key drivers include land- and sea-use change, direct exploitation of organisms, climate change, and pollution. These anthropogenic pressures significantly enhance the occurrence of biological invasions (IPBES, 2023), which play a critical role in altering and diminishing global biodiversity (Bellard et al., 2016; Blackburn et al., 2019) and contribute substantially to economic losses (Haubrock et al., 2022).

Biological invasions are particularly damaging to freshwater ecosystems (Vitousek et al., 1996). Historically, these ecosystems have been geographically isolated, fostering the evolution of many endemic species and, at times, low biodiversity (Lodge, 1993). However, increased connectivity driven by human activities (Rahel, 2007), numerous introduction pathways, and insufficient monitoring have rendered aquatic ecosystems, in general, vulnerable to biological invasions (Haubrock et al., 2023). Freshwater habitats occupy less than 1% of the Earth's surface, yet they are biodiversity hotspots that support around 10% of all known species, about a third of all vertebrate species (Strayer & Dudgeon, 2010) and 51% of the world's fish species (WWF, 2021). Furthermore, their importance in terms of ecosystem services (e.g., water supply, food, and economic productivity through fisheries and aquaculture) (Carpenter et al., 2011) is extremely high. Freshwater fish species, an integral part of this ecosystem, are one of the most threatened groups of organisms in the world (Olden et al., 2010), as well as one of the most introduced *taxa* (Gozlan, 2008). Globally, 551 non-native freshwater fish species have been recorded as established (Bernery et al., 2022). Once established, non-native fish can proliferate, spread, and cause ecological and/or socioeconomic impacts, becoming then a biological invasion (Lewis et al., 2016) harmful to native species and to the overall ecosystem.

Competition, predation, hybridization, disease/parasite transmission and interaction with native habitats (digging and grazing or browsing) are deemed in the Global Invasive Species Database (GISD) (ISSG, 2015) as the main mechanisms responsible for the majority of the ecological and socioecological impacts of invasive freshwater fish (Bernery et al., 2022), greatly contributing for the decline in freshwater biodiversity (Dudgeon et al., 2006; Simberloff et al., 2013; Doherty et al., 2016). Moreover, IAS can cause significant economic impacts, according to a study published in 2022 by Haubrock et al., the total (observed and potential) economic costs related to invasive fish species in Europe between 1960 and 2020 amount to 5.01 billion US dollars. Moreover, most estimates are likely very conservative, not only because cost data are scarce for most invasive alien fish species, but also because it is difficult to assign a monetary value to impacts that are not directly quantifiable, such as damage to ecosystems and human well-being (Millennium Ecosystem Assessment, 2005; Haubrock et al., 2021, 2022).

Situated within the Mediterranean basin, one of the planet's most critical biodiversity hotspots (Myers et al., 2000), the Iberian Peninsula, displays a distinctive freshwater fish fauna with exceptionally high levels of endemism (Doadrio, 2001; Collares-Pereira et al., 2021). However, the region's rivers have been extensively modified by human activities, with many being impounded or diverted (Hermoso et al., 2011; Costa et al., 2021), and some reservoirs even dating as far back as the Roman times (Clavero et al., 2013). As mentioned previously, these modifications increase the vulnerability of these ecosystems to IAS (Leprieur et al., 2008; Clavero

et al., 2013). Today, Iberian rivers rank among the most invaded ecosystems in the Mediterranean region (Leprieur et al., 2008). According to estimates by Anastácio et al. (2019), approximately 14 new freshwater species are introduced into Portugal every decade, being non-native fish about one third of this value. Such non-native fish introductions are often of piscivorous predators (Ribeiro et al., 2009; Gkenas et al., 2015; Martelo et al., 2021), that pose significant threats to the highly endemic native fish populations, which are poorly adapted to intense predation pressures (Elvira & Almodóvar, 2001; Encina et al., 2006; Ribeiro et al., 2009).

The European catfish, *Silurus glanis* (Linnaeus, 1758), an invasive species in Portugal, is native to regions stretching from Western Asia to Germany and Flanders (Belgium) (Verreycken et al., 2007). Known for its impressive size, reaching up to 2.8 metres in total length and weighing as much as 130 kg (Boulêtreau & Santoul, 2016), this top predator, which is confined to freshwater ecosystems, became greatly sought after for angling, and saw their spread boosted by both authorized introductions for aquaculture and stocking, and unauthorized releases mainly for angling (Copp et al., 2009; Cucherousset et al., 2018). This species has now established self-sustaining populations in major river basins across several European countries and has even spread as far as Tunisia and Brazil (Cucherousset et al., 2018). It arrived to the Iberian Peninsula via eastern Spain in 1974 (Benejam et al., 2007), with its first record in Portugal dating to 2014 (Gkenas et al., 2015). It is thought to have invaded the Tagus River through anthropogenic dispersal events, with natural downstream movement further aiding its spread (Gago et al., 2016). Currently, in Portugal, this invasive fish inhabits the main stems of Tagus and Douro rivers (Gago et al., 2016; Gkenas et al., 2023).

The invasion success of a non-native species depends not only on its introduction or dispersal events but also on its ability to survive and thrive in new environments (Bernery et al., 2022). The European catfish possesses several traits that enhance its success as an invader, including rapid growth rates, long lifespans, high fecundity, and large egg sizes (Copp et al., 2009; Panfili et al., 2024; Gkenas et al., 2025). Preferring deep lentic or slow-moving lotic waters (Copp et al., 2009; Capra et al., 2017), it typically selects habitats near river margins with dense vegetation or large tree roots (Carol et al., 2007; Copp et al., 2009). This species also demonstrates strong site fidelity, often defending small home ranges of 1.3 to 1.5 km², which expand with rising water temperatures and vice-versa (Carol et al., 2007; Brevé et al., 2014; Slavík et al., 2014). This resident behaviour, hypothesized as a way to conserve energy (Slavík et al., 2014), is occasionally disrupted in invaded areas, where flood events coupled with low water temperatures have been shown to increase movement ranges (Slavík et al., 2014; Chevallier et al., 2023). Such observations highlight the importance of abiotic factors like temperature and river flow in influencing behavioural changes. Additionally, the European catfish exhibits remarkable adaptability, occupying shallower depths in spring and summer while retreating to greater depths in winter (Encina et al., 2023; Říha et al., 2024; Santos et al., 2025).

Most often described as an opportunistic forager with great adaptability to new prey sources, this apex predator (Carol et al., 2009; Copp et al., 2009; Vejřík et al., 2017) has been shown to impact fish assemblages (Encina et al., 2023). For instance, in the Torrejón reservoir, its predation on the Iberian barbel (*Luciobarbus bocagei*, Steindachner, 1864) has significantly decreased its abundance, going from over 74% of total catch (CPUE) and biomass (BPUE) per unit of effort in 2010, to 32% total CPUE and 21% total BPUE in 2020 (Encina et al., 2023). Meanwhile, in a river in south-west France, it was found that Allis shad (*Alosa alosa*, Linnaeus, 1758) accounted for 88.5% of the prey identified in its diet (Boulêtreau et al., 2021). In a recent study in the Lower Tagus River native migratory and highly valuable European eel (*Anguilla anguilla*, Linnaeus,

1758) and, native species of mullets (*Chelon* spp.) and barbels (*Luciobarbus* spp.) have been identified as the most consumed *taxa* ranging from 20-60% of frequency of occurrence (Moncada, 2024). Based on this information, it is likely that the European catfish's predation pressure in the Lower Tagus River has been impacting its biodiversity, especially its native fish species, as observed in many other invaded areas (Cucherousset et al., 2012).

Biotelemetry studies have revealed that European catfish exhibit notable seasonal and regional differences in activity patterns. In their native range, they become lethargic during winter, with activity levels increasing in spring and summer as water temperatures rise. While their physiological optimum temperature is between 22–27 ºC (Copp et al., 2009; Lindell, 2021), spring activity begins at temperatures as low as 2.5 ºC, becoming more pronounced between 7–12 ºC (Kuzishchin et al., 2018). In contrast, in warmer non-native regions like the Iberian Peninsula, the species maintains year-round activity. For instance, in Tagus reservoirs such as Belver (Portugal) and Torrejón (Spain), winter activity shows only a slight decrease compared to other seasons (Encina et al., 2023; Santos et al., 2025). This suggests that in warmer regions, catfish activity during colder months are due to elevated metabolic rates, potentially leading to higher feeding frequencies and expanded movement ranges during winter (Bergé, 2012; Capra et al., 2014; Santos et al., 2025).

Catfish activity patterns also vary by time of day due to its hunting behaviour. In their native range, European catfish typically display a diel activity pattern, with peaks of movement primarily occurring at night throughout the year, though this behaviour can shift seasonally (Slavík et al., 2007). However, in invaded areas such as the Ebro River in Spain, the Po River in Italy or the Tagus River in Portugal, the species has also demonstrated strong crepuscular activity, with higher movement frequency concentrated from dusk until dawn (Carol et al., 2007; Nyqvist et al., 2022; Santos et al., 2025). These variations highlight the species' ability to adapt its behaviour to differing environmental conditions, particularly following the seasonal patterns of catfish prey availability and activity.

While extensive work on microhabitat preferences (e.g. Brevé et al., 2014; Capra et al., 2017, 2018), space use as in: longitudinal home-ranges (e.g. Carol et al., 2007; Slavík et al., 2007; Daněk et al., 2014; Capra et al; 2017, 2018; Nyqvist et al., 2022; Chevallier et. al., 2023; Říha et al., 2024; Santos et al., 2025) and vertical distribution in the water column (e.g. Capra et al., 2017, Ferreira, 2019; Říha et al., 2024; Santos et al., 2025) were conducted, most research focused on lentic systems such as lakes and reservoirs and used passive telemetry techniques. Catfish movement studies in lotic systems are comparatively sparse, primarily investigating the impact of hydropower plants (e.g. Brevé et al., 2014; Capra et al., 2017, 2018), the influence of colder tributaries (e.g. Nyqvist et al., 2022), or describing catfish long range movements (e.g. Franquet et al., 2025). Additionally, current research on activity levels relies on location-based estimations, which may obscure finer details of their behaviour (e.g. Lindell 2021; Říha et al., 2024; Santos et al., 2025). Given the European catfish's growing presence in free-flowing lotic systems like the Tagus River, which supports a diverse prey community, including seasonally abundant diadromous and endemic fish species (Moncada, 2024), and considering the species' year-round activity levels observed in this region (Santos et al., 2025), further research is urgently needed to investigate its activity patterns and putative ecological impacts in these environments.

This study aimed to address the identified research gap by using biotelemetry coupled with biologging to investigate the behaviour of European catfish in an invaded free-flowing temperate

river system—the lower Tagus River. Twelve adult specimens were tagged with radio telemetry archival tags equipped with sensors recording temperature, pressure (i.e., depth), and accelerometery data as a proxy for fish activity. The detailed data retrieved from these tags, combined with active radio tracking, provided high-resolution insights into fish movements along a lotic stretch of the Tagus River. More specifically, the collected data were used to: (1) analyse longitudinal space use from manual tracking locations; (2) assess vertical space use and activity patterns from biologging (pressure and accelerometery sensors) and relate them with other abiotic factors; and (3) identify possible predatory activity from the accelerometery data and relate it to local environmental factors. On a more applied basis, this research aims to advance understanding of the species' behaviour, supporting the assessments of its impact on native biota and providing new insights for managing and controlling its further spread, including the collection of information that can maximize the cost-efficiency of removal actions.

2. Methodology

2.1 Study area

The Tagus River is one of the largest in the Iberian Peninsula, spanning around 1000 km, originating in east-central Spain in the Sierra de Albarracín and flowing into the Atlantic Ocean at Lisbon in Portugal, draining about 80,600 km^2 (Sabater et al., 2009). Biogeographically within the Mediterranean region, this river basin experiences mild climatic conditions with average annual mean air temperatures between 14 and 17 ºC in the middle and lower catchment valleys (Sabater et al., 2009). Annual precipitation varies from 500 to 1000 mm across the basin, with values closer to 500 mm being more representative (Sabater et al., 2009). Nearly 80% of the annual precipitation occurs during the three winter months, with floods predominantly taking place in December and January (Sabater et al., *2*009).

This catchment is primarily dominated by arable land (45.6%), followed by natural grasslands (28.8%) and forests (21.5%) (Sabater et al., 2009). Supporting the water needs of about eleven million people, the basin's current morphology has been heavily shaped by dam construction (Sabater et al., 2009), which has reduced the frequency of high flows and sedimentation rates (Vide et al., 2002). In the case of the studied river stretch riparian strips are narrow and consist of resilient species like *Tamarix africana* (Aguiar & Ferreira, 2005) and *Salix sp.*, *Populus sp.*, *Alnus glutinosa*, *Fraxinus angustifolia* (Rosete et al., 2019).

The Tagus River basin is home to 28 native fish species, including 11 endemic to the Iberian Peninsula, two Lusitanian endemisms, and seven diadromous species (Collares-Pereira et al., 2021). Over the past century, 16 non-native fish species have been introduced into the basin (Collares-Pereira et al., 2021), including the European catfish (*Silurus glanis*), first recorded in 2006 (Gkenas et al., 2015).

The study area selected to conduct this work encompasses a 28 km lotic section of the lower Tagus River within Santarém district, Portugal. This stretch begins at the Pego weir (Abrantes: 39°28'53.7"N, 8°06'58.0"W) and extends downstream to Almourol (Vila Nova da Barquinha: 39°27'37.1"N, 8°23'12.6"W). Between these two places, a weir in Abrantes (39°27'00.9"N, 8°12'19.6"W) divides this section in two areas: the upstream area, with approximately 9.5 km from the Pego weir to the Abrantes weir, and downstream area, with approximately 18.5 km from the Abrantes weir to Almourol (Figure 2.1). During the study period, daily mean temperature (°C) changed as shown in Figure 2.2, with the lowest values recorded in February and the highest in July, followed closely by August. Daily mean river flow (m^3/s) (Figure 2.2) peaked during the winter months, with a notable high-flow event occurring in mid-December.

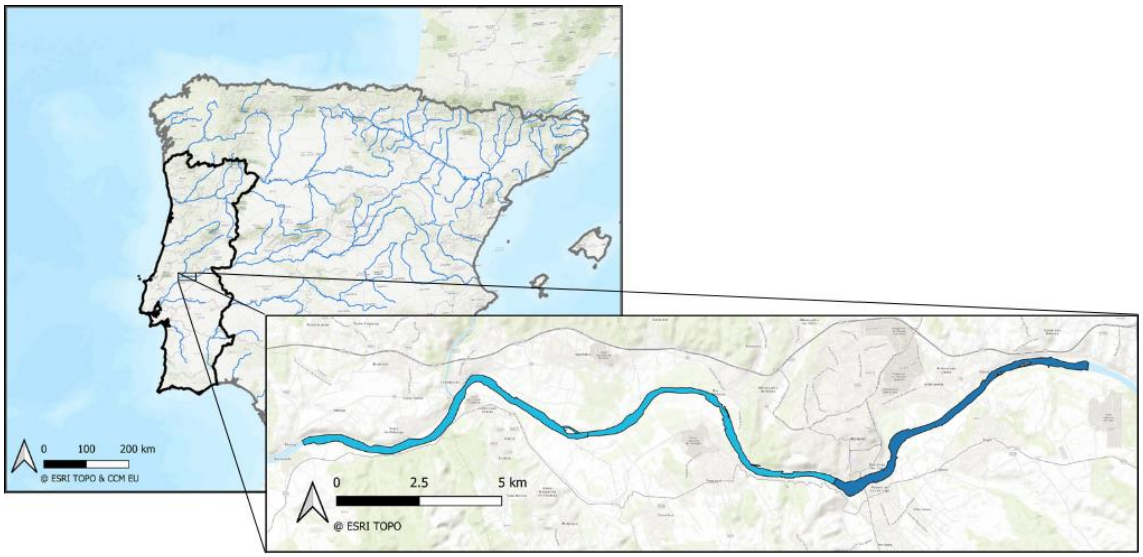

Figure 2.1 – Study area location within the Iberian Peninsula and its respective locality within the lotic stretch of the Tagus River. Detailing the 28 km long lotic section between the Pego weir (39°28'53.7"N, 8°06'58.0"W) and Almourol (39°27'37.1"N, 8°23'12.6"W), divided by the Abrantes weir (39°27'00.9"N, 8°12'19.6"W), upstream (dark blue) and downstream (light blue).

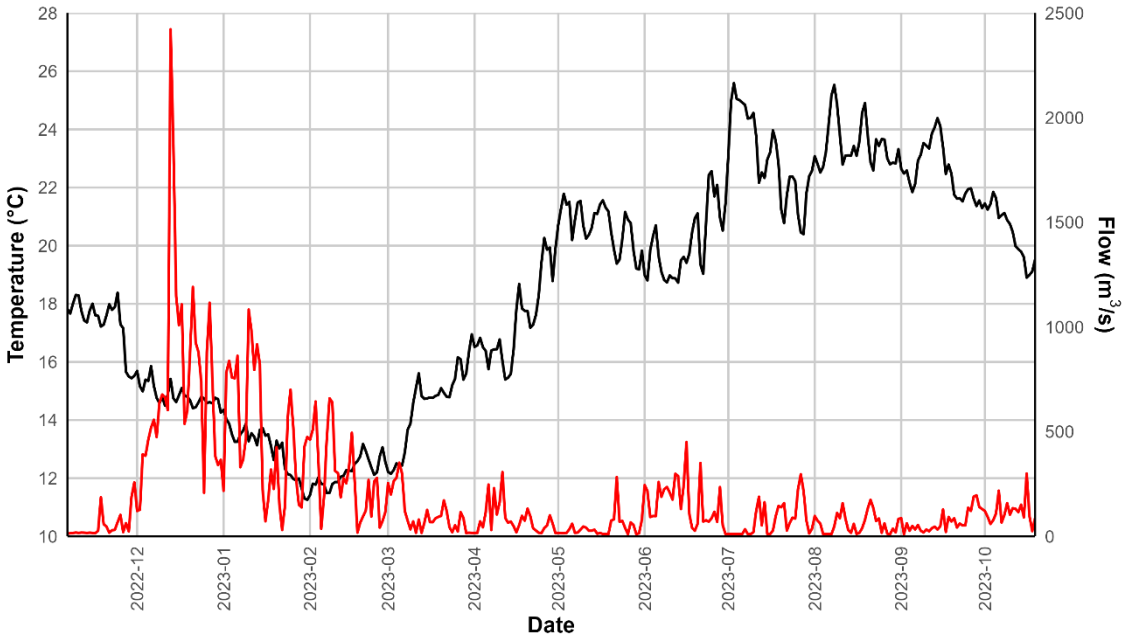

Figure 2.2 – Variation in daily mean water temperature (ºC) and river flow (m^3/s) throughout the study period. Water temperature data, recorded by fish tags (black), and mean river flow data from the Belver Dam, provided by EDP S.A. (red).

2.2 Biotelemetry and biologging

Over the past 50 years, advancements in technology have made electronic tags widely accessible for studying wildlife, including freshwater species (Cooke et al., 2013). In the last two decades, biotelemetry has been at the forefront of ecological research by linking animal movements with physiological and environmental data (Hussey et al., 2015), combining tracking devices with sensors such as thermometers, barometers, and accelerometers (Yang et al., 2021). While acoustic telemetry and passive integrated transponder (PIT) tagging have become increasingly popular, with the former now being the dominant tracking method, radio telemetry has historically been the most widely used technology in freshwater studies (Cooke et al., 2013). Despite this shift, it remains highly relevant, particularly for studies focusing on non-native species behaviour in dynamic, complex environments like the lower Tagus River (Ferreira, 2019; Santos et al., 2025).

Research in large river systems often faces challenges due to hydraulic complexity, leading to the widespread use of passive telemetry methods, where fish trajectories and speeds are inferred from detections across listening stations spaced kilometres apart (Capra et al., 2018). Although significantly more labour-intensive, active manual tracking provides more detailed and adaptable data collection, offering flexibility in defining study area boundaries and tracking fish movement at finer temporal and spatial scales. This approach is particularly well-suited for monitoring species like the European catfish, whose behavioural patterns in invaded environments are still poorly understood.

A key advantage of using radio telemetry in this study relies on the deployment of MCFT3-SP (MCFT3-L) VHF data-logging transmitters from Lotek (Annex I, Figure I.1). These are compact transmitters measuring 85 mm in length, 16 mm in diameter, and weighing 30 g, less than 1% of the tagged fish's body weight (Winter, 1983; Brown et al., 1999). They are equipped with sensors that record temperature (ºC), pressure (mbars) - later converted into depth (m)- and three-dimensional (3D) acceleration (conveying activity), at every 40 seconds. Their high archival capacity, combined with an operational battery life of approximately one year, significantly enhanced data collection compared to passive methods such as acoustic telemetry, which requires the fish to be within the receiver's range for data to be recorded.

The acceleration sensor featured in these tags, a 3D accelerometer, recorded and showed values for movement along three axes: longitudinal (X-axis), vertical (Y-axis), and lateral (Z-axis). ASum, the vector sum of acceleration, was an additional measurement provided by the tag and it was used to quantify activity by assessing tag movements in 3D space during the preceding log interval. This value was internally calculated and logged every 40 seconds using the formula: $ASum = V_{sum} \times (4/255)$, where $V_{sum}(i) = SQRT(X(i)^2 + Y(i)^2 + Z(i)^2)$. V_{sum} represented activity as the rate of acceleration change in gravitational force ($1g = 9.81\ m/s^2$). Each V_{Sum} value was converted into an absolute acceleration rate and recorded as a fractional number (e.g., a reading of 0.7 represents 0.7g of acceleration change). Ultimately, activity (ASum) was logged and showed as a discrete variable, categorized into fixed increments of 0.03, ranging from 0 to 1.5.

Additionally, the tags broadcasted radio signals every two seconds at specific operating frequencies (Table 2.1 and 2.2) allowing them to be manually tracked with a radio receiver . This advanced design and data-collection capability significantly enhanced the capacity to track and analyse fine scale fish behaviour in complex freshwater environments.

2.3 Capture and tagging

In this study, 12 adult European catfish (*Silurus glanis*), with total lengths (TL) ranging from 82 to 138 cm, were captured and tagged. As this species exhibits no obvious external sexual dimorphism, preventing differentiation between males and females based solely on external characteristics (Copp et al., 2009), all individuals were classified as adults, as the estimated length at sexual maturity in this region is 72.9 cm for females and 68.8 cm for males (Copp et al., 2009; Gkenas et al., 2025) (Table 2.1 and 2.2).

Two out of the 12 catfish were used in the 3D accelerometer sensor testing (detailed in Section 2.4) were captured by fishermen near Constância (Table 2.1). The remaining 10 individuals were part of the tracking experiment conducted in the Tagus River (detailed in Section 2.5). Of these, five (#1 to #5) were captured downstream near Constância, while the other five (#6 to #10) were caught upstream of the Abrantes weir (Table 2.2). Adult catfish were collected using large-mesh gill nets (>180 mm) and baited longlines, following the procedures described by Vejřík et al. (2024) (Annex I, Figures II.2 and II.3). All individuals were measured (TL ± 1 mm), tagged, and released—those tested in the 3D accelerometer sensor trials were transferred to outdoor experimental tanks, while those in the tracking study were returned near their capture sites, immediately after being captured and tagged, in November 2022.

All the specimens were implanted with MCFT3-SP (MCFT3-L) VHF data logging transmitters from Lotek (Annex I, Figure I.1). To perform the procedure, fish were anesthetized in a solution of 2-phenoxyethanol (0.4 ml per litre of water), and the transmitters were inserted through a surgical incision (≈ 2 cm) in the peritoneal cavity, with the wound area previously disinfected with an iodine solution. With the assistance of a hollow needle, the external antenna was positioned on the exterior of the individual's body. Finally, the incision was sutured with two to three independent sutures and subsequently disinfected again with the iodine solution (Annex I, Figure I.4). Each transmitter was labelled with contact information, and the fish were externally tagged with an anchor tag for identification upon potential recapture. All surgical instruments were sterilized with a 96% alcohol solution. Following surgery, fish were placed in recovery for approximately one hour at the capture site before release (Annex I, Figure I.5). The described tagging process ensured minimal harm and maximized post-surgical recovery and tracking success in the field.

2.4 Sensor (3D accelerometer) testing in a controlled outdoor water enclosure

A preliminary experiment was conducted under controlled conditions to validate activity readings in relation to catfish behaviour and establish threshold values for different behavioural categories. These thresholds were later used to analyse activity data and aid in result interpretation. Additionally, this experiment enabled testing of the tagging procedure and assessment of the transmitters' potential impact on fish behaviour and well-being.

For this experiment, the two adult European catfish were maintained separately in large 3,000 L water enclosures both equipped with oxygenation air pumps and wooden panels to provide shade. Water was changed daily, and fish were fed daily with red swamp crayfish (*Procambarus clarkii*). As previously mentioned (Section 2.3), fish were measured (TL ± 1 mm) and tagged following the procedure outlined in the same section (Table 2.1).

Table 2.1 – Information on the tagged European catfish for the sensor (3D accelerometer) testing. Identification (ID) of the tagged catfish, with code of external mark (Anchor tag), transmitter frequency (Freq.) and total length (TL).

ID	Anchor tag	Freq.	TL (cm)
1	0202	150.400	129
2	0203	150.970	115

Three weeks after the tagging procedure experimental tests to establish threshold values for different behavioural categories were conducted. Five experimental trials, each lasting 30 minutes, were performed on each specimen, totalling two hours and 30 minutes of testing. In each experimental trial start and end time were registered. Specimens were exposed to different stimuli in order to induce various swimming speeds (behaviours): 1) a prey (crayfish) was presented inside of a small dipnet and moved at different speeds; 2) a stick was used to prompt movement at varying speeds; and 3) a control period with no stimuli. During this procedure, each observer was continuously registering the behaviour of each specimen, dividing the response periods into the following categories: **immobile (I); mobile (M); or burst movement (B)** and assigning it a specific time stamp. Before this an extra trial set, with a reduced time frame, was filmed so the two observers could standardize behaviour categories: **immobile periods** corresponded to when the specimen was completely stationary; **mobile periods** corresponded to swimming movements achieved by the movement of the caudal fin, that could either be a longer straight swimming movement (less frequent) or a circular swim with a turn on itself (more frequent); **burst movements** were characterized by rapid swimming, always followed by a bite on the object used to stimulate the specimen. Both mobile and burst movements were almost exclusively reactions to exterior stimuli.

Upon completion of all tests, both specimens were euthanized following the ethical procedures for this species and complying with the National and European regulations on handling wild animals (Decreto-Lei n.º 92/2019; Directive 2010/63/EU). The transmitters were then extracted, deactivated to halt data collection, and the recorded data was downloaded. Data retrieval was performed using Lotek's specialized software, MCFT3 Data Log Host. This process involved connecting the computer running the MCFT3 Host app to a Data Logger Communication (DLC) reader (physical connection) that subsequently was connected to the retrieved tag enabling data transfer. The retrieved data was stored in comma-separated value (CSV) files containing the parameters outlined in Section 2.2. Finally, all recorded observations from the trials, including timestamps, observed behaviours, and stimuli, were compared with the corresponding activity data obtained from the transmitters.

2.5 Manual tracking in the Tagus River

A total of 10 fish (Table 2.2) were tracked between November 2022 and November 2023, adding up to 45 tracking days, of which 19 were done fortnightly in single tracking days and 26 completed in seven recapturing attempts (with durations from two to five days, between July and November 2023) (Table 2.3). The tagged fish were tracked using a manual radio tracking receiver (model R410) and a 4-element Yagi antenna, both from Advanced Telemetry Systems. Upon signal detection, triangulation was carried out to refine the specimens' positions, after which their geographical coordinates and detection times were recorded (Annex I, Figure I.6).

Single-day tracking campaigns were either conducted from the riverbank or from a boat depending on field safety conditions (e.g. high flows) or operational conditions (e.g. boat availability). These campaigns spanned the entire study area, as represented in Figure 2.1. However, due to the absence of detections for some fish within the designated area, two tracking campaigns were conducted beyond the study limits. These extended 12 km downstream from Almourol to Chamusca (39°23'19.4"N, 8°27'15.6"W), as detailed in Table 2.3.

Recapturing campaigns involved intense active tracking by boat and along the riverbanks (Table 2.3). Once the tagged fish position was identified, gillnets or baited longlines were deployed together with simultaneous boat electric fishing. When recaptured, fish were euthanized as described in section 2.4. After this, transmitters were retrieved, and total length (TL ± 1 mm) and sex information were recorded. Subsequently, the data was downloaded as outlined in section 2.4.

Table 2.2 – Information on the tagged European catfish for the lotic lower Tagus River tracking. Identification (ID) of the tagged catfish, with code of external mark (Anchor tag), transmitter frequency (Freq.), capture and release date and location (Date and Location), size upon capture (TL), date of recapture (Recapture), last date of detection (Last detection), number of monitored months (No. months) and total number of detections (No. of detections).

ID	Anchor tag	Freq.	Date and Location	TL (cm)	Recapture	Last detection	No. of months	No. of detections
1	71	150.400	4-11-2022 Constância	102.0	-	31-10-2023	11	14
2	75	150.460	4-11-2022 Constância	82.0	26-10-2023*	-	11	10
3	62	150.580	4-11-2022 Constância	120.0	-	24-11-2023	12	15
4	54	150.520	4-11-2022 Constância	112.0	24-04-2023^{F}	-	5	7
5	53	150.640	4-11-2022 Constância	120.0	-	22-12-2022	1	2
6	34	150.430	25-11-2022 Abrantes	138.5	-	25-11-2022	-	1
7	66	150.490	25-11-2022 Abrantes	118.0	-	13-09-2023	10	12
8	63	150.850	25-11-2022 Abrantes	103.0	13-09-2023^{M}	-	10	23
9	32	150.700	25-11-2022 Abrantes	106.0	-	11-05-2023*^{1}	6	10
10	58	150.550	25-11-2022 Abrantes	99.0	20-07-2023^{F}	-	8	19

*Only the tag was recovered.; *^{1} A previously tagged individual (confirmed by scar analysis) was recovered at the usual site of this individual on 12-09-2023, although no tag was recovered; ^{F} Female specimen, ^{M} Male specimen.

Table 2.3 – Summary of tracking and recapture efforts. Campaigns are organized by number (No.) and type (Type), which are categorized as: SDT- single day tracking or RAT- recapturing attempt tracking. It also details each campaign: start and end dates (Dates); Duration in days (Duration); river section covered (Section) with "All" indicating both upstream and downstream sections and distance covered in km (Distance).

No.	Type	Dates	Duration	Section	Distance
1	SDT	25/11/2022	1	All	28
2	SDT	07/12/2022	1	All	28
3	SDT	22/12/2022	1	All	28
4	SDT	04/01/2023	1	All	28
5	SDT	18/01/2023	1	All	28
6	SDT	02/02/2023	1	All	28
7	SDT	16/02/2023	1	All	28
8	SDT	02/03/2023	1	All	28
9	SDT	17/03/2023	1	All	28
10	SDT	31/03/2023	1	All*	40
11	SDT	15/04/2023	1	All	28
12	SDT	25/04/2023	1	Downstream*	31
13	SDT	27/04/2023	1	Upstream	9
14	SDT	11/05/2023	1	All	28
15	SDT	26/05/2023	1	All	28
16	SDT	11/06/2023	1	All	28
17	SDT	27/06/2023	1	Upstream	9
18	SDT	29/06/2023	1	Downstream	19
19	RAT	16 - 20/07/2023	5	All	28
20	RAT	16 - 18/08/2023	3	All	28
21	SDT	30/08/2023	1	All	28
22	RAT	11 - 14/09/2023	4	All	28
23	RAT	27 - 28/09/2023	2	All	28
24	RAT	23 - 27/10/2023	5	All	28
25	RAT	30/10/2023 - 1/11/2023	3	All	28
26	RAT	21 - 24/11/2023	4	Downstream	19

*Includes tracking out of the bounds of the study area, 12 km further downstream.

2.6 Data analysis

For longitudinal space use data analysis, QGIS 3.34 (QGIS Development Team, 2023) was employed to calculate three spatial metrics: Home Range (HR), Core Range (CR), and Mid-Stream Linear Range (MSLR). Home and Core Ranges were estimated using Kernel Density Estimation (KDE), a method known for its effectiveness in minimizing bias, particularly when working with small sample sizes (Seaman & Powell, 1996). Following Seaman et al. (1999), KDE was applied only to individuals with ten or more recorded location points to ensure reliable range estimates. These metrics were computed using the publicly available "Home Range Analysis by Kernel Density Estimation" model (Frate, 2022). The integration of MSLR provided a valuable dimension to the analysis by capturing longitudinal spatial use in a linear environment such as rivers, where space is naturally constrained. This straightforward metric enhances robustness in studies with limited observations (Kay, 2004) and enables meaningful comparisons across research using linear distance measures (Ovidio et al., 2002; Capra et al., 2018; Nyqvist et al., 2022).

The KDE at 95%, representing the "Home Range"- is the smallest area within which there is a 95% probability of detecting the animal over a year, that in this case is represented by the study period which varied between 6 to 12 months. The KDE at 50%, referred to as the "Core Range" - indicating the smallest area with a 50% detection probability over the aforementioned period. Finally, the mid-stream linear range (MSLR) was determined as the mid-stream linear distance in kilometres between the most upstream and downstream locations, using basic QGIS tools.

Model application began by generating a raster layer from a point shapefile containing individual detection locations. A kernel function was then applied, creating a smooth, bell-shaped surface over each detection point, with density values highest at the point itself and decreasing symmetrically with distance until reaching zero at the search radius or bandwidth limit (Silverman, 1986). This approach ensures that areas closer to detection points contribute more significantly to the overall density estimate, while influence diminishes with increasing distance.

The search radius was determined using the algorithm described in the Esri ArcGIS Pro resource for kernel density analysis (Frate, 2022). Density calculations followed Silverman (1986) quartic kernel function, with density at each raster cell determined by summing the contributions of overlapping kernels. Cells near detection points exhibited higher densities due to greater kernel overlap, while those farther away had lower values. This process generated a smooth density distribution across the raster, effectively producing a heatmap that visually represented spatial use intensity within the study area.

From this heatmap, raster statistics and reclassification tools were applied to create HR and CR layers. Finally, these raster layers were vectorized into polygons using GDAL's polygonize tool and clipped to fit the river boundaries. The areas corresponding to the 95% KDE and 50% KDE were calculated using the field calculator in QGIS.

A total of 10 maps were then constructed, seven with all detection locations, HR area and CR area for each individual, and three with only the detection locations of the individuals where KDE could not be computed due to low number of detections. Additionally, the percentage of detections occurring outside each tagged fish's defined HR and the percentage of detections near river margins were calculated (locations up to 20 metres from the margin line).

From the 10 tagged fish, only four were recaptured (Table 2.2.). After downloading the data from the tags depth values were derived using the hydrostatic pressure equation, applying freshwater-specific constants to the recorded pressure data. For activity, the 3D acceleration sensor recorded four parameters: X-axis, Y-axis, Z-axis, and ASum, as mentioned in section 2.2. To simplify the

data selection for the activity response variable, Pearson correlations (*cor ()* function, *stats* package) were computed between all four parameters in R-project (R 4.0.5). The correlation matrix revealed that all three individual axis parameters (X-axis, Y-axis, Z-axis) were highly correlated (above 0.8) with ASum, which is the vector sum of these components as described in Section 2.2. Given its comprehensive representation of overall activity, ASum was selected as the activity response variable.

A preliminary filtration was then applied to the data, excluding data from the first 48h to account for possible behavioural changes caused by manipulation for tagging (Rees et al., 2013). Additionally, all data from the 24h previous to the recapture time were excluded, to avoid including data affected by potential changes in behaviour associated with fish struggling to release from the fishing gear used during the recapture campaigns. The process for individual #2 is noteworthy because only the tag was recovered (Table 2.2). This required accounting for the possibility that the tag had been expelled sometime before its recovery. Preliminary analyses revealed a cessation of activity on October 20th, so, to ensure accuracy, only data up to 00:00h of that day was considered, although the tag was recovered on the 26th. Moreover, any negative depth values in all recorded data were set to zero, to correct any erroneous measurements made by the tag's sensors.

Depth and activity data from the filtered dataset were grouped by season, month, day, and hour using the *dplyr* package and visualized with *ggplot2* from R (R 4.0.5). Datetime formatting was handled with the *lubridate* package. Seasonal variations in activity and depth were tested for significance using the Kruskal-Wallis rank sum test (*kruskal.test()*, base R). Pairwise comparisons were conducted using Dunn's post-hoc test (*dunn.test()*, *dunn.test* package), with Bonferroni-adjusted p-values. Generally, a 5% significance level was applied to all tests, excepting for Bonferroni-adjusted p-values (Zar, 2010).

Generalized Additive Models (GAMs) were developed to identify environmental variables influencing activity and depth use, as preliminary analysis indicated potential non-linear relationships between the response variables and some predictors (Wood, 2017). These models were implemented using the *mgcv* package in R (R 4.0.5). The response variables were examined as daily averages for both depth and activity data. Predictors for daily averages included water temperature, river flow, moonlight intensity, Julian Day of the year, season and finally activity in models with depth as the response variable and depth in models with activity as the response variable (Table 2.4). Water temperature values were recorded directly by the tags, while river flow data corresponded to the Belver Dam's daily mean affluent flow obtained from EDP, S.A. (personal communication). Moonlight intensity was calculated using the *getMoonIllumination()* function from the *suncalc* package, providing values between 0 (new moon) and 1 (full moon) from R (R 4.0.5). Julian Day of the year was derived using the *yday()* function from the *lubridate* package from R (R 4.0.5).

All models were fitted using a log-linked gamma distribution, suitable for strictly positive continuous data. The smoothing parameter for all models was estimated using the Maximum Likelihood (ML) method, which provides reliable and comparable estimates of model fit (Wood, 2017). To account for variability among individual tagged fish and prevent pseudo-replication, a random effect was included (Brewster et al., 2021, Santos et al., 2025). The selection of reference levels for parametric predictors should align with the study's objectives and research questions. In this study, the goal is to facilitate straightforward comparisons among the four seasons as such, to provide a stable baseline, the reference level was set to the season with the lowest variance. "Spring" was chosen as the reference for the response variable depth, while "Winter" was selected for activity.

In GAMs, assessing nonlinear correlations among predictors, known as "concurvity" (Wood, 2008), is essential. Concurvity was evaluated using the *concurvity()* function in the *mgcv* package, with an arbitrary cutoff of 0.7 applied for the most pessimistic measure when selecting predictors. An exhaustive model selection was conducted by testing all possible combinations of predictors and ranking models based on Akaike Information Criterion (AIC) and Bayesian Information Criterion (BIC), with AIC serving as the primary selection criterion. For all tested models, the shrinkage approach (Marra & Wood, 2011) was applied to confirm the significance of predictors. This method modifies the smoothing penalty with an additional shrinkage term, allowing them to shrink to zero if they are not meaningful, effectively taking them out of the model. Finally, if the model chosen as best (through AIC) presented any non-significant explicative variable a likelihood ratio test (LRT) was performed (Wood, 2017) regarding the next best performing model, if the simpler model did not present as significantly different (p-value > 0.05) it was confirmed as the best option. The final models were validated through diagnostic checks, including Q-Q plots, histograms of residuals, plots of response versus fitted values, and residuals versus the linear predictor.

To further investigate activity data, an additional model was developed to study Burst Movements (Section 2.4) that are potentially associated with predatory or agonistic behaviours, following Santos et al. (2025). Initially, activity data from the experiment trial (Section 2.4) was visualized through barplots created with the *ggplot2* R (version 4.0.5) package. Subsequently, additional boxplots were generated by grouping the data by behavioural categories (mobile [M], immobile [I], and burst movement [B]). Grouping was performed using the *group_by()* function, followed by the application of the *summarise()* and *quantile()* functions from R's *dplyr* package to extract the 25th, 50th, and 75th percentiles (first, second, and third quartiles, respectively). These percentiles were then used to get threshold values for the three behavioural categories and, afterward used to classify activity data from tagged fish in the lower Tagus River (section 2.5). Additionally, activity data recovered from this experiment were grouped (*dplyr* package) and visualized (*ggplot2* package) by hour in R (R 4.0.5).

Immobility events were excluded using the *filter()* function from *dplyr*, isolating mobility and burst movement events. The response variable was then defined as the hourly rate of Burst Movements. This zero-inflated count data was analysed using a two-part Hurdle model, implemented with the *hurdle()* function from the *pscl* package (Zeileis et al., 2008). The model consists of two components: (1) a logistic regression to model the presence-absence of burst movements (zero counts) and (2) a truncated count model for positive counts. This structure allows for independent testing of predictors on both the occurrence of burst movements and their frequency.

The absolute number of Burst Movements was initially introduced as the response variable. However, an offset parameter in the *hurdle()* function was included to adjust the counts relative to the total number of movement records, effectively modelling the rate (or proportion) of Burst Movements per detection (Santos, 2021). To account for potential overdispersion in the data, two distribution families—Poisson and Negative Binomial—were tested for the count component, with the latter being better suited for over dispersed data (Hoef & Boveng, 2007). The predictors used in this analysis were mean hourly values for water temperature, river flow, depth of the individual, season and period of the day (Table 2.4). All parameters were obtained as described for the GAMs with the addition of period of the day, determined using the *getSunlightTimes()* function from the *suncalc* package also from R (R 4.0.5). Reference levels were also chosen as

described for GAMs with "Winter" being chosen as reference level for season and "day" for period of the day. A rootogram was the chosen graphical tool for assessing the fit of these models. It compares the frequencies of the observed distribution on a square root scale with the curve of the fitted count model (Kleiber & Zeileis, 2016).

Table 2.4 – **List of predictors analysed in Generalized Additive Models (GAMs)** with daily means for activity (3D accelerometer data) and depth use (pressure data) as response variables and **Hurdle models** with hourly ratio of the number of burst movements per number of movement records as response variable. Variables are organized by model Type (Model) detailing the variables and the respective units (Variable, unit) used for each, maximum and minimum range (Range), variable abbreviation (Acronym) and the origin of the raw data (Source).

Model	Variable, unit	Range	Acronym	Source
GAMs	Mean daily depth, m	0.340 - 14.789	mean_depth	MCFT3-L, Lotek
	Mean daily activity, g	0.002 - 0.144	mean_ASum	MCFT3-L, Lotek
	Mean daily temperature, °C	10.800 - 26.320	mean_temp	MCFT3-L, Lotek
	Mean daily river flow, m^3/s	9.814 - 2422.430	mean_flow	EDP, S.A.
	Season, factor	"Winter", "Spring", "Summer", "Autumn"	Season	RStudio
	Moonlight intensity, fraction	0-1	mean_moon	RStudio
	Julian Day of the year, ordinal	1-365	mean_JD	RStudio
Hurdle	Mean hourly depth, m	0.000 - 15.882	mean_depth	MCFT3-L, Lotek
	Mean hourly temperature, °C	9.779 – 28.691	mean_temp	MCFT3-L, Lotek
	Mean hourly river flow, m^3/s	0.000 – 3709.550	mean_flow	EDP, S.A.
	Season, factor	"Winter", "Spring", "Summer", "Autumn"	Season	RStudio
	Period of the day, factor	"Day", "Dusk", "Night", "Dawn"	Period	RStudio
	Mean hourly depth, m	0.000 - 15.882	mean_depth	MCFT3-L, Lotek
	Mean hourly temperature, °C	9.779 – 28.691	mean_temp	MCFT3-L, Lotek

3. Results

3.1 Longitudinal habitat use

The maximum linear distance of river used by each individual (i.e., MSLR) was calculated for nine out of 10 tagged fish with a total number of 113 detections, ranging from 2 to 23 for each individual. Along the annual cycle, individuals used a median MSLR of 3.34 km (mean 4.81 km ± 3.26 km SD), ranging between 1.92 km and 10.16 km (Table 3.1). Home Range (HR) and Core Range (CR) were only possible to estimate for seven out of the 10 tagged fish with a total number of detections of 104, ranging from 10 to 23 for each individual. The HR area ranged from 0.101 to 0.742 km², with a median of 0.292 km² (mean 0.353 km² ± 0.245 km² SD). The CR area ranged from 0.011 to 0.308 km² with a median of 0.032 km² (mean 0.090 km² ± 0.113 km² SD) (Table 3.1).

Table 3.1 – Summary of spatial metrics for longitudinal habitat use of the four recaptured European catfish. Results are organized by Identification (ID) of the tagged catfish and detailing mid-stream linear range (MSLR) in km, Home Range (HR) in km²; Core Range (CR) in km², number of HR zones (No. HR) and number of CR zones (No. CR).

ID	MSLR (Km)	HR (km²)	CR (km²)	No. HR	No. CR
1	4.19	0.357	0.019	2	1
2	2.38	0.292	0.044	2	1
3	9.16	0.251	0.011	2	1
4	3.89	-	-	-	-
5	0.60	-	-	-	-
6	-	-	-	-	-
7	10.16	0.742	0.308	2	1
8	1.92	0.101	0.023	4	2
9	2.51	0.109	0.032	2	3
10	3.34	0.621	0.182	2	2

Individual longitudinal space use maps revealed relatively minor differences among the tracked European catfish (Figures 3.1-3.10). Most individuals divided their activity between two distinct zones within their HR area (Table 3.1), while one specimen used four distinct zones and was recorded shifting between these sections at least 10 times (Figure 3.8). Unidirectional movement patterns within their HR area were observed for three out of the seven fish, these fish did not return to their initial zones during the study (Figures 3.1, 3.3 and 3.10). The other four fish were recorded shifting zones at least once (Figures 3.2, 3.7, 3.8 and 3.9). Regarding CR areas, most of the studied fish maintained a single CR zone (Figure 3.1, 3.2, 3.3 and 3.7), while other fish occupied two or three zones (Figures 3.8, 3.9 and 3.10). A high number of detections (42.11%) occurred near the riverbank, primarily in refuge areas characterized by abundant riparian vegetation, extensive canopy coverage or anthropogenic structures such as bridges (Fig. 3.11).

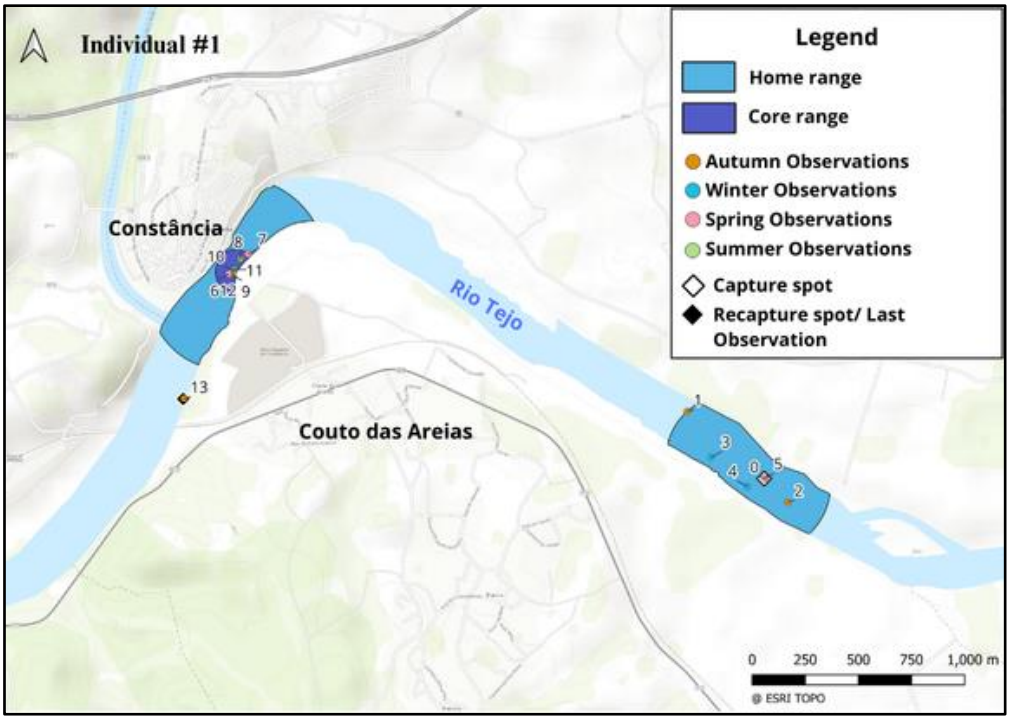

Figure 3.1 – **Map of the longitudinal space use of individual #1 with manual tracking locations (#0-#13) and Home Range and Core Range areas/zones. Date of all observations represented: 0** - 04/11/2022; **1** - 25/11/2022; **2** - 07/12/2022; **3** - 02/03/2023; **4** - 17/03/2023; **5** - 31/03/2023; **6** - 25/04/2023; **7** - 26/05/2023; **8** - 19/07/2023; **9** - 16/08/2023; **10** - 12/09/2023; **11** - 13/09/2023; **12** - 14/09/2023; **13** - 31/10/2023.

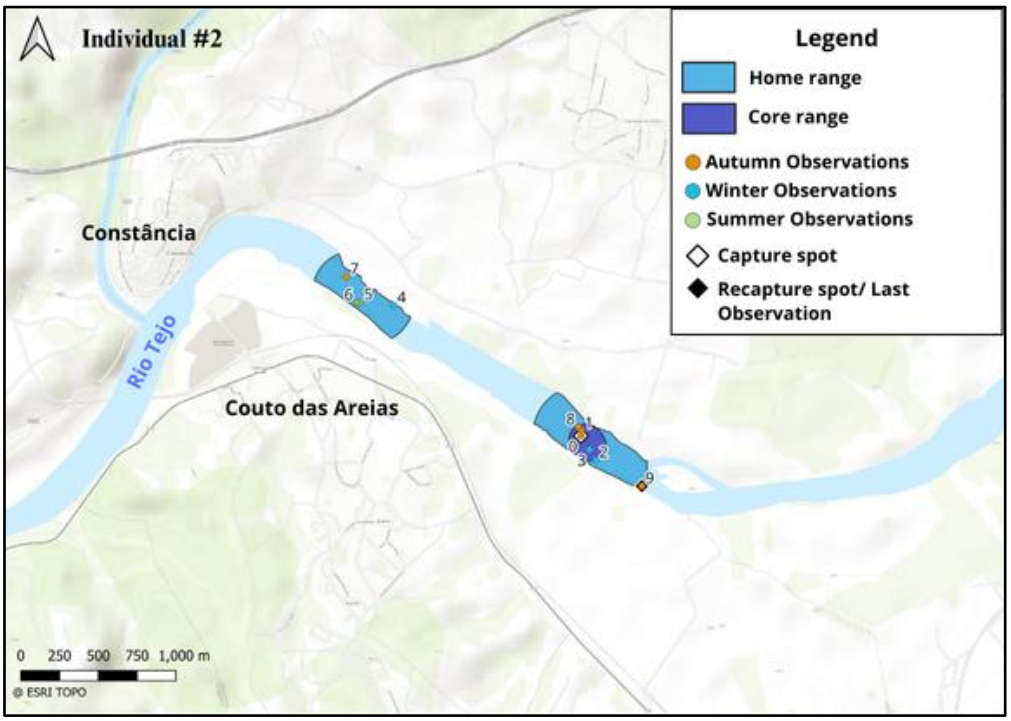

Figure 3.2 – **Map of the longitudinal space use of individual #2 with manual tracking locations (#0-#9) and Home Range and Core Range areas/zones. Date of all observations represented: 0** - 04/11/2022; **1** - 07/12/2022; **2** - 22/12/2022; **3** - 04/01/2023; **4** - 18/01/2023; **5** - 12/09/2023; **6** - 13/09/2023; **7** - 27/09/2023; **8** – 25/10/2023; **9** - 26/10/2023.

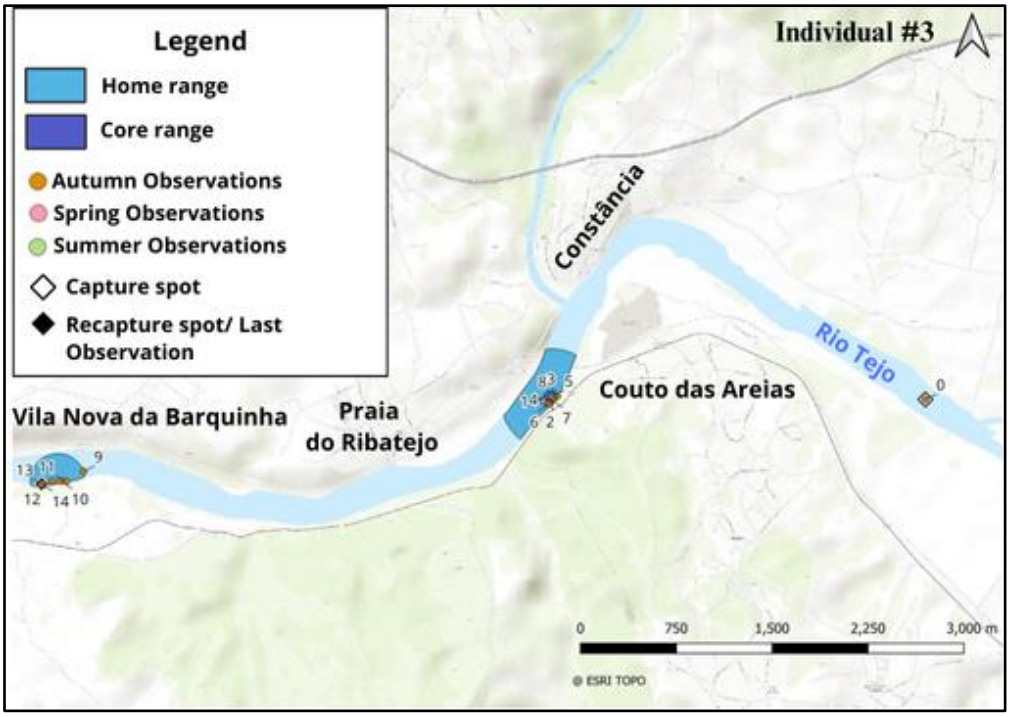

Figure 3.3 – **Map of the longitudinal space use of individual #3 with manual tracking locations (#0-#14) and Home Range and Core Range areas/zones. Date of all observations represented: 0** - 04/11/2022; **1** - 26/05/2023; **2** - 29/06/2023; **3** - 18/08/2023; **4** - 30/08/2023; **5** - 12/09/2023; **6** - 28/09/2023; **7** - 27/10/2023; **8** - 30/10/2023; **9** - 31/10/2023; **10** - 01/11/2023; **11** - 21/11/2023; **12** - 22/11/2023; **13** - 23/11/2023; **14** - 24/11/2023.

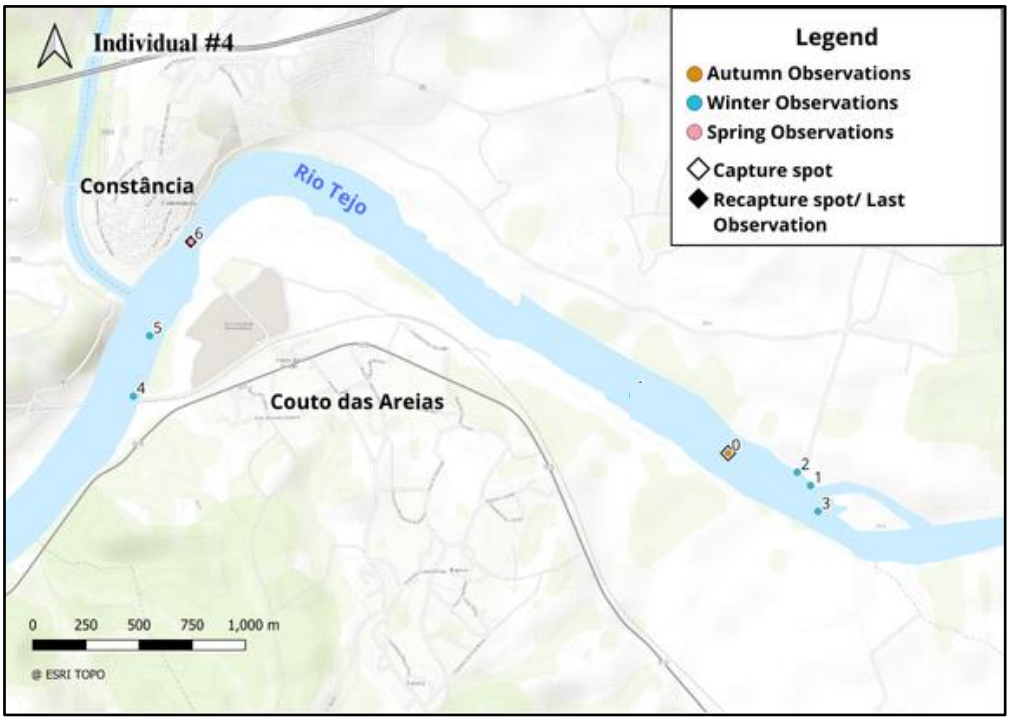

Figure 3.4 – **Map of the longitudinal space use of individual #4 with manual tracking locations (#0-#6) and Home Range and Core Range areas/zones. Date of all observations represented: 0** - 04/11/2022; **1** - 22/12/2022; **2** - 04/01/2023; **3** - 18/01/2023; **4** - 02/03/2023; **5** - 17/03/2023; **6** - 24/04/2023.

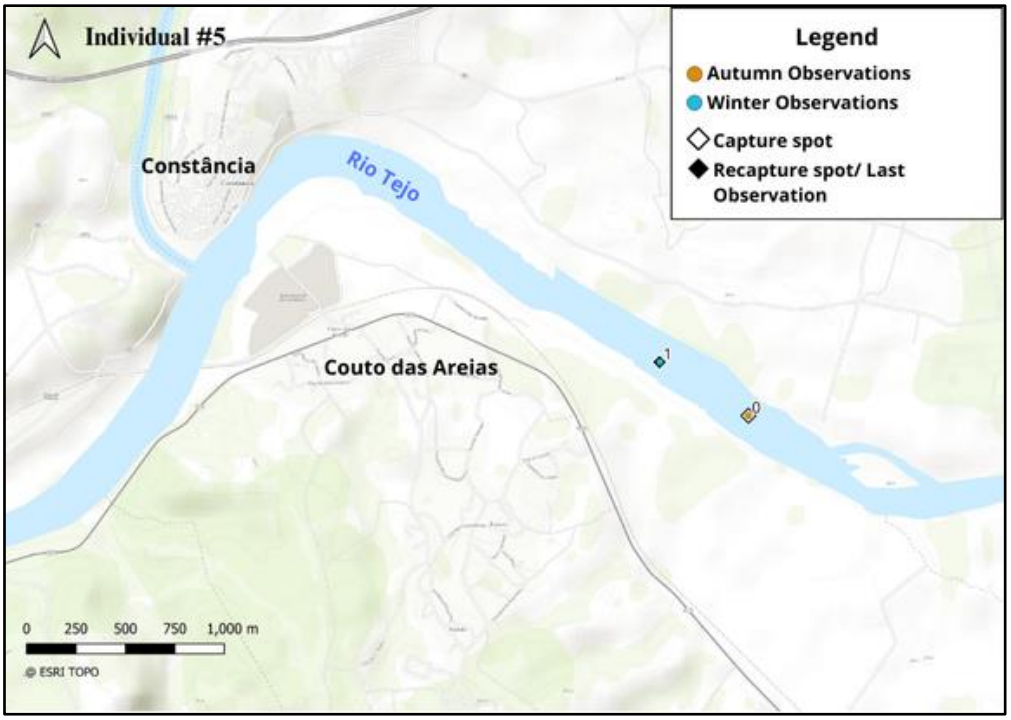

Figure 3.5 – **Map of the longitudinal space use of individual #5 with manual tracking locations (#0-#1). Date of all observations represented: 0** - 04/11/2022; **1** - 22/12/2022.

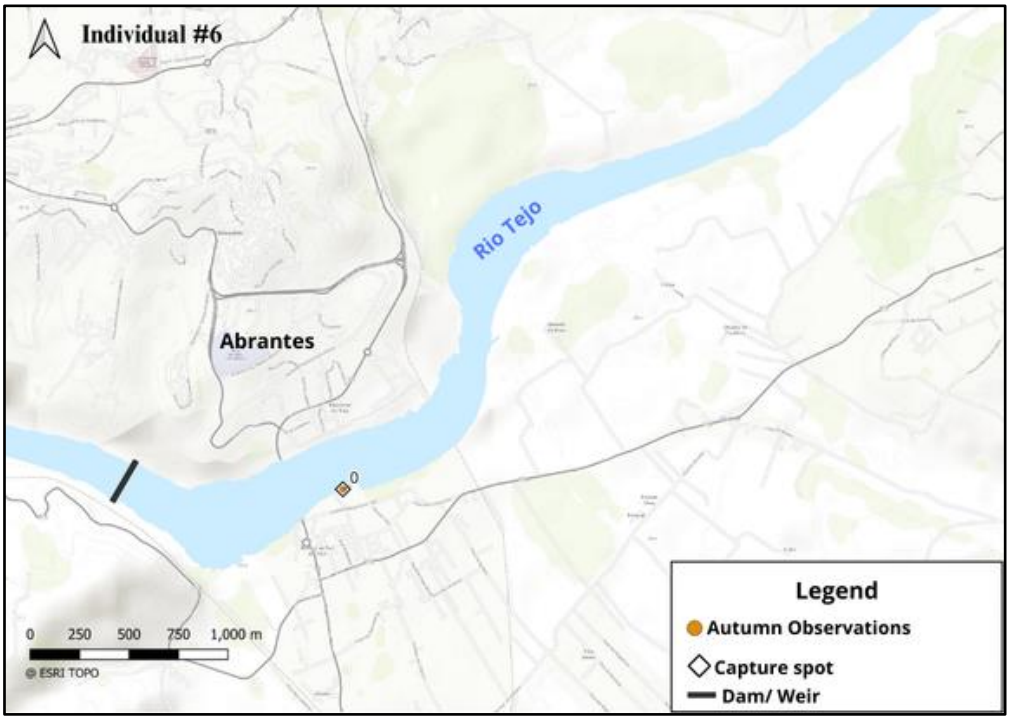

Figure 3.6 – **Map of the longitudinal space use of individual #6 with manual tracking locations (#0). Date of all observations represented: 0** - 25/11/2022.

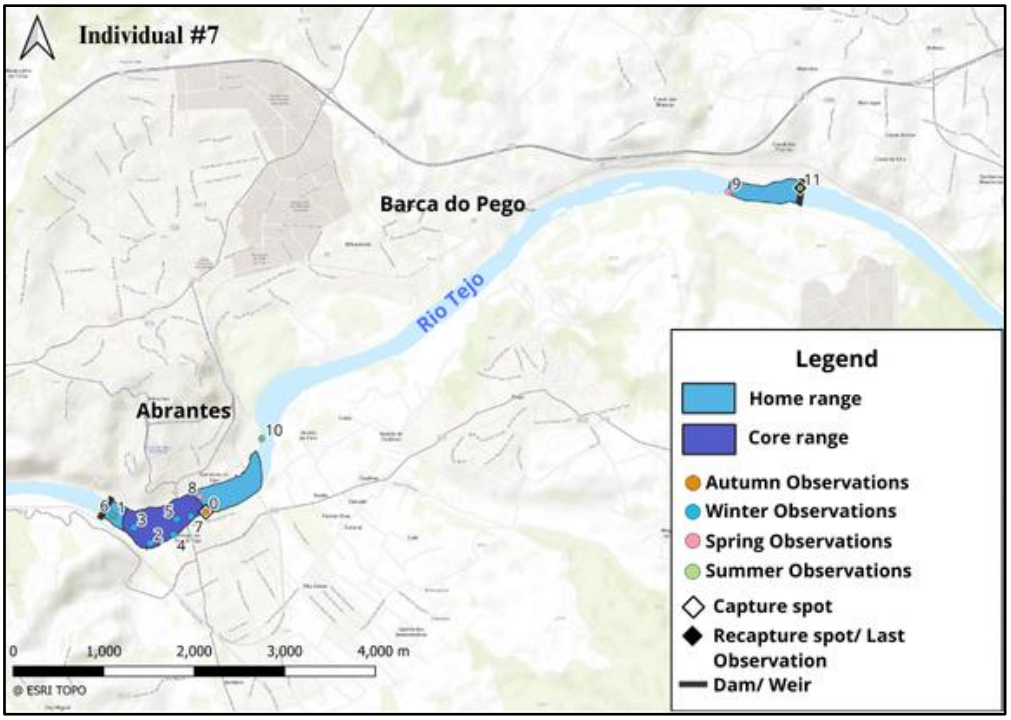

Figure 3.7 - Map of the longitudinal space use of individual #7 with manual tracking locations (#0-#11) and Home Range and Core Range areas/zones. Date of all observations represented: 0 - 25/11/2022; **1** - 07/12/2022; **2** - 22/12/2022; **3** - 18/01/2023; **4** - 02/02/2023; **5** - 16/02/2023; **6** - 02/03/2023; **7** - 17/03/2023; **8** - 31/03/2023; **9** - 11/05/2023; **10** - 16/07/2023; **11** - 13/09/2023.

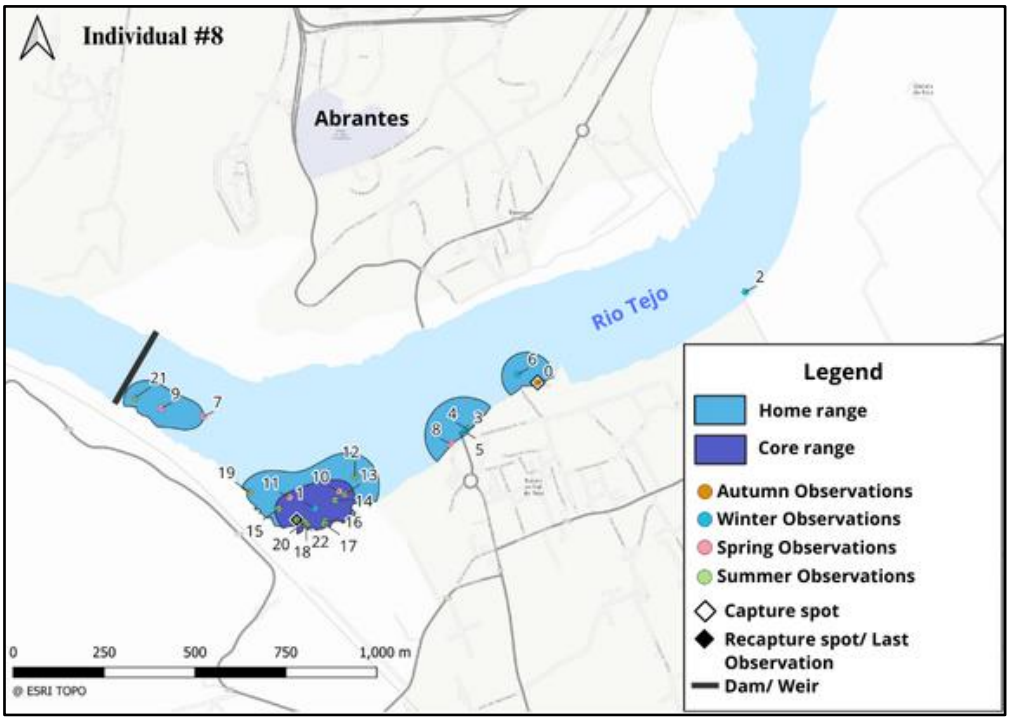

Figure 3.8 – Map of the longitudinal space use of individual #8 with manual tracking locations (#0-#22) and Home Range and Core Range areas/zones. Date of all observations represented: 0 - 25/11/2022; **1** - 22/12/2022; **2** - 18/01/2023; **3** - 02/02/2023; **4** - 16/02/2023; **5** - 02/03/2023; **6** - 17/03/2023; **7** - 31/03/2023; **8** - 15/04/2023; **9** - 27/04/2023; **10** - 11/05/2023; **11** - 11/06/2023; **12** - 27/06/2023; **13** - 16/07/2023; **14** - 17/07/2023; **15** - 18/07/2023; **16** - 19/07/2023; **17** - 16/08/2023; **18** - 18/08/2023; **19** - 30/08/2023; **20** - 11/09/2023; **21** - 12/09/2023; **22** - 13/09/2023. Second Core Range area zone is very small, and it is covered by detections **#3** to **#5**.

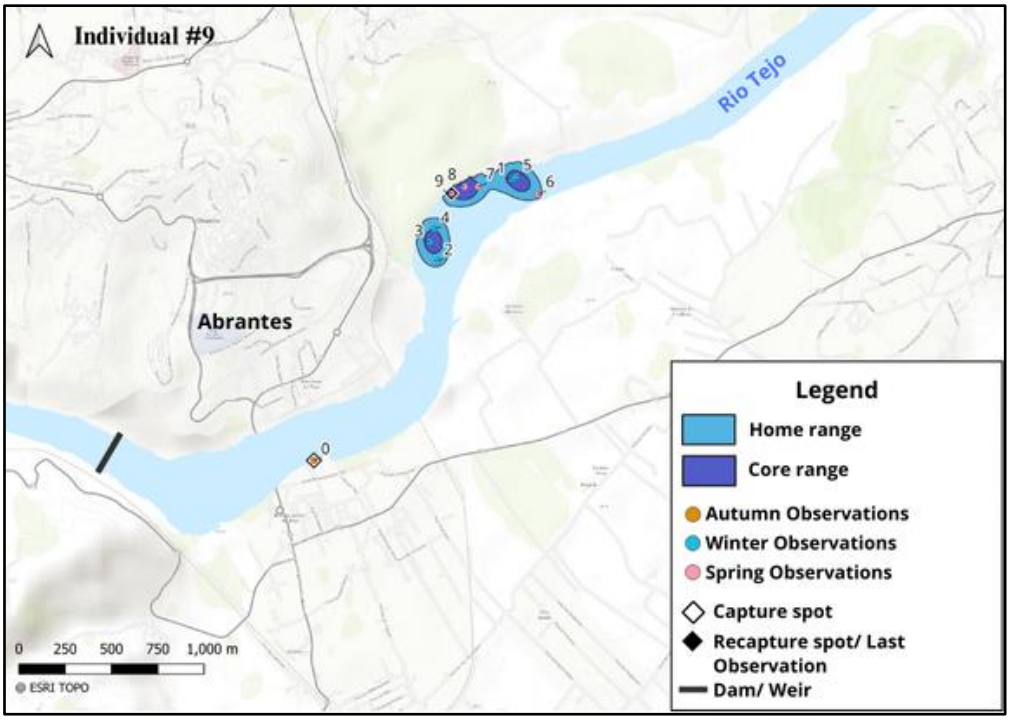

Figure 3.9 – Map of the longitudinal space use of individual #9 with manual tracking locations (#0-#9) and Home Range and Core Range areas/zones. Date of all observations represented: 0 - 25/11/2022; **1** - 18/01/2023; **2** - 02/02/2023; **3** - 16/02/2023; **4** - 02/03/2023; **5** - 17/03/2023; **6** - 31/03/2023; **7** - 15/04/2023; **8** - 27/04/2023; **9** - 11/05/2023.

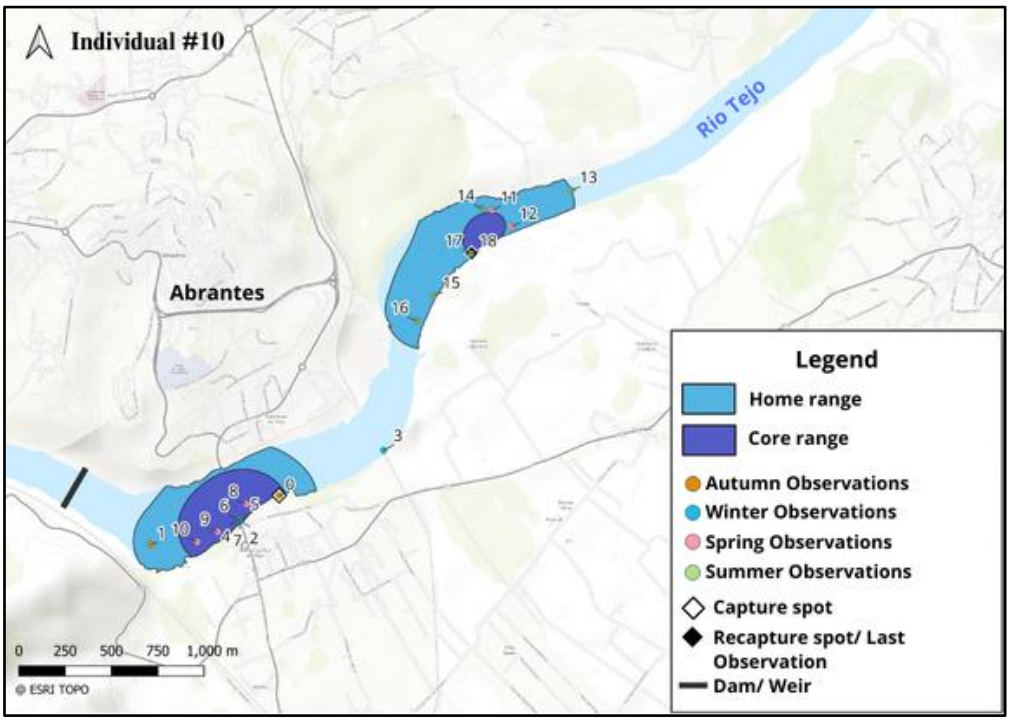

Figure 3.10 – **Map of the longitudinal space use of individual #10 with manual tracking locations (#0-#18) and Home Range and Core Range areas/zones. Date of all observations represented: 0** - 25/11/2022; **1** - 07/12/2022; **2** - 04/01/2023; **3** - 18/01/2023; **4** - 02/02/2023; **5** - 16/02/2023; **6** - 2/03/2023; **7** - 17/03/2023; **8** - 31/03/2023; **9** - 15/04/2023; **10** - 27/04/2023; **11** - 26/05/2023; **12** - 11/06/2023; **13** - 27/06/2023; **14** - 16/07/2023; **15** - 17/07/2023; **16** - 18/07/2023; **17** - 19/07/2023; **18** - 20/07/2023.

Figure 3.11 – **Photographs illustrative of the locations used as refuge areas for individual: A) #1** from detections #6 to #9 (Fig.3.1); **B) #1** from detections #10 to #12 (Fig.3.1); **C) #3** from detection #1 to #8. (Fig.3.3); **D) #8** from detection #3 to #5 and #8 (Fig.3.8) and, for individual **#10** from detection #2 to #6 (Fig.3.10).

3.2 Vertical habitat use

Four fish were recaptured, resulting in a total of 2,177,835 datetime stamps associated with sensor (pressure, 3D accelerometery) data. These were used in the following analysis (Table 3.2).

Table 3.2 – Summary of the number of datetime stamps of the four recaptured European catfish. Identification (ID)of the tagged catfish and number of datetime stamps per individual (No. of datetime stamps) with pressure (i.e., depth) and 3D accelerometer (i.e., activity) data.

ID	No. of datetime stamps
2	729,863
4	351,876
8	605,850
10	490,246

The pressure sensor data revealed a seasonal variation in the European catfish's depth use (Figure 3.12). Overall, the tagged fish predominantly occupied shallow waters throughout the year. Summer registered the shallowest median depth at 1.6 m and winter the deepest median depth at 3 m. Monthly analysis supports this seasonal pattern, with the winter months of January and February showing the highest median depths of 3.1 m and the month of June and July recording the shallowest median depths at 1.2 m and 1.5 m, respectively. The variability of vertical habitat use was higher during February, while June registered minor variability in depth occupation. Maximum observed depths reached nearly 17 m, particularly from January to March. Although September and October both decreased in median depth and variability with the latter showing the shallowest depth, diverging from the seasonal trend, they were not considered due to their low sample sizes (of two and one individuals). The Kruskal-Wallis test confirmed that there are significant differences in seasonal depth use values ($\chi 2$ = 242831, df=3, p-value <0,0001),

moreover Dunn's test indicates significant differences in depth for any of the seasons' pairwise comparisons (all p-values <0,0001).

Circadian patterns in European catfishes' depth use seemed to follow the same pattern throughout the year (Figure 3.13). Tagged fish tended to dwell in shallower depths during the day period (9/10h until 18h/19h) overall, occupying deeper areas during dusk, night and dawn, with a more evident variation during the summer months of June, July and August. Autumn months of October, November and December showed a different pattern where the shallowest depths were registered during the dusk, night and dawn, and higher depths being reached during the day, as well as a slightly higher variation.

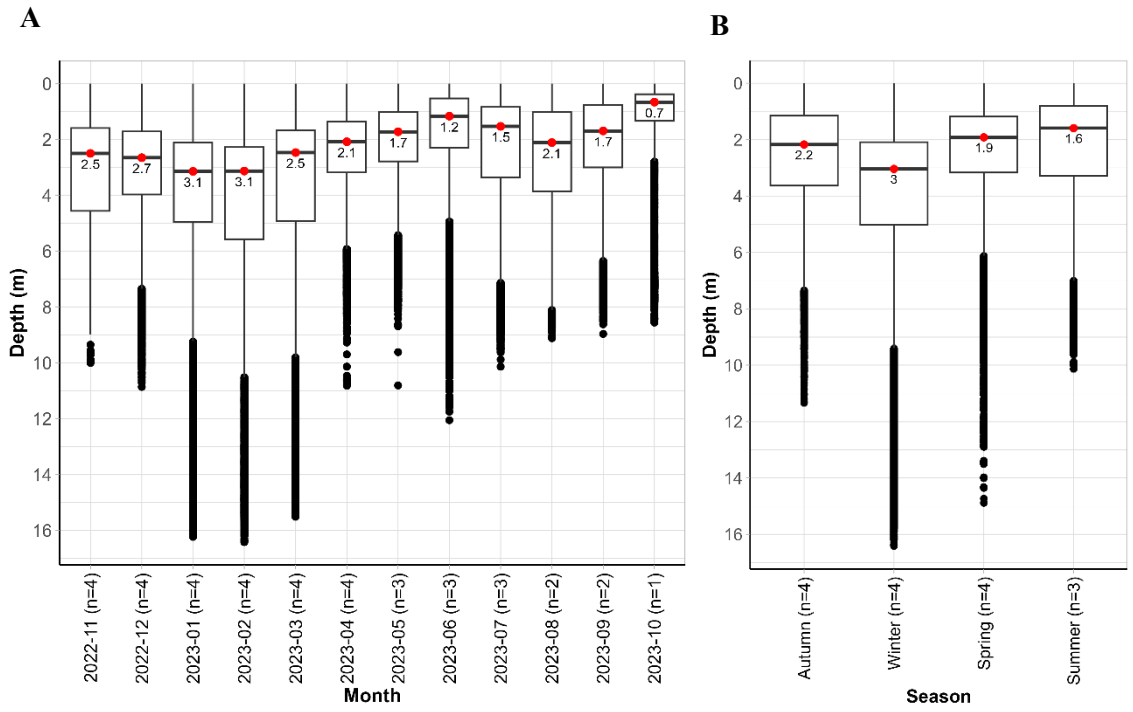

Figure 3.12 – Seasonal vertical habitat used (i.e., depth) along the study period considering the data collected from the four recaptured European catfish. Represented by boxplots for each month **(A)** and annual season **(B)** with median values shown below the red dots.

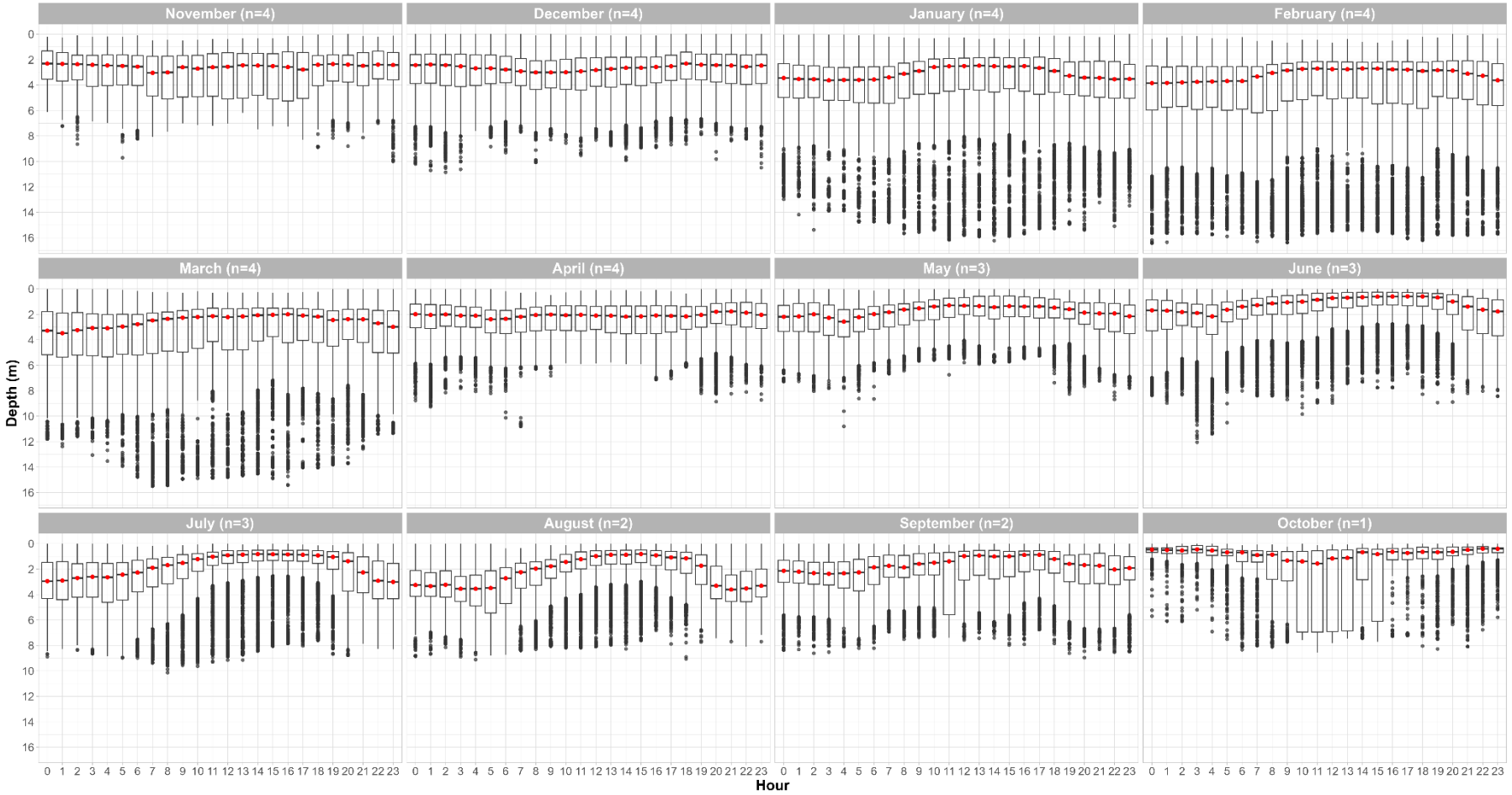

Figure 3.13 – Circadian vertical habitat use (i.e., depth) along the study period considering the data collected from the four recaptured European catfish . Represented by boxplots for each monitored month with medians accentuated by the red dots.

A total of 63 explanatory models were developed to analyse daily mean depth values (Annex II, Table II.1). The top ten models based on AIC values were identified together with other key model selection criteria (Table 3.3). The best-performing model included all explanatory variables (Table 2.4); however, penalized p-values indicated that moonlight intensity was not a significant predictor. Consequently, a LRT was performed to compare if the inclusion of this predictor improved model performance. The full model was compared to model d_d_58, which excluded moonlight intensity as a predictor and coincidentally had the second-best AIC and deviance explained. The LRT revealed no significant improvement (p-value > 0.05), leading to the selection of the simpler model, d_d_58, in line with the principle of parsimony.

Concurvity analysis revealed high values for temperature (0.974), river flow (0.731), and Julian Day of the year (0.979), this was largely due to shared seasonal patterns, particularly apparent in the strong correlation between temperature and Julian Day of the year (0.958) and the inclusion of the parametric variable Season. Despite these relationships, all variables were retained in the model due to their complementary ecological and physical information. For example, while both temperature and Julian Day reflect seasonality, temperature represents an environmental condition, whereas Julian Day relates to temporal patterns that may encompass additional temporal factors like reproduction or seasonal resource availability.

Partial effect plots for the selected model, d_d_58 (Figure 3.14) show that temperature exhibited a nearly linear negative relationship with depth, indicating that fish tend to occupy shallower depths as temperatures increase. River flow showed a non-linear relationship with depth, increasing up to approximately 1000 m^3/s. Activity also showed a non-linear relationship with depth, that although significant, is less visible than the others, pointing out that generally higher activity events occur at shallower depths. A non-linear relationship was observed between depth use and Julian Day of the year, with fish occupying greater depths from late June (day 180) to early August (day 220), followed by a gradual shift to shallower depths until late October (day 300). This seasonal pattern may have been influenced by the behaviour exhibited by individuals #2 and #8, which consistently occupied greater depths during July and August. This trend is evident in the individual monthly boxplots for depth use (Annex II, Figure II.1) and the individual depth GAMs (Annex II, Table II.2 and Figure II.2). Furthermore, high concurvity among some variables suggests that the effects of Julian Day of the year and season on depth use may have been partially absorbed, with temperature likely playing a dominant role. As a result, the partial plot for Julian Day highlights a more evident summer peak, which may amplify seasonal differences, potentially underestimating winter depth values that should be higher. This finding suggests that fish may utilize deeper habitats during summer due to an unidentified factor independent from those analysed. Individual Perspective plots of the models' daily mean depth predictions can be found in Annex II and Figure II.3.

Table 3.3 – Summary on the selection process of the predictors on Generalized Additive Models (GAMs) of the daily mean depth, of the four recaptured European catfish, as the response variable. The Akaike Information Criterion (AIC), the Bayesian Information Criterion (BIC) and the deviance explained are presented for each fitted model.

Model ID	Depth Model Formula	AIC	BIC	Deviance explained (%)
d_d_23	Y ~ s(mean_temp) + s(mean_flow) + s(mean_JD) + s(Ind, bs = "re")	3108.99	3231.58	48.88
d_d_49	Y ~ s(mean_temp) + s(mean_ASum) + s(mean_JD) + Season + s(Ind, bs = "re")	3108.80	3221.01	48.69
d_d_45	Y ~ s(mean_temp) + s(mean_flow) + s(mean_JD) + s(mean_moon) + s(Ind, bs = "re")	3108.43	3235.47	48.99
d_d_61	Y ~ s(mean_temp) + s(mean_ASum) + s(mean_JD) + s(mean_moon) + Season + s(Ind, bs = "re")	3103.86	3221.70	49.03
d_d_42	Y ~ s(mean_temp) + s(mean_flow) + s(mean_ASum) + s(mean_JD) + s(Ind, bs = "re")	3101.67	3247.71	49.68
d_d_60	Y ~ s(mean_temp) + s(mean_flow) + s(mean_JD) + s(mean_moon) + Season + s(Ind, bs = "re")	3101.22	3215.85	49.09
d_d_57	Y ~ s(mean_temp) + s(mean_flow) + s(mean_ASum) + s(mean_JD) + s(mean_moon) + s(Ind, bs = "re")	3100.30	3251.28	49.84
d_d_46	Y ~ s(mean_temp) + s(mean_flow) + s(mean_JD) + Season + s(Ind, bs = "re")	3099.12	3228.57	49.48
d_d_58	**Y ~ s(mean_temp) + s(mean_flow) + s(mean_ASum) + s(mean_JD) + Season + s(Ind, bs = "re")**	**3093.81**	**3227.68**	**49.82**
d_d_63	Y ~ s(mean_temp) + s(mean_flow) + s(mean_ASum) + s(mean_JD) + s(mean_moon) + Season + s(Ind, bs = "re")	3091.30	3230.11	50.03

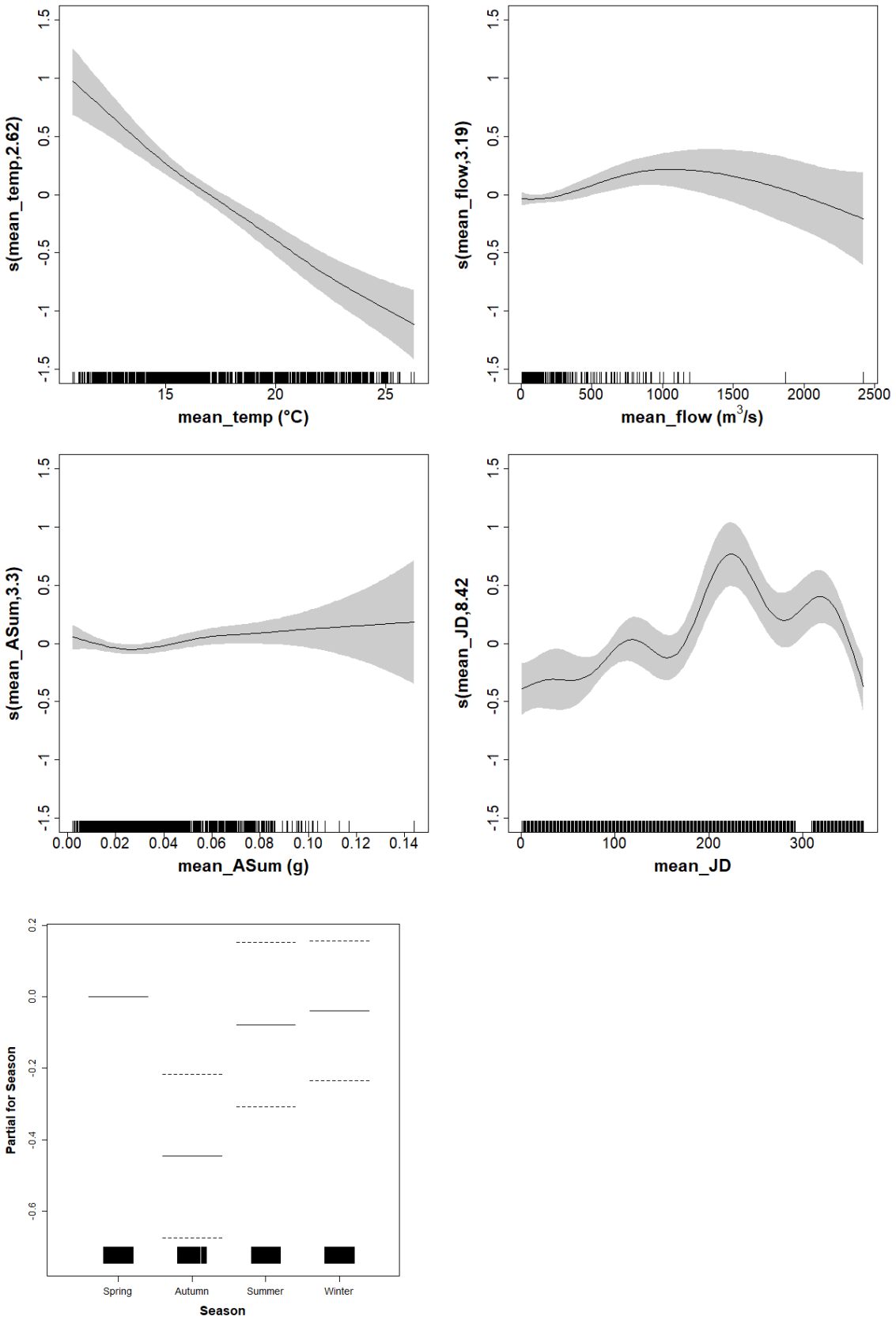

Figure 3.14 – Partial effect plots of the chosen depth use GAM (model d_d_58) revealing the correlations between the predictors and the mean daily depth use as response variable. The plot for the parametric variable season of the year as a different scale.

3.3 Activity patterns

3.3.1 Sensor (3D accelerometer) calibration in a controlled outdoor water enclosure for behavioural activity

Preliminary analysis of one month of data from the two individuals tested in a controlled water enclosure revealed a high frequency of zero values for 3D accelerometry (ASum) (Figure 3.15). As a result, mean and median activity values were extremely low, complicating the analysis of daily and hourly variations. To better evaluate overall trends, activity was instead assessed as a percentage of activity events. To classify activity events data from the experimental tests conducted in a controlled water enclosure (Section 2.4) were used to assess 3D accelerometer recordings in relation to observed catfish behaviour. Three behavioural categories were defined *a priori*: immobile (I), mobile (M), and burst movement (B). Their activity distributions were analysed using boxplots (Figure 3.16), and thresholds were established based on key percentiles of activity data dispersion (ASum) (Table 3.4). Activity values below the first quartile (Q1 = 0.03) of the M distribution were classified as I behaviour, indicating periods when the fish was stationary or exhibited minimal movement. Values between Q1 (0.03) of the M distribution and the first quartile (Q1 = 0.78) of the B distribution were categorized as M behaviour, representing moderate and continuous movement. Finally, values exceeding Q3 (0.78) of the B distribution were defined as B behaviour, characterized by high-intensity, sudden bursts of activity. Activity events include all events classified as M or B. All analyses were conducted on data from both studied fish, which showed no noteworthy differences in distribution values when analysed individually. Both tested specimens exhibited a circadian pattern, with peak activity occurring from dusk through the night until dawn, and the lowest activity levels recorded during the day (Figure 3.17).

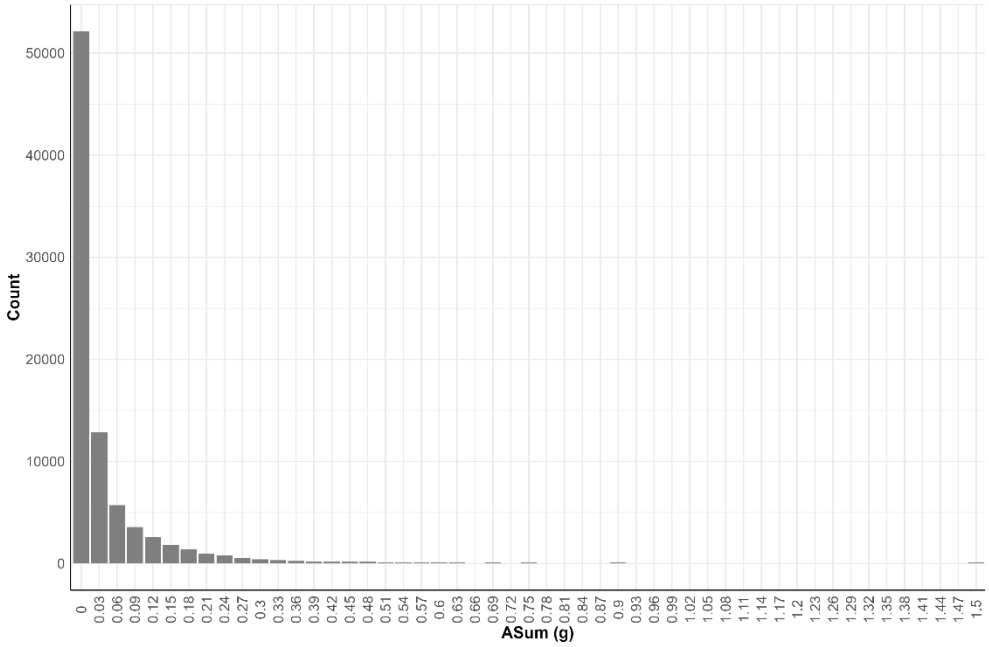

Figure 3.15 – Distribution of activity levels considering the 3D accelerometer data (ASum) collected from the two European catfish maintained in the water enclosure, during three weeks. Represented by a bar plot with count data for each activity level (ASum).

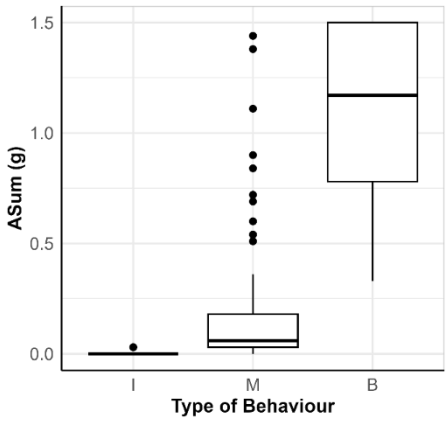

Figure 3.16 – Threshold values of activity for each behavioural category considering the 3D accelerometer data (ASum) collected from the two European catfish maintained in the water enclosure, during the experimental tests. Represented by boxplots for each behavioural category, with I as immobile; M as mobile and B as burst movement.

Table 3.4 – Key percentiles of the 3D accelerometer data (i.e., activity) recorded during the experimental tests conducted with two European catfish in a water enclosure associated to each behavioural category thresholds. With I as immobile, M as mobile and B as burst movement.

Behaviour	Q1	Q2	Q3
Immobile (I)	0.00	0.00	0.00
Mobile (M)	0.03	0.06	0.18
Burst Movement (B)	0.78	1.17	1.50

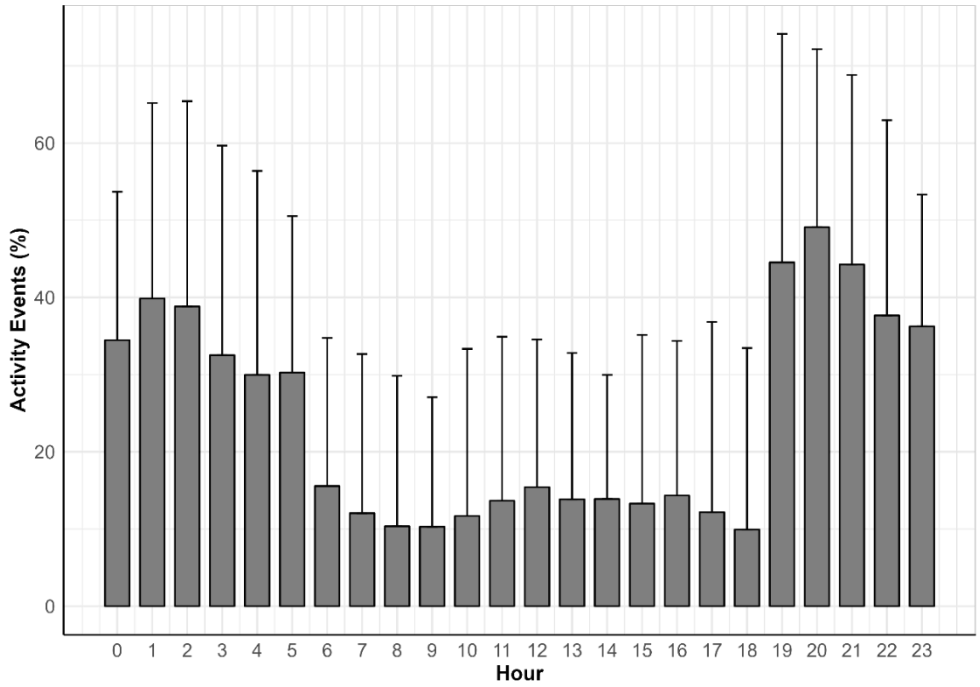

Figure 3.17 – Circadian activity considering the 3D accelerometer data collected from the two European catfish maintained in the water enclosure, during three weeks. Represented by a bar plot with mean values of percentage of activity events and standard deviation for each hour.

3.3.2. General activity

The 3D accelerometer sensor data revealed that overall, in warmer seasons European catfish's activity levels were higher and, although lower in colder seasons, still substantial (Figure 3.18). Monthly analysis supports this overall seasonal pattern with April (spring) and August (summer) revealing the highest levels of activity, the lowest levels of activity were registered in October (autumn) followed by February (winter).

The Kruskal-Wallis test indicates that there are significant differences in seasonal activity ($\chi 2$ = 108919, df=3, p-value <0,0001) values. Similarly, Dunn's test indicates there are differences in activity for any of the seasons' pairwise comparisons (all p-values <0,0001).

Circadian patterns in European catfishes' activity levels showed a clear diel pattern where levels were lower during the day and started to increase from dusk through the night and until dawn. However, from October until December, the circadian pattern appeared to change and become less clear (Figure 3.19).

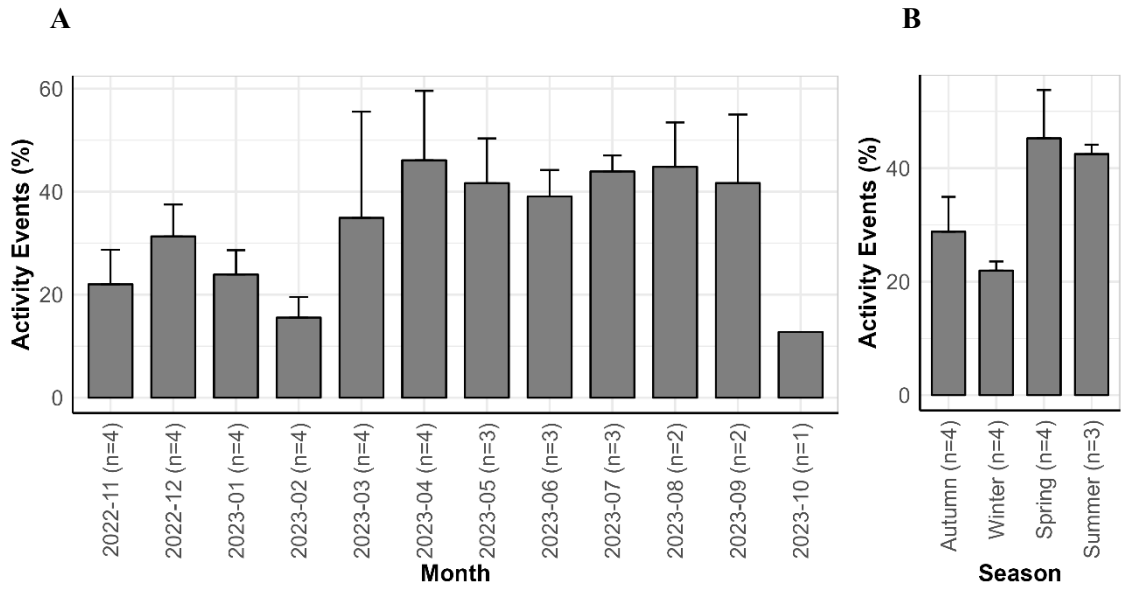

Figure 3.18 – Seasonal activity along the study period considering the 3D accelerometer data collected from the four recaptured European catfish. Represented by bar plots with mean values of percentage of activity events and standard deviation for each month **(A)** and annual season **(B)**.

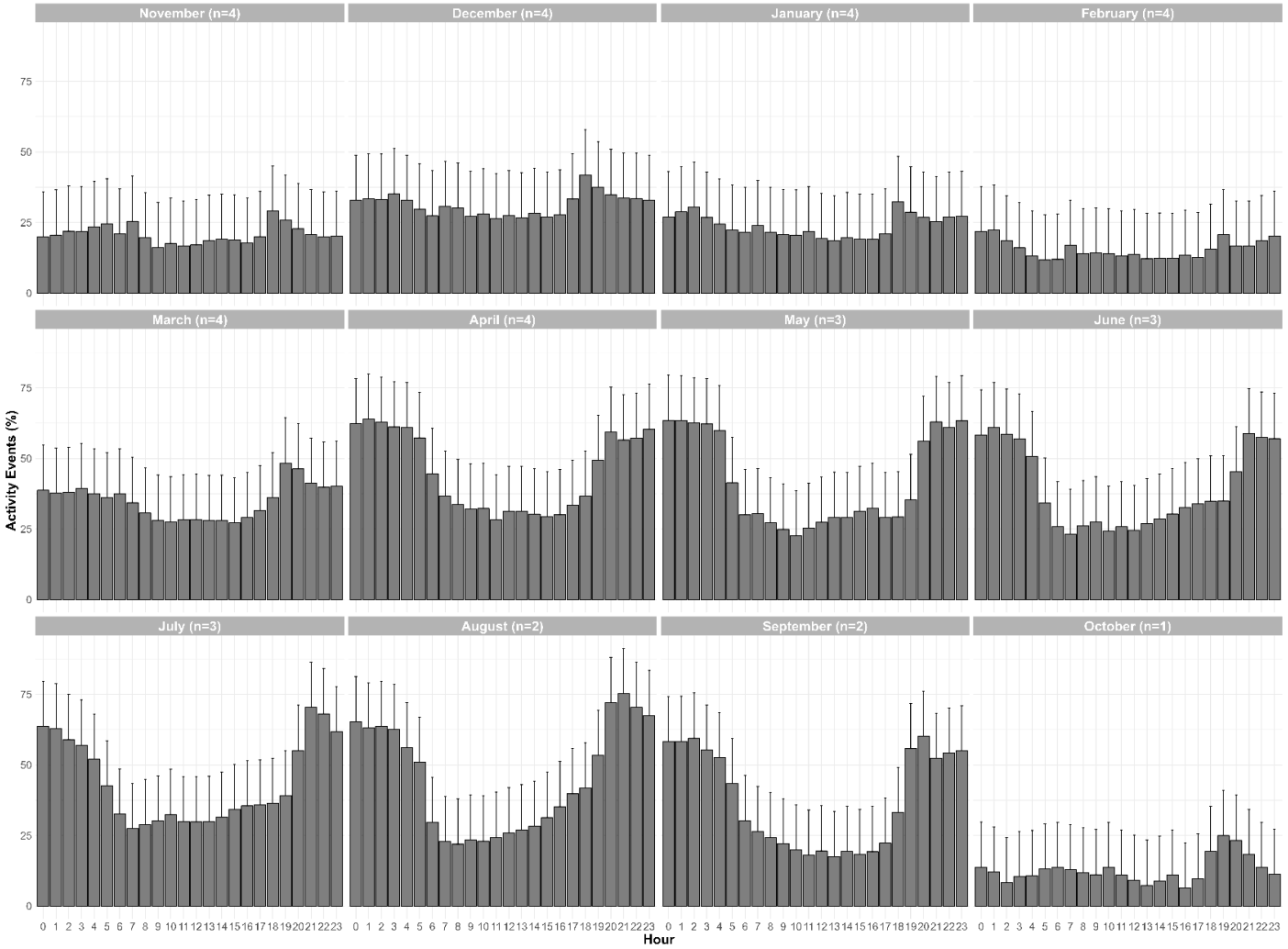

Figure 3.19 – Circadian activity along the study period considering the 3D accelerometer data collected from the four recaptured European catfish. Represented by bar plots with mean values of percentage of activity events and standard deviation, for each month.

A total of 63 explanatory models were developed (Annex II, Table II.3) to analyse daily activity. Among the top ten models (Table 3.5), the best model, a_d_58, included all explanatory variables except moonlight intensity. Concurvity analysis indicated high values for temperature (0.974), river flow (0.732), and Julian Day of the year (0.979). These high values were attributed to shared seasonal patterns and intrinsic relationships between these variables. Specifically, the strong correlation between temperature and Julian Day (0.958) reflects the pronounced seasonality of temperature. Despite these high concurvity values, all variables were retained in the model due to their complementary roles in explaining the response variable (Section 3.2).

Partial effects plots for the selected model, a_d_58, (Figure 3.20) revealed a non-linear positive relationship between temperature and activity, with higher activity levels associated with higher temperatures. Regarding river flow, activity followed a non-linear trend, with the lowest activity levels occurring at the lowest flow values, furthermore, activity increased as river flow rose, but observations were limited beyond the 1000 m^3/s threshold. Activity showed a non-linear relationship with depth, with a tendency to increase until reaching 8 m depth, after which it steadily decreased, showing its lowest levels at greatest depths. Regarding Julian Day of the year, it is possible to observe an increase in activity from around day 100 (early April), peaking near day 150 (late May), before declining until day 200 (late July). Activity showed a slight increase around day 240 (late August) before declining again, reaching its lowest levels around day 290 (mid-October). Finally, fish were more active during summer and least active in winter. Individual Perspective plots of the models' daily mean activity predictions can be found in Annex II and Figure II.4.

Table 3.5 – Summary on the selection process of the predictors on Generalized Additive Models (GAMs) of the daily mean activity, of the four recaptured European catfish, as the response variable. The Akaike Information Criterion (AIC), the Bayesian Information Criterion (BIC) and the deviance explained are presented for each fitted model.

Model ID	Activity Model Formula	AIC	BIC	Deviance explained (%)
a_d_57	Y ~ s(mean_temp) + s(mean_flow) + s(mean_depth) + s(mean_JD) + s(mean_moon) + s(Ind, bs = "re")	-6144.17	-5975.58	55.17
a_d_42	Y ~ s(mean_temp) + s(mean_flow) + s(mean_depth) + s(mean_JD) + s(Ind, bs = "re")	-6146.20	-5982.30	55.17
a_d_56	Y ~ s(mean_depth) + s(mean_JD) + s(mean_moon) + Season + s(Ind, bs = "re")	-6150.60	-6024.87	54.70
a_d_62	Y ~ s(mean_flow) + s(mean_depth) + s(mean_JD) + s(mean_moon) + Season + s(Ind, bs = "re")	-6150.65	-6020.07	54.79
a_d_39	Y ~ s(mean_depth) + s(mean_JD) + Season + s(Ind, bs = "re")	-6152.49	-6031.50	54.70
a_d_53	Y ~ s(mean_flow) + s(mean_depth) + s(mean_JD) + Season + s(Ind, bs = "re")	-6152.63	-6026.85	54.79
a_d_61	Y ~ s(mean_temp) + s(mean_depth) + s(mean_JD) + s(mean_moon) + Season + s(Ind, bs = "re")	-6153.67	-6008.35	55.16
a_d_49	Y ~ s(mean_temp) + s(mean_depth) + s(mean_JD) + Season + s(Ind, bs = "re")	-6155.06	-6015.28	55.13
a_d_63	Y ~ s(mean_temp) + s(mean_flow) + s(mean_depth) + s(mean_JD) + s(mean_moon) + Season + s(Ind, bs = "re")	-6158.23	-5994.00	55.67
a_d_58	**Y ~ s(mean_temp) + s(mean_flow) + s(mean_depth) + s(mean_JD) + Season + s(Ind, bs = "re")**	**-6160.37**	**-6000.43**	**55.69**

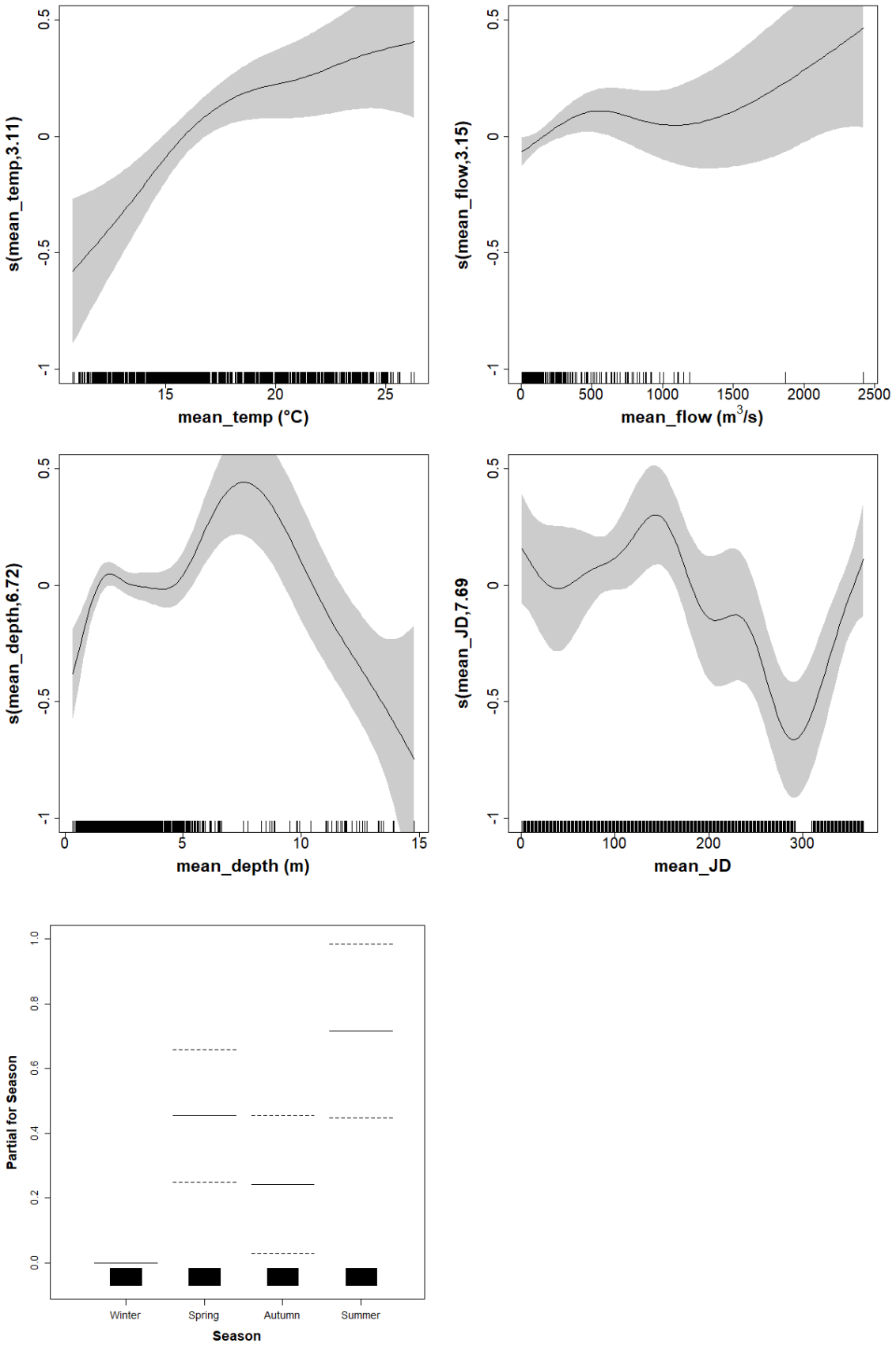

Figure 3.20- Partial effect plots of the chosen activity use GAM (model a_d_58) revealing the correlations between the predictors and the mean daily activity (i.e., 3D accelerometer) as response variable. The plot for the parametric variable season of the year as a different scale.

3.3.3. Burst activity

A total of 62 Hurdle models were created during the process of finding the best explanatory model of the rate of burst movements (Annex II, Table II.4). The chosen Hurdle model had the lowest AIC and BIC among all models and included temperature, river flow, period of the day, and season of the year as predictors, model 28, (Table 3.6). The results of the selected model (Table 3.7) indicate that while temperature does not significantly influence the likelihood of burst movements occurring (zero hurdle component), it has a positive association with their frequency when they do occur (count component). River flow positively affects the probability of extreme activity occurring but has only a weak effect on its frequency. The model reveals that burst movements are most likely at night, followed by dusk and dawn, compared to daytime. Similarly, when extreme activity does occur, its frequency is highest at night, with a more minor increase observed at dawn. Regarding seasonal patterns, the model indicates that burst movements are significantly more likely in spring, summer, and autumn compared to winter. However, the frequency of these events is significantly higher only in spring. The rootogram confirms the model's fit and robustness (Annex II, Figure II.5).

Table 3.6 – Summary on the selection process of the predictors on Hurdle models of the rate of European catfish burst movements (Y). Predictors tested for both count and zero Hurdle (binomial) parts of the Hurdle model are presented, as well as the distribution used for the count part – Negative Binomial (NB) and Poisson. The Akaike Information Criterion (AIC) and the Bayesian Information Criterion (BIC) are also presented for each of the fitted models.

Model ID		Burst Movement Hurdle Model Formula		Distribution	AIC	BIC
		Zero Hurdle	Count			
59	Y ~	mean_temp + mean_flow + Period + Season	mean_temp + mean_flow + Period + Season	Poisson	21889.20	22015.55
62	Y ~	mean_temp + mean_flow + mean_depth + Period + Season	mean_temp + mean_flow + mean_depth + Period + Season	Poisson	21889.13	22029.53
25	Y ~	mean_depth + Period + Season	mean_depth + Period + Season	NB	21782.72	21902.06
15	Y ~	Period + Season	period + Season	NB	21779.80	21885.10
29	Y ~	mean_temp + mean_depth + Period + Season	mean_temp + mean_depth + Period + Season	NB	21768.41	21901.79
21	Y ~	mean_temp + Period + Season	mean_temp + Period + Season	NB	21766.95	21886.28
30	Y ~	mean_flow + mean_depth + Period + Season	mean_flow + mean_depth + Period + Season	NB	21754.93	21888.31
24	Y ~	mean_flow + Period + Season	mean_flow + Period + Season	NB	21753.25	21872.58
31	Y ~	mean_temp + mean_flow + mean_depth + Period + Season	mean_temp + mean_flow + mean_depth + Period + Season	NB	21736.92	21884.34

28	**Y ~**	**mean_temp + mean_flow + Period + Season**	**mean_temp + mean_flow + Period + Season**	**NB**	**21735.26**	**21868.64**

Table 3.7 – Results of the selected two-part Hurdle model (model 28) of the rate of European catfish burst movements. Predictors and model intercept for each Hurdle component (zero Hurdle and count parts) are presented with respective coefficients (Coef), standard error (Std. Error), statistic test (z value) and p-value (p).

Zero Hurdle Model Coefficients (binomial with logit link)

Logit	Coef	Std. Error	Z value	p
mean_temp	0.02144	0.01291	1.660	0.0969
mean_flow	0.00045	0.00009	5.168	0.0000
Period "Dusk"	1.06500	0.10160	10.485	0.0000
Period "Night"	0.68180	0.05426	12.566	0.0000
Period "Dawn"	0.40640	0.09663	4.206	0.0000
Season "Spring"	1.34100	0.09574	14.010	0.0000
Season "Summer"	1.12700	0.13890	8.114	0.0000
Season "Autumn"	-0.38990	0.09241	-4.219	0.0000
(Intercept)	0.07926	0.24850	0.319	0.7498

Count Model Coefficients (truncated negative binomial with log link)

NB	Coef	Std. Error	Z value	p
mean_temp	0.04005	0.00914	4.381	0.0000
mean_flow	0.00011	0.00006	1.925	0.0542
Period "Dusk"	-0.02708	0.05547	-0.488	0.6255
Period "Night"	0.16870	0.03758	4.490	0.0000
Period "Dawn"	0.13480	0.06245	2.159	0.0309
Season "Spring"	0.16330	0.07427	2.198	0.0279
Season "Summer"	-0.11670	0.10260	-1.137	0.2557
Season "Autumn"	0.02867	0.08056	0.356	0.7219
(Intercept)	-4.47600	0.14520	-30.835	0.0000

4. Discussion

This study presents the first continuous high-resolution analysis of European catfish activity and depth-use behaviour in a lotic system, offering new insights regarding riverine fish ecology. As far as can be determined from the available literature, this marks the first application of this particularly advanced radio telemetry technology in riverine fish. Utilizing data-logging transmitters equipped with temperature, pressure, and 3D-accelerometer sensors a robust dataset (with 2,177,835 observations) was obtained, despite the limited number of tagged and recaptured individuals (four out of 10). European catfish revealed year-round activity with lower values during winter and autumn and higher values during spring and summer. Seasonal differences in depth use were also evident, with fish occupying greater depths in winter and shallower habitats in summer. Circadian patterns in depth use remained stable for most of the year, except in autumn. In general, fish occupied shallower depths during the day and deeper habitats at night, reaching their peak depth at dawn. Activity peaked at dusk and was lowest during the day. Activity and depth patterns were strongly correlated with water temperature and flow, Julian Day of the year and season as well as individuals' depth in the case of activity and individuals' activity in the case of depth. This study is also the first to incorporate high-resolution activity data to comprehensively assess fish behaviour, from general activity-inactivity states to the identification of high-intensity burst movements, which are presumed to represent predatory events. These extreme activity events were primarily observed in spring at dusk and were influenced by water temperature, flow, season, and period of the day. By integrating longitudinal space use (manual tracking campaigns), vertical habitat use (pressure sensor data), and activity levels (3D-accelerometer sensors), this study provides a holistic understanding of adult European catfish habitat preferences in an invaded riverine system.

Despite some limitations encountered during this study, their impact on the overall findings was minimal. One of the primary challenges was detecting and locating individuals during tracking campaigns, as some fish reached depths (> 5 m) beyond the detection range of the radio receiver. This reduced spatial resolution and constrained the ability to accurately identify fine-scale space-use patterns. Additionally, the difficulty in recapturing tagged individuals to retrieve the multi-sensor logging transmitters resulted in a small sample size of four fish (40% of the tagged fish). Furthermore, at least two tags were expelled from the individuals, potentially contributing to the reduced sample size. However, as previously mentioned, the robust dataset with more than two million observations and the consistency between the general activity and depth patterns with previous studies conducted in the River Tagus seem to support the representativeness of the collected data.

4.1. Habitat use

European catfish generally exhibits small Home Ranges, consistently occupying littoral areas of rivers (Carol et al., 2007; Slavík et al., 2007; Brevé et al., 2014). In the lotic section of the Tagus River, Home Range areas ranged from 0.101 to 0.742 km², with a mean of 0.353 km² (median of 0.292 km²). These values were considerably lower than those reported in other non-native areas, such as the Belver Reservoir in the Tagus River, which had a mean Home Range of 1.66 km² (Ferreira, 2019; Santos, 2021). Conversely, they were higher than those recorded in native habitats, such as the Berounka River in the Czech Republic, where the mean Home Range was 0.016 km² (Slavík et al., 2007). Mid-stream linear range values ranged from 1.92 km to 10.16 km, with a mean of 4.81 km (median of 3.34 km). These values were slightly higher than those reported in other non-native environments, such as a reservoir in the Ebro River (Spain) (Carol et

al., 2007) and the Po River in Italy (Nyqvist et al., 2022), where values were mostly lower than 2 km. The differences in Home Range size may be attributed to various reasons like, variations in sample size related to tracking frequency or methodological differences in Home Range estimation, but they do not contradict the broader space use pattern that European catfish exhibits in its native range by remaining within a relatively confined area throughout the year. Additionally, the higher mid-stream linear range values could also be attributed to low detection rates, as smaller sample sizes are more susceptible to outliers. However, these elevated mid-stream linear range values could also indicate seasonal movements exceeding 10 kilometres, similar to those observed by Franquet et al. (2025) in an estuarine habitat without migration barriers. This suggests that European catfish in this study area may exhibit comparable large-scale seasonal movements, as also observed by Ferreira (2019). A high percentage of detections near river margins with dense vegetation and large tree roots suggests a strong preference for sheltered habitats. These areas likely serve as aggregation sites (Westrelin et al., 2023) or resting zones, as previously described by Carol et al. (2007).

Seasonal variations in depth use were observed, along with distinct circadian patterns in vertical movement. While median seasonal depth use remained relatively stable, winter was the season of the year with the greatest depth use, with fish typically dwelling around three metres and occasionally reaching depths up to 17 metres. This increased depth use during winter may have been driven by lower temperatures, promoting reduced activity levels and refuge behaviour, also associated with higher river flows (i.e., more stressful water currents for swimming behaviour), as indicated by the depth use models and as observed in both native (Říha et al., 2022) and non-native (Santos et al., 2025) ranges. In contrast, summer recorded the shallowest median depth, with fish generally occupying depths around 1.6 metres. A notable shift occurred from winter to spring, as median depth decreased from three metres to 1.9 metres, possibly linked to the establishment of nesting sites for reproduction (Copp et al., 2009) in shallower waters. In fact, this pattern is consistent with the peak spawning period (March-June) of the European catfish in this area (Gkenas et al., 2025). A detailed analysis of partial effect plots for season and Julian Day of the year revealed an increased depth use during summer (June-August). This behaviour may have been influenced by environmental factors not accounted for in this study, such as dissolved oxygen, or by additional ecological drivers. Moncada et al. (*in review*) observed that, in summer, European catfish prey heavily on *Chelon spp.* and *Luciobarbus spp.*, with the latter being a benthic species (Romão et al., 2017). This suggests that prey availability shift towards above mentioned species, combined with the catfish's highly opportunistic hunting behaviour (Copp et al., 2009), may explain the observed change in depth use during this period.

A study conducted in the Belver Reservoir (Tagus River) showed that between December and March, European catfish exhibited a clear daily vertical movement pattern, from deeper depths during the day to shallower depths at night (Santos et al., 2025), indicating a consistent circadian pattern throughout most of the year. However, in the lotic stretch of the Tagus River, a reversed pattern was observed from January to September, with catfish occupying deeper depths at night (≈3 m), associated with higher variation, and moving to shallower depths during the day (≈1.5 m) with comparatively lower depth range variation, with the opposite occurring in autumn, from October to December. Moncada (2024) also identified *Luciobarbus spp.* as one of the most frequently preyed-upon species in autumn by the European catfish, exhibiting a second migratory peak (after spring spawning migration) to upstream areas between October and November (Rato et al., 2024). Moreover, distinct behavioural patterns of preys can also influence circadian diurnal preference of European catfish as an opportunistic hunter as observed elsewhere (Copp et al., 2009; Boulêtreau et al., 2021). In summer, daily depth fluctuations became more pronounced, prompting European catfish to adjust their vertical movements in response to prey behaviour or habitat use change as observed by Moncada et al. (*in review*).

4.2 Activity patterns

This study demonstrated that European catfish remain active year-round, exhibiting significant seasonal variations in activity levels, likely influenced by prey availability and environmental conditions (Encina et al., 2023; Rato et al. 2024; Santos et al., 2025). The activity patterns recorded by the 3D accelerometer sensors not only align with previous studies that used longitudinal fish movements as a proxy for activity in invaded areas but also reinforce findings from Santos et al. (2025), the only other study that employed direct activity measurements.

European catfish exhibited peak activity levels during spring closely followed by summer, partially aligning with findings from Slavík et al. (2007) and Daněk et al. (2016) for native populations in Central Europe and Nyqvist et al. (2022) and Santos et al. (2025) for non-native populations in the Po River (Italy) and the Belver reservoir in the Tagus River, respectively. Although, in all the above-mentioned studies, summer had the highest levels of catfish activity, in the present study tagged individuals were slightly more active in spring than in the summer. This may be explained by findings from Moncada (2024), which identified spring as the season when European catfish had the most diverse diet in this barrier-free study area, where fish can migrate freely to the sea. During this period, catfish primarily targeted migratory fish, such as *Alosa* spp., which are more vulnerable due to their spawning behaviour and reproductive courtship (Boulêtreau et al., 2020; Boulêtreau et al., 2021). Winter activity levels in the lotic Tagus River remained relatively high, despite being lower than in warmer seasons, as also reported by Santos et al. (2025) and in contrast to Daněk et al. (2016). This suggests that even in colder months, European catfish, which has been described to start pronounced activity with temperatures between 7-12 ºC (Kuzishchin et al., 2018), remain active in the lotic section of the Tagus River whose colder water temperatures only reach 10-11ºC. This sustained activity is likely facilitated by increased foraging efficiency linked, for example, to the increased vertical exploration of the water column as seen in depth data. High river flows might also help explain the relatively high winter activity, possibly due to increased movement as supported by the activity model results and previously observed by Santos et al. (2025) and Chevallier et al. (2023). Conversely, the low river flow and decreasing water temperatures in autumn may contribute to the observed lower activity levels during this season, despite the relative warm water temperatures (≈18 ºC). During warmer months, increased activity levels correspond to rising water temperatures, which approach the species' physiological optimum of 25–27°C (Copp et al., 2009). The activity model confirms this positive relationship between water temperature and activity, consistent with previous findings in native populations (Slavík et al., 2007; Daněk et al., 2016) and non-native (Nyqvist et al., 2022; Santos et al., 2025). The highest activity levels, recorded in April 2023, coincided with peak reproduction season (Gkenas et al., 2025) as previously mentioned. Other high levels, namely in summer, recorded in August 2023 coincided with peak water temperatures (~26°C). The metabolic increase associated with these temperatures likely drives higher foraging and prey consumption (Bergé, 2012; Capra et al., 2014; Santos et al., 2025).

European catfish displayed a consistent circadian activity pattern, with overall higher nocturnal activity and reaching maximum levels at dusk, as found by Santos et al. (2025) in the Belver Reservoir. These activity peaks mostly align with diel vertical movements, where greater depth variation may be associated with foraging behaviour. Adding to this, findings from Santos et al. (2025) showed that some migratory fish are more active after sundown. Conversely, reduced daytime activity, often occurring in shallower depths, likely indicates that European catfish stay stationary in refuge areas with dense vegetation, submerged tree trunks, large stones (Carol et al., 2007) or even man-made structures like bridges, mostly near river margins.

4.3 Predatory activity

The European catfish burst movements measured in this study, acting as proxy for predatory activity, seemed to be strongly influenced by season, diel period, river flow and water temperature (Santos et al., 2025). Burst movements were significantly more likely to occur in spring, summer and autumn, in this order, compared to winter. However, while the probability of occurrence in summer did not differ significantly from winter, the frequency of extreme events—when they did occur—was notably lower than in spring. These hight burst movement levels in spring further corroborate the previously mentioned highest general activity levels (section 4.2) as well as their connection to anadromous fish (Belo et al., 2021; Collares-Pereira et al., 2021). Moreover, during the establishment of nesting sites European catfish have been known to exhibit high aggressive behaviours between males (Cech, Martin, personal communication) which could suggest that these seasonal burst movement patterns may also be linked to the establishment of spawning/nest territories, aligning with findings from Santos et al. (2025).

A clear circadian pattern was observed, with extreme movement events occurring most likely at dusk, followed by night and dawn, and least likely during the day. This supports the hypothesis that burst movements are primarily linked to predatory activity, as European catfish are known to hunt actively during nocturnal periods in their native range (Slavík et al., 2007) and during nocturnal and crepuscular periods in non-native environments (Carol et al., 2007; Nyqvist et al., 2022; Santos et al., 2025). These hunting patterns may largely be driven by increased prey activity, as seen in European eel (*Anguilla anguilla*), a frequently targeted species that overall is perceived to move during the night (Monteiro et al., 2023). However, the occurrence of burst movements during the day, albeit in a lower frequency, suggests that European catfish, despite being less active, continues to exploit opportunistic foraging strategies (Copp et al., 2009). This behaviour is evident in their predation on Iberian barbel during autumn (Moncada, 2024), which has been observed to be more active, during daylight hours (Rato et al., 2024). In fact, the declining Iberian barbel population in the Torrejón Reservoir (Spain) may be linked to sustained catfish predation, even during periods where European catfish activity levels are reduced (Encina et al., 2023). Additionally, higher river flow appears to increase the likelihood of extreme movement events, suggesting that environmental conditions may influence catfish movement, either by raising energetic swimming demands or altering prey availability that are displaced by increased flow.

5. Final remarks

As an invasive species in the Iberian Peninsula, the European catfish has had a substantial impact on freshwater ecosystems. Its large size, high fecundity, and strong predatory potential (Copp et al., 2009; Moncada, 2024; Gkenas et al., 2025) enable it to exert incredible pressure on endemic fish assemblages in the region (Encina et al., 2023). Dietary studies in the lower Tagus River (Portugal) indicate a preference for native species, including mullets (*Chelon* spp.) and barbels (*Luciobarbus* spp.), as well as endangered species such as the European eel (*Anguilla anguilla*, L., 1758) and the twaite and allis shads (*Alosa* spp.) (Moncada, 2024). This predatory behaviour poses a major ecological threat to native fish populations. If the European catfish continues to expand into Tagus tributaries or other Iberian rivers, it may further increase predation pressure on already vulnerable fish species, such as the near-threatened Iberian barbel (*Luciobarbus comizo*, Steindachner, 1864) and the endangered Lisbon-arched-mouth nase (*Iberochondrostoma olisiponense*, Gante, Santos, and Alves, 2007) (Veríssimo et al., 2018; Collares-Pereira et al., 2021). Given these ecological risks, immediate management and control measures should be implemented to prevent further expansion and mitigate the species' impact on the aforementioned freshwater species.

Firstly, to prevent the further spread of European catfish in Portugal, it is strongly recommended that competent authorities, such as the Portuguese Institute for Nature and Forests Conservation (ICNF) and the Portuguese Environmental Agency (APA) implement preventive measures to restrict its dispersal into other reservoirs and hydrographic basins. Currently, this species is confirmed mostly in the main stems of the Tagus and Douro Rivers (Gago et al., 2016; Gkenas et al., 2023). Recreational anglers are the primary vector for the introduction of this species into non-native waters across the Iberian Peninsula (Gago et al., 2016; Gkenas et al., 2023). Many European catfish anglers perceive the species as having no negative impact on local fish communities and commonly practice catch and release, even when illegal, as observed in southern Germany (Fromherz et al., 2024), and in Portugal where one in two anglers release individuals back to the water, upon capture even though it is also illegal (Gago et al., 2025). To mitigate these risks, it is essential to increase angler awareness through educational outreach initiatives highlighting the threats European catfish pose to native fish communities and their potential impact on the abundance of other recreationally important species (Banha et al., 2024; Gago et al., 2025). This effort can be supported by findings from this study, which demonstrate the species' highly opportunistic behaviour. Encouraging a joint approach that actively incorporates anglers' perspectives may help in shaping effective management strategies. By addressing misconceptions and highlighting ecological consequences, anglers may be discouraged from translocating catfish to new river systems or releasing captured individuals, thereby reducing further introductions and limiting the species' spread.

Secondly, since European catfish is well established in the region, population control is of utmost importance in order to reduce its impact (Vejřík et al., 2024; Moncada, 2024; Rivaes et al., *in review*). While previous work has been done to study and understand this species ecology and behaviour in reservoirs (Santos et al., 2025), so as to improve and develop strategies for population control, this work adds crucial information on how to replicate the control actions on lotic stretches, increasing the spatial/temporal effectiveness of removal actions, maximizing the capture of individuals (Vejřík et al., 2024). Considering results from this work it is proposed that removal efforts in the lotic Tagus River should focus on spring and summer (particularly from April to June) and, for maximal effectiveness, gill nets and/or longlines should be deployed in areas with dense vegetation during the day so as to catch the fish after sundown and night when European catfish is more active. In these seasons, the fishing gear should aim for depths ranging from 3 to 1.5 metres.

In Vejřík et al. (2024), long-lines were efficient in capturing catfish, proving cost-effective and technically undemanding, requiring an average of 5.6 bait fish to catch one European catfish per day, and outperforming other techniques. This method has also shown to be highly selective, producing a very low rate of bycatch in non-native areas (Castro, B. personal observation), which can be helpful when fishing in areas composed of highly singular fish assemblages with several high-value fish (mostly migratory species), as this one.

Accompanying the above-mentioned measures it also important to mention that, in its native range, European catfish is highly valued as both a trophy species and a culinary delicacy. It is described as highly palatable and has even been the subject of research on optimal aquaculture practices (Linhart et al., 2002). However, in non-native areas, large catfish are often released under the false assumption that they are inedible, contributing to their continued establishment and expansion (Fromherz et al., 2024). Similarly, the Indo-Pacific lionfish, an invasive marine fish, has been successfully integrated into commercial harvest strategies (Blakeway et al., 2021). This could also be a solution applied to European catfish. Research on lionfish has demonstrated that public perception, environmental concern, and educational outreach significantly influence willingness to consume the species (Blakeway et al., 2021). Moreover, in the south of Portugal, increased awareness of the invasive Weakfish (*Cynoscion regalis*, Bloch & Schneider, 1801) through a substantial media push has already yielded a 90% positive response regarding its introduction into consumers' diets (Cerveira et al., 2022). Following this model, ongoing research is exploring the feasibility of integrating European catfish into both the food industry and livestock feed production (Gago, personal communication). By increasing its commercial value, European catfish could become a more attractive target for consumption, thereby reducing catch-and-release rates among anglers and mitigating its ecological impact. Other measures like specific fishing competitions are also being implemented and funded by Fundo Ambiental (Gago, personal communication).

Further research is needed to expand knowledge and understanding on European catfish behaviour. Future studies should incorporate controlled laboratory experiments with constant video monitoring to increase accuracy in linking the 3D accelerometer records with specific behaviours. Additionally, a sample size increase on this studies' radio-tracking component would enhance the robustness of spatial and behavioural analyses, providing a more comprehensive assessment of the species' movement patterns and habitat use in this region. Furthermore, to optimize tagging success, future procedures should position incisions more laterally, allowing musculature to prevent tag expulsion and improve retention. Given the species' preference for anadromous prey and recent vast seasonal distance travelled in estuarine habitats (Franquet et al., 2025), future research should also explore activity and depth use in areas with tidal influence. Finally, studies employing predation tags (tags implanted on potential prey species that when consumed start sending a distinct acoustic signal indicating a predatory event), similar to the research conducted in Southwestern France by Boulêtreau et al. (2020), could provide valuable insights into predator-prey interactions, further advancing knowledge on the trophic dynamics of this invasive species.

References

Aguiar, F., & Ferreira, M. (2005). Human-disturbed landscapes: Effects on composition and integrity of riparian woody vegetation in the Tagus River basin, Portugal. *Environmental Conservation, 32*(1), 30–41. https://doi.org/10.1017/S0376892905001992

Anastácio, P., Ribeiro, F., Capinha, C., Banha, F., Gama, M., Filipe, A., Rebelo, R., & Sousa, R. (2019). Non-native freshwater fauna in Portugal: A review. *Science of the Total Environment, 650*(2), 1923–1934. https://doi.org/10.1016/j.scitotenv.2018.09.251

Banha, F., Gago, J., Margalejo, D., Feijão, J., Casals, F., Anastácio, P. M., & Ribeiro, F. (2024). Angler's preferences, perceptions and practices regarding non-native freshwater fish. *Reviews in Fish Biology and Fisheries*, *34*(1), 385–404. https://doi.org/10.1007/s11160-023-09819-x

Bellard, C., Genovesi, P., & Jeschke, J. M. (2016). Global patterns in threats to vertebrates by biological invasions. *Proceedings of the Royal Society B: Biological Sciences, 283*(1823), 20152454. https://doi.org/10.1098/rspb.2015.2454

Belo, A. F., Cardoso, G., Pereira, E., Quintella, B. R., Mateus, C. S., Alexandre, C. M., Batista, C., Telhado, A., Quadrado, M. F., & Almeida, P. R. (2021). Fish pass use by shads (*Alosa alosa* L. and *Alosa fallax* [Lacépède, 1803]): Implications for monitoring and management. *Ecohydrology*. https://doi.org/10.1002/eco.2292

Benejam, L., Carol, J., Alcaraz, C., García-Berthou, E., & Zamora, L. (2007). On the spread of the European catfish (*Silurus glanis*) in the Iberian Peninsula: First record in the Llobregat river basin. *Limnetica, 26*(1), 169–171. https://doi.org/10.23818/limn.26.14

Bergé, J. (2012). *Apport de la télémétrie acoustique pour la compréhension de l'utilisation dynamique des habitats par les poissons dans un grand fleuve aménagé, le Rhône* (Doctoral dissertation, Irstea, Université Lyon 1).

Bernery, C., Bellard, C., Courchamp, F., Brosse, S., Gozlan, R. E., Jarić, I., Teletchea, F., & Leroy, B. (2022). Freshwater fish invasions: A comprehensive review. *Annual Review of Ecology, Evolution, and Systematics, 53*(1), 427–456. https://doi.org/10.1146/annurev-ecolsys-032522-015551

Blackburn, T. M., Bellard, C., & Ricciardi, A. (2019). Alien versus native species as drivers of recent extinctions. *Frontiers in Ecology and the Environment, 17*(4), 203–207. https://doi.org/10.1002/fee.2020

Blakeway, R. D., Ross, A. D., & Jones, G. A. (2021). Insights from a Survey of Texas Gulf Coast Residents on the Social Factors Contributing to Willingness to Consume and Purchase Lionfish. *Sustainability, 13*(17), 9621. https://doi.org/10.3390/su13179621

Boulêtreau, S., & Santoul, F. (2016). The end of the mythical giant catfish. *Ecosphere, 7*(11), e01606. https://doi.org/10.1002/ecs2.1606

Boulêtreau, S., Carry, L., Meyer, E., Filloux, D., Menchi, O., Mataix, V., & Santoul, F. (2020). High predation of native sea lamprey during spawning migration. Scientific Reports, *10*(6122). https://doi.org/10.1038/s41598-020-62916-w

Boulêtreau, S., Fauvel, T., Laventure, M., Delacour, R., Bouyssonnié, W., Azémar, F., & Santoul, F. (2021). "The giants' feast": Predation of the large introduced European catfish on spawning migrating allis shads. *Aquatic Ecology*, 55, 1–9. https://doi.org/10.1007/s10452-020-09811-8

Brevé, N. W. P., Verspui, R., de Laak, G. A. J., Bendall, B., Breukelaar, A. W., & Spierts, I. L. Y. (2014). Explicit site fidelity of European catfish (*Silurus glanis*, L., 1758) to man-

made habitat in the River Meuse, Netherlands. *Journal of Applied Ichthyology, 30*(3), 472–478. https://doi.org/10.1111/jai.12408

Brewster, L. R., Cahill, B. V., Burton, M. N., Dougan, C., Herr, J. S., Norton, L. I., McGuire, S. A., Pico, M., Urban-Gedamke, E., Bassos-Hull, K., Tyminski, J. P., Hueter, R. E., Wetherbee, B. M., Shivji, M., Burnie, N., & Ajemian, M. J. (2021). First insights into the vertical habitat use of the whitespotted eagle ray Aetobatus narinari revealed by pop-up satellite archival tags. *Journal of fish biology*, *98*(1), 89–101. https://doi.org/10.1111/jfb.14560

Brown, R. S., Cooke, S. J., Anderson, W. G., & McKinley, R. S. (1999). Evidence to challenge the "2% rule" for biotelemetry. *North American Journal of Fisheries Management, 19*(3), 867–871. https://doi.org/10.1577/1548-8675(1999)019<0867:ETCTRF>2.0.CO;2

Capra, H., Pella, H., & Ovidio, M. (2014, June). Movements of endemic and exotic fish in a large river ecosystem (Rhône, France). In *Proceedings of the 10th International Conference on Ecohydraulics*, Trondheim, Norway

Capra, H., Pella, H., & Ovidio, M. (2018). Individual movements, home ranges and habitat use by native rheophilic cyprinids and non-native catfish in a large regulated river. *Fisheries Management and Ecology, 25*(1), 1–14. https://doi.org/10.1111/fme.12272

Capra, H., Plichard, L., Bergé, J., Pella, H., Ovidio, M., McNeil, E., & Lamouroux, N. (2017). Fish habitat selection in a large hydropeaking river: Strong individual and temporal variations revealed by telemetry. *Science of the Total Environment, 578*, 109–120. https://doi.org/10.1016/j.scitotenv.2016.10.155

Carol, J., Benejam, L., Benito, J., & García-Berthou, E. (2009). Growth and diet of European catfish (*Silurus glanis*) in early and late invasion stages. *Fundamental and Applied Limnology*, *174*(4), 317–328. https://doi.org/10.1127/1863-9135/2009/0174-0317

Carol, J., Zamora, L., & García-Berthou, E. (2007). Preliminary telemetry data on the movement patterns and habitat use of European catfish (*Silurus glanis*) in a reservoir of the River Ebro, Spain. *Ecology of Freshwater Fish, 16*(4), 450–456. https://doi.org/10.1111/j.1600-0633.2007.00235.x

Carpenter, S. R., Stanley, E. H., & Vander Zanden, M. J. (2011). State of the world's freshwater ecosystems: Physical, chemical, and biological changes. *Annual Review of Environment and Resources, 36*(1), 75–99. https://doi.org/10.1146/annurev-environ-021810-094524

Cerveira, I., Baptista, V., Teodósio, M. A., & Morais, P. (2022). What's for dinner? Assessing the value of an edible invasive species and outreach actions to promote its consumption. *Biological Invasions, 24*(3), 815–829. https://doi.org/10.1007/s10530-021-02685-3

Chevallier, E., Denys, G. P. J., Marlot, R., Duntze, M., Mierral, A., Fasquel, A., Maël Dhainaut, & Julien Boucault. (2023). Behaviour of two predator fishes *Esox lucius* Linnaeus, 1758 and *Silurus glanis* Linnaeus, 1758 during two successive floods in the French Aisne River. *Cybium: Revue Internationale d'Ichtyologie, 47*(1), 79–99. https://doi.org/10.26028/cybium/2023-471-007

Clavero, M., Hermoso, V., Aparicio, E., & Godinho, F. N. (2013). Biodiversity in heavily modified waterbodies: Native and introduced fish in Iberian reservoirs. *Freshwater Biology, 58*(6), 1190–1201. https://doi.org/10.1111/fwb.12120

Collares-Pereira, M. J., Alves, M. J., Ribeiro, F., Domingos, I., Almeida, P. R., Costa, L., Gante, H., Filipe, A. F., Aboim, M. A., Rodrigues, P. M., & Magalhães, M. F. (2021). *Guia dos Peixes de água doce e migradores de Portugal Continental* (2nd ed.). Edições Afrontamento. http://hdl.handle.net/10174/32043

Cooke, S. J., Midwood, J. D., Thiem, J. D., Klimley, P., Lucas, M. C., Thorstad, E. B., Eiler, J., Holbrook, C., & Ebner, B. C. (2013). Tracking animals in freshwater with electronic tags: past, present and future. *Animal Biotelemetry*, *1*(1), 5. https://doi.org/10.1186/2050-3385-1-5

Copp, G., Britton, J., Cucherousset, J., García-Berthou, E., Kirk, R., Peeler, E., & Stakėnas, S. (2009). Voracious invader or benign feline? A review of the environmental biology of European 25 catfish *Silurus glanis* in its native and introduced ranges. *Fish and Fisheries*, *10*(3), 252–282. https://doi.org/10.1111/j.1467-2979.2008.00321.x

Costa, M. J., Duarte, G., Segurado, P., & Branco, P. (2021). Major threats to European freshwater fish species. *Science of the Total Environment, 797*, 149105. https://doi.org/10.1016/j.scitotenv.2021.149105

Cucherousset, J., Bouletreau, S., Azemar, F., Compin, A., & Guillaume, M. (2012). "Freshwater Killer Whales": Beaching behaviour of an alien fish to hunt land birds. *PLoS ONE, 7*(12), e50840. https://doi.org/10.1371/journal.pone.0050840

Cucherousset, J., Horky, P., Slavík, O., Ovidio, M., Arlinghaus, R., Boulêtreau, S., Britton, R., García- Berthou, E., & Santoul, F. (2018). Ecology, behaviour and management of the European catfish. *Reviews in Fish Biology and Fisheries*, *28*, 177–190. https://doi.org/10.1007/S11160 017-9507-9

Daněk, T., Horký, P., Kalous, L., Filinger, K., Břicháček, V., & Slavík, O. (2016). Seasonal changes in diel activity of juvenile European catfish *Silurus glanis* (Linnaeus, 1758) in Byšická Lake, Central Bohemia. *Journal of Applied Ichthyology, 32*(6), 1093–1098. https://doi.org/10.1111/jai.13146

Daněk, T., Kalous, L., Petryl, M., & Horký, P. (2014). Move or die: Change in European catfish (*Silurus glanis* L.) behaviour caused by oxygen deficiency. *Knowledge and Management of Aquatic Ecosystems, 414*, 08. https://doi.org/10.1051/kmae/2014030

Doadrio, I. (Ed.). (2001). *Atlas y libro rojo de los peces continentales de España* [Atlas and Red Book of Spain's Freshwater Fish]. Consejo Superior de Investigaciones Científicas (CSIC) & Ministerio de Medio Ambiente. https://www.researchgate.net/profile/Ignacio-Doadrio/publication/248658934_Atlas_y_Libro_Rojo_de_Los_Pesces_Continentales_de_Espana/links/5853a3bf08ae95fd8e1d86bc/Atlas-y-Libro-Rojo-de-Los-Pesces-Continentales-de-Espana.pdf

Doherty, T. S., Glen, A. S., Nimmo, D. G., Ritchie, E. G., & Dickman, C. R. (2016). Invasive predators and global biodiversity loss. *Proceedings of the National Academy of Sciences of the United States of America*, *113*(40), 11261–11265. https://doi.org/10.1073/pnas.1602480113

Dudgeon, D., Arthington, A. H., Gessner, M. O., Kawabata, Z., Knowler, D. J., Lévêque, C., Naiman, R. J., Prieur-Richard, A. H., Soto, D., Stiassny, M. L., & Sullivan, C. A. (2006). Freshwater biodiversity: importance, threats, status and conservation challenges. *Biological reviews of the Cambridge Philosophical Society*, *81*(2), 163–182. https://doi.org/10.1017/S1464793105006950

Elvira, B., & Almodóvar, A. (2001). Freshwater fish introductions in Spain: Facts and figures at the beginning of the 21st century. *Journal of Fish Biology, 59*(Suppl. A), 323–331. https://doi.org/10.1111/j.1095-8649.2001.tb01393.x

Encina, L., Rodríguez-Ruiz, A., & Granado-Lorencio, C. (2006). The Iberian ichthyofauna: Ecological contributions. *Limnetica, 25*(1–2), 349–368. https://doi.org/10.23818/limn.25.24

Encina, L., Rodríguez-Ruiz, A., Orduna, C., Cid, J. R., Ilaria, D.M., & Granado-Lorencio, C. (2023). Impact of invasive European catfsh (Silurus glanis) on the fish community of

Torrejón reservoir (Central Spain) during a 11-year monitoring study. *Biological Invasions, 26*(3), 745–756. https://doi.org/10.1007/s10530-023-03204-2

Ferreira, M. (2019). European catfish (S*ilurus glanis*) movements and diet ecology in a newly established population in the Tagus drainage [Universidade de Lisboa]. http://hdl.handle.net/10451/40493

Franquet, S., Verhelst, P., Bervoets, L., Baeyens, R., Vermeersch, S., Schoelynck, J., Van den Neucker, T., & Pauwels, I. (2025). Large-scale movement patterns of European catfish (*Silurus glanis* L.) in the Scheldt River basin, Belgium. *Journal of Fish Biology*. https://doi.org/10.1111/jfb.16066

Frate, L. (2022). *Home-range analysis through Kernel Density Estimation in QGIS (Version 3.16)* [QGIS model]. GitHub. https://github.com/ludovico85/Home-range-analysis-through-Kernel-Density-Estimation-in-QGIS

Fromherz, M., Baer, J., Roch, S., Geist, J., & Brinker, A. (2024). Characterization of specialist European catfish anglers in southern Germany: Implications for future management. *Fisheries Research, 279*, 107144–107144. https://doi.org/10.1016/j.fishres.2024.107144

Gago, J., Anastácio, P., Gkenas, C., Banha, F., & Ribeiro, F. (2016). Spatial distribution patterns of the non-native European catfish, *Silurus glanis*, from multiple online sources – A case study for the River Tagus (Iberian Peninsula). *Fisheries Management and Ecology, 23*(6), 503–509. https://doi.org/10.1111/fme.12189

Gago, J., Rivaes, R., Ribeiro, D., Dias, D., Castagné, P., Santoul, F., & Ribeiro, F. (2025). Anglers' perceptions about European catfish *Silurus glanis* in a newly invaded region. *Preprints*. https://doi.org/10.20944/preprints202502.0420.v1

Gkenas, C., Gago, J., Mesquita, N., Alves, M. J., & Ribeiro, F. (2015). First record of Silurus glanis Linnaeus, 1758 in Portugal (Iberian Peninsula). *Journal of Applied Ichthyology, 31*(4), 756 - 758. https://doi.org/10.1111/jai.12806.

Gkenas, C., Martelo, J., Ribeiro, D., Gago, J., Santos, G., Dias, D., & Ribeiro, F. (2023). Westwards expansion of the European catfish *Silurus glanis* in the Douro River (Portugal). *Limnetica, 43*(1). https://doi.org/10.23818/limn.43.01

Gkenas, C., Sequeira, V., Ribeiro, D., Gago, J., Dias, D., Verma, C. R., Kumkar, P., & Ribeiro, F. (2025). Reproductive traits of the European catfish (*Silurus glanis*) during the early stages of invasion. *Journal of Vertebrate Biology, 74*(24122). https://doi.org/10.25225/jvb.24122

Gozlan, R. E. (2008). Introduction of non-native freshwater fish: Is it all bad? *Fish and Fisheries, 9*(1), 106–115. https://doi.org/10.1111/j.1467-2979.2007.00267.x

Haubrock, P. J., Bernery, C., Cuthbert, R. N., Liu, C., Kourantidou, M., Leroy, B., Turbelin, A. J., Kramer, A. M., Verbrugge, L. N. H., Diagne, C., Courchamp, F., & Gozlan, R. E. (2022). Knowledge gaps in economic costs of invasive alien fish worldwide. *Science of the Total Environment, 803,* 149875. https://doi.org/10.1016/j.scitotenv.2021.149875

Haubrock, P. J., Cuthbert, R. N., & Haase, P. (2023). Long-term trends and drivers of biological invasion in Central European streams. *Science of the Total Environment, 876,* 162817. https://doi.org/10.1016/j.scitotenv.2023.162817

Haubrock, P. J., Turbelin, A. J., Cuthbert, R. N., Novoa, A., Taylor, N. G., Angulo, E., Ballesteros-Mejia, L., Bodey, T. W., Capinha, C., Diagne, C., Essl, F., Golivets, M., Kirichenko, N., Kourantidou, M., Leroy, B., Renault, D., Verbrugge, L., & Courchamp, F. (2021). Economic costs of invasive alien species across Europe. *NeoBiota, 67*, 153–190. https://doi.org/10.3897/neobiota.67.58196

Hermoso, V., Clavero, M., Blanco-Garrido, F., & Prenda, J. (2011). Invasive species and habitat degradation in Iberian streams: An analysis of their role in freshwater fish diversity loss. *Ecological Applications*, *21*(1), 175–188. https://doi.org/10.1890/09-2011.1

Hoef, J. M., & Boveng, P. L. (2007). 'Quasi-Poisson vs. negative binomial regression: How should we model overdispersed count data?'. *Ecology, 88*(11), 2766–2772. https://doi.org/10.1890/07-0043.1

Hussey, N. E., Kessel, S. T., Aarestrup, K., Cooke, S. J., Cowley, P. D., Fisk, A. T., Harcourt, R. G., Holland, K. N., Iverson, S. J., Kocik, J. F., Flemming, J. M., & Whoriskey, F. G. (2015). Aquatic animal telemetry: A panoramic window into the underwater world. *Science, 348*(6240). https://doi.org/10.1126/science.1255642

Intergovernmental Science-Policy Platform on Biodiversity and Ecosystem Services (IPBES). (2019). *Global assessment report on biodiversity and ecosystem services: Summary for policymakers*. IPBES Secretariat. https://doi.org/10.5281/zenodo.3553579

Intergovernmental Science-Policy Platform on Biodiversity and Ecosystem Services (IPBES). (2023). *Assessment report on invasive alien species and their control*. IPBES Secretariat. https://www.ipbes.net/IASmediarelease

Invasive Species Specialist Group (ISSG). (2015). *The Global Invasive Species Database* (Version 2015.1). International Union for Conservation of Nature. http://www.iucngisd.org/gisd/

Kay, W. R. (2004). Movements and home ranges of radio-tracked *Crocodylus porosus* in the Cambridge Gulf region of Western Australia. *Wildlife Research*, *31*(5), 495–508. https://doi.org/10.1071/WR04037

Kleiber, C., & Zeileis, A. (2016). Visualizing Count Data Regressions Using Rootograms. *American Statistician, 70*(3), 296–303. https://doi.org/10.1080/00031305.2016.1173590

Kuzishchin, K. V., Gruzdeva, M. A., & Pavlov, D. S. (2018). Traits of Biology of European Wels Catfish *Silurus glanis* from the Volga–Ahtuba water system, the Lower Volga. *Journal of Ichthyology, 58*(6), 833–844. https://doi.org/10.1134/S0032945218060103

Leprieur, F., Beauchard, O., Blanchet, S., Oberdorff, T., & Brosse, S. (2008). Fish Invasions in the World's River Systems: When Natural Processes are Blurred by Human Activities. *PLoS Biology, 6*(2), e28. https://doi.org/10.1371/journal.pbio.0060028

Lewis, M. A., Petrovskii, S. V., & Potts, J. R. (2016). Dynamics of biological invasions. In M. A. Lewis, S. V. Petrovskii, & J. R. Potts (Eds.), *The mathematics behind biological invasions* (pp. 19–68). Springer International Publishing. https://doi.org/10.1007/978-3-319-33922-1

Lindell, N. (2021). *Habitat preference and activity pattern of wels catfish (Silurus glanis) at its northernmost distribution area* (PhD Thesis).

Linhart, O., Štěch, L., Švarc, J., Rodina, M., Audebert, J. P., Grecu, J., & Billard, R. (2002). The culture of the European catfish, *Silurus glanis*, in the Czech Republic and in France. *Aquatic Living Resources, 15*(2), 139–144. https://doi.org/10.1016/S0990-7440(02)01153-1

Lodge, D. M. (1993). Biological invasions: Lessons for ecology. *Trends in Ecology & Evolution, 8*(4), 133-137. https://doi.org/10.1016/0169-5347(93)90025-K

Marra, G., & Wood, S. N. (2011). Practical variable selection for generalized additive models. *Computational Statistics and Data Analysis, 55*(7), 2372–2387. https://doi.org/10.1016/j.csda.2011.02.004

Martelo, J., da Costa, L. M., Ribeiro, D., Gago, J., Magalhães, M. F., Gante, H. F., Alves, M. J., Cheoo, G., Gkenas, C., Banha, F., Gama, M., Anastácio, P. M., Tiago, P. M., & Ribeiro, F. (2021). Evaluating the range expansion of recreational non-native fishes in

Portuguese freshwaters using scientific and citizen science data. *BioInvasions Records, 10*(2), 378–389. https://doi.org/10.3391/bir.2021.10.2.16

Millennium Ecosystem Assessment. (2005). *Ecosystems and human well-being: Biodiversity synthesis*. World Resources Institute. https://www.millenniumassessment.org/documents/document.354.aspx.pdf

Moncada, M. (2024). Catfished: how metabarcoding diet analysis increases knowledge on predation by the invasive *Silurus glanis* [Universidade de Lisboa]. http://hdl.handle.net/10451/64472

Monteiro, R. M., Domingos, I., Almeida, P. R., Costa, J. L., Pereira, E., Belo, A. F., Portela, T., Telhado, A., Quintella, B. R. (2023). Upstream movement of juvenile eels (*Anguilla anguilla* L.) in a southwestern European river. *Environmental Biology of Fishes, 106*, 1313–1325. https://doi.org/10.1007/s10641-023-01417-x

Myers, N., Mittermeier, R. A., Mittermeier, C. G., da Fonseca, G. A. B., & Kent, J. (2000). Biodiversity hotspots for conservation priorities. *Nature, 403*(6772), 853–858. https://doi.org/10.1038/35002501

Nyqvist, D., Calles, O., Forneris, G., & Comoglio, C. (2022). Movement and activity patterns of non-native Wels catfish (*Silurus glanis* Linnaeus, 1758) at the Confluence of a Large River and its Colder Tributary. *Fishes*, *7*(6), 325. https://doi.org/10.3390/fishes7060325

Olden, J. D., Kennard, M. J., Leprieur, F., Tedesco, P. A., Winemiller, K. O., & García-Berthou, E. (2010). Conservation biogeography of freshwater fishes: recent progress and future challenges. *Diversity and Distributions*, *16*(3), 496–513. https://doi.org/10.1111/j.1472-4642.2010.00655.x

Ovidio, M., Baras, E., Goffaux, D., Birtles, C., & Philippart, J. C. (2002). Seasonal variations of activity pattern of brown trout (*Salmo trutta*) in a small stream, as determined by radio-telemetry. *Hydrobiologia, 470*(1), 195–202. https://doi.org/10.1023/A:1015625500918

Panfili, J., Nicolas, D., Diop, K., & Crivelli, A. (2024). Life-history traits of the invasive and biggest European freshwater fish, the wels catfish (*Silurus glanis*), show high potential for colonisation in Southern Europe. *Marine and Freshwater Research, 75*, MF24187. https://doi.org/10.1071/MF24187

Rahel, F. J. (2007). Biogeographic barriers, connectivity, and homogenization of freshwater faunas: It's a small world after all. *Freshwater Biology*, *52*(4), 696–710. https://doi.org/10.1111/j.1365-2427.2006.01708.x

Rato, A. S., Alexandre, C. M., Pedro, S., Mateus, C. S., Pereira, E., Belo, A. F., Quintella, B. R., Quadrado, M. F., Telhado, A., Batista, C., & Almeida, P. R. (2024). New evidence of alternative migration patterns for two Mediterranean potamodromous species. *Scientific Reports, 14*(1), 23910. https://doi.org/10.1038/s41598-024-74959-4

Rees, A., Britton, R., Godard, M., Crooks, N., Miller, J., Wesley, K., & Copp, G. (2013). Efficacy of tagging European catfish *Silurus glanis* (L., 1758) released into ponds. *Journal of Applied Ichthyology, 30*(1), 127–129. https://doi.org/10.1111/jai.12254

Ribeiro, F., Collares-Pereira, M. J., & Moyle, P. B. (2009). Non-native fish in the fresh waters of Portugal, Azores & Madeira Islands: A growing threat to aquatic biodiversity. *Fisheries Management and Ecology, 16*(4), 255–264. https://doi.org/10.1111/j.1365-2400.2009.00659.x

Říha, M., Rabaneda-Bueno, R., Jarić, I., Souza, A., Vejřík, L., Draštík, V., Blabolil, P., Holubová, M., Jůza, T., Gjelland, K., Rychtecký, P., Sajdlová, Z., Kočvara, L., Tušer, M., Prchalová, M., Šeda, J., & Peterka, J. (2022). Seasonal habitat use of three

predatory fishes in a freshwater ecosystem. *Hydrobiologia, 849*(15), 3351–3371. https://doi.org/10.1007/s10750-022-04938-1

Říha, M., Rabaneda-Bueno, R., Vejřík, L., Jarić, I., Prchalová, M., Šmejkal, M., Čech, M., Draštík, V., Blabolil, P., Holubová, M., Jůza, T., Gjelland, K. Ø., Sajdlová, Z., Kočvara, L., & Tušer, M. (2024). Hungry catfish – effect of prey availability on movement dynamics of a top predator. *BioRxiv (Cold Spring Harbor Laboratory)*. https://doi.org/10.1101/2024.08.30.610378

Romão, F., Quaresma, A. L., Branco, P., Santos, J. M., Amaral, S., Ferreira, M. T., Katopodis, C., & Pinheiro, A. N. (2017). Passage performance of two cyprinids with different ecological traits in a fishway with distinct vertical slot configurations. *Ecological Engineering, 105*, 180–188. https://doi.org/10.1016/j.ecoleng.2017.04.031

Rosete, J., Lameirinhas, A., & Corley, M. F. (2019). The Moths of Constância (Ribatejo, Portugal) - a brief sampling (Insecta: Lepidoptera). *SHILAP Revista de lepidopterología*, *47*(187), 519–533. https://doi.org/10.57065/shilap.548.

Sabater, S., Muñoz, I., Feio, M. J., Romaní, A. M., & Graça, M. A. (2009). Chapter 4—Iberian Rivers. In Rivers of Europe (pp. 113–149). Academic Press.

Santos, G. (2021). Activity patterns and tridimensional space use by the European catfish (Silurus glanis) in Belver reservoir [Universidade de Lisboa]. https://repositorio.ul.pt/bitstream/10451/51885/1/TM_Gil_Santos.pdf

Santos, G. S., Ribeiro, F., Pereira, E., Silva, A. F., Almeida, P. R., Ribeiro, D., & Quintella, B. R. (2025). Behaviour of the apex predator European catfish (*Silurus glanis*) on a recently invaded reservoir. *Ecology of Freshwater Fish, 34*, e12817. https://doi.org/10.1111/eff.12817

Seaman, D. E., Millspaugh, J. J., Kernohan, B. J., Brundige, G. C., Raedeke, K. J., & Gitzen, R. A. (1999). Effects of Sample Size on Kernel Home Range Estimates. *Journal of Wildlife Management, 63*(2), 739–747. https://doi.org/10.2307/3802664

Seaman, D. E., & Powell, R. A. (1996). An evaluation of the Accuracy of Kernel Density Estimators for Home Range Analysis. *Ecology, 77*(7), 2075–2085. https://doi.org/10.2307/2265701

Silverman, B. W. (1986). *Density Estimation for Statistics and Data Analysis*. Springer US. https://doi.org/10.1007/978-1-4899-3324-9

Simberloff, D., Martin, J.-L., Genovesi, P., Maris, V., Wardle, D. A., Aronson, J., Courchamp, F., Galil, B., García-Berthou, E., Pascal, M., Pyšek, P., Sousa, R., Tabacchi, E., & Vilà, M. (2013). Impacts of biological invasions: What's what and the way forward. *Trends in Ecology & Evolution*, *28*(1), 58–66. https://doi.org/10.1016/j.tree.2012.07.013

Slavík, O., Horký, P., Bartoš, L., Kolářová, J., & Randák, T. (2007). Diurnal and seasonal behaviour of adult and juvenile European catfish as determined by radio-telemetry in the River Berounka, Czech Republic. *Journal of Fish Biology, 71*(1), 101–114. https://doi.org/10.1111/j.1095-8649.2007.01529.x

Slavík, O., Horký, P., & Závorka, L. (2014). Energy cost of European Catfish Space Use as Determined by Biotelemetry. *PLoS ONE, 9*(6), e98997. https://doi.org/10.1371/journal.pone.0098997

Strayer, D., & Dudgeon, D. (2010). Freshwater biodiversity conservation: Recent progress and future challenges. *Journal of the North American Benthological Society, 29*(1), 344-358. https://doi.org/10.1899/08-171.1

Vejřík, L., Vejříková, I., Blabolil, P., Bartoň, D., Sajdlová, Z., Kočvara, L., Peterka, J., Muška, M., Duras, J., Jůza, T., Ribeiro, F., Rivaes, R. P., Ribeiro, D., Cordeiro, M. M., Castro, B., & Čech, M. (2024). Long-lines for research monitoring and efficient population

regulation of an invasive apex predator, European catfish (*Silurus glanis*). *Heliyon, 10*(14), e34125. https://doi.org/10.1016/j.heliyon.2024.e34125

Vejřík, L., Vejříková, I., Blabolil, P., Eloranta, A., Kočvara, L., Peterka, J., Sajdlová, Z., The Chung, S. H., Šmejkal, M., Kiljunen, M., & Čech, M. (2017). European catfish (Silurus glanis) as a freshwater apex predator drives ecosystem via its diet adaptability. Scientific Reports, 7(1). https://doi.org/10.1038/s41598-017-16169-9

Veríssimo, A., Gante, H., Santos, C., Cheoo, G., Oliveira, J., Cereja, R., & Ribeiro, F. (2018). Distribution and demography of the critically endangered Lisbon arched-mouth nase, *Iberochondrostoma olisiponense*. *Fishes in Mediterranean Environments, 2018.* https://doi.org/10.29094/FiSHMED.2018.002

Verreycken, H., Anseeuw, D., Van Thuyne, G., Quataert, P., & Belpaire, C. (2007). The non-indigenous freshwater fishes of Flanders (Belgium): review, status, and trends over the last decade. *Journal of Fish Biology, 71,* (Supplement D), 160–172. https://doi.org/10.1111/j.1095-8649.2007.01679.x

Vide, J., Martin-Moreta, P., López-Querol, S., Machado, M., & Benito, G. (2002, October). TAGUS RIVER: Historical floods at Talavera de la Reina. In V. R. Thorndycraft, G. Benito, M. Barriendos, & M. C. Llasat (Eds.), *Palaeofloods, historical floods and climatic variability: Applications in flood risk assessment*. PHEFRA Workshop.

Vitousek, P. M., D'Antonio, C. M., Loope, L. L., Rejmanek, M., & Westbrooks, R. G. (1996). Introduced species: A significant component of human-caused global change. *New Zealand Journal of Ecology, 21,* 1-16.

Westrelin, S., Moreau, M., Fourcassié, V., & Santoul, F. (2023). Overwintering aggregation patterns of European catfish *Silurus glanis*. *Movement Ecology, 11*(9). https://doi.org/10.1186/s40462-023-00373-6

Winter, J. D. (1983). Underwater biotelemetry. In L. A. Nielsen & D. L. Johnson (Eds.), *Fisheries techniques* (pp. 371–395). American Fisheries Society.

Wood, S. N. (2008). Fast stable direct fitting and smoothness selection for generalized additive models. *Journal of the Royal Statistical Society: Series B (Statistical Methodology), 70*(3), 495–518. https://doi.org/10.1111/j.1467-9868.2007.00646.x

Wood, S. N. (2017). *Generalized additive models: An introduction with R* (2nd ed.). Chapman and Hall/CRC. https://doi.org/10.1201/9781315370279

WWF. (2021). *The world's forgotten fishes*. World Wildlife Fund. https://wwf.panda.org/discover/our_focus/freshwater_practice/the_world_s_forgotten_fishes/

Yang, Y., Lu, J., Pflugrath, B. D., Li, H., Martinez, J. J., Regmi, S., Wu, B., Xiao, J., & Deng, Z. D. (2021). Lab-on-a-Fish: Wireless, miniaturized, fully integrated, implantable biotelemetric tag for real-time *in vivo* monitoring of aquatic animals. *IEEE Internet of Things Journal*. *PP*(1), 1–1. https://doi.org/10.1109/JIOT.2021.3126614

Zar, J. H. (2010). *Biostatistical analysis* (5th ed.). Pearson.

Zeileis, A., Kleiber, C., & Jackman, S. (2008). Regression models for count data in R. *Journal of Statistical Software, 27*(8), 1–25. https://doi.org/10.18637/jss.v027.i08

* References conducted following APA 7th edition

Supplementary materials

Annex I

This annex contains supplementary material about the fish capturing, tags and tagging process.

Figure I.1- MCFT3-L VHF data logging transmitters from Lotek

Two types of fishing gear were selected to suit the size of the fish targeted for capture: gill nets and long lines. The gill nets had mesh sizes of 180 to 220 mm, lengths of 100 to 130 m, and heights ranging from 5 to 6.3 m (Fig. I.2). The long lines consisted of a main float line approximately 60 m long, with ten 2.5 m bait lines, each holding live bait at the bottom with a 1.5 L plastic bottle on top, every 5 m (Fig. I.3) as described in Vejřík L., et al., 2024.

Figure I.2- Deployment of gill nets

Figure I.3- Deployment of long lines

Figure I.4- Tagging procedure major steps: A) 2 cm incision; **B)** insertion of exterior antenna, with hollow needle; **C)** sutures to close the incision.

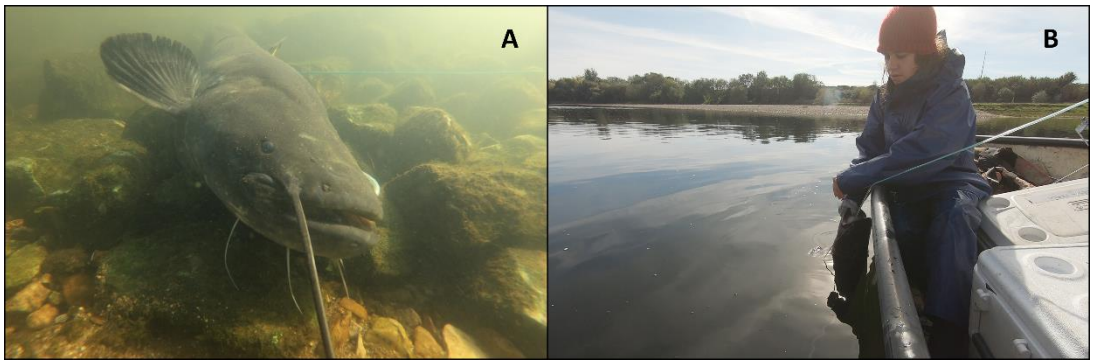

Figure I.5- Images of European catfish **A)** in recovery; **B)** being released in capture spot.

Figure I.6- Images of the manual active radio tracking procedure, by boat, using a manual radio tracking receiver (model R410) and a 4-element Yagi antenna, both from Advanced Telemetry Systems.

Annex II

This annex contains supplementary material about European catfish depth use, model lists, individual GAM's for depth/activity and model predictions for depth/activity.

Table II.1 – Full table on the selection process of the predictors on Generalized Additive Models (GAMs) of the daily mean depth of catfish as the response variable. The Akaike Information Criterion (AIC), the Bayesian Information Criterion (BIC) and the deviance explained are presented for each fitted model.

Model ID	Depth Model Formula	AIC	BIC	Deviance explained (%)
d_d_1	Y ~ s(mean_temp) + s(Ind, bs = "re")	3232.73	3293.84	41.26
d_d_2	Y ~ s(mean_flow) + s(Ind, bs = "re")	3502.18	3548.89	24.16
d_d_3	Y ~ s(mean_ASum) + s(Ind, bs = "re")	3522.96	3569.70	22.69
d_d_4	Y ~ s(mean_JD) + s(Ind, bs = "re")	3241.87	3310.33	40.92
d_d_5	Y ~ s(mean_moon) + s(Ind, bs = "re")	3676.58	3705.96	10.36
d_d_6	Y ~ Season + s(Ind, bs = "re")	3397.64	3437.00	30.96
d_d_7	Y ~ s(mean_temp) + s(mean_flow) + s(Ind, bs = "re")	3220.17	3298.62	42.32
d_d_8	Y ~ s(mean_temp) + s(mean_ASum) + s(Ind, bs = "re")	3231.69	3297.39	41.42
d_d_9	Y ~ s(mean_temp) + s(mean_JD) + s(Ind, bs = "re")	3120.43	3219.91	47.87
d_d_10	Y ~ s(mean_temp) + s(mean_moon) + s(Ind, bs = "re")	3232.71	3299.02	41.38
d_d_11	Y ~ s(mean_temp) + Season + s(Ind, bs = "re")	3200.81	3245.19	42.62
d_d_12	Y ~ s(mean_flow) + s(mean_ASum) + s(Ind, bs = "re")	3414.56	3485.49	30.70
d_d_13	Y ~ s(mean_flow) + s(mean_JD) + s(Ind, bs = "re")	3207.83	3293.68	43.15
d_d_14	Y ~ s(mean_flow) + s(mean_moon) + s(Ind, bs = "re")	3503.13	3554.56	24.22
d_d_15	Y ~ s(mean_flow) + Season + s(Ind, bs = "re")	3370.44	3427.59	33.13
d_d_16	Y ~ s(mean_ASum) + s(mean_JD) + s(Ind, bs = "re")	3227.09	3318.35	42.23
d_d_17	Y ~ s(mean_ASum) + s(mean_moon) + s(Ind, bs = "re")	3519.53	3571.69	23.09
d_d_18	Y ~ s(mean_ASum) + Season + s(Ind, bs = "re")	3390.09	3449.50	31.96
d_d_19	Y ~ s(mean_JD) + s(mean_moon) + s(Ind, bs = "re")	3240.74	3314.09	41.09
d_d_20	Y ~ s(mean_JD) + Season + s(Ind, bs = "re")	3210.82	3293.88	42.93
d_d_21	Y ~ s(mean_moon) + Season + s(Ind, bs = "re")	3396.32	3440.65	31.17
d_d_22	Y ~ s(mean_temp) + s(mean_flow) + s(mean_ASum) + s(Ind, bs = "re")	3213.06	3315.61	43.23

d_d_23	Y ~ s(mean_temp) + s(mean_flow) + s(mean_JD) + s(Ind, bs = "re")	3108.99	3231.58	48.88
d_d_24	Y ~ s(mean_temp) + s(mean_flow) + s(mean_moon) + s(Ind, bs = "re")	3220.92	3304.55	42.40
d_d_25	Y ~ s(mean_temp) + s(mean_flow) + Season + s(Ind, bs = "re")	3193.28	3255.37	43.40
d_d_26	Y ~ s(mean_temp) + s(mean_ASum) + s(mean_JD) + s(Ind, bs = "re")	3113.06	3236.34	48.70
d_d_27	Y ~ s(mean_temp) + s(mean_ASum) + s(mean_moon) + s(Ind, bs = "re")	3228.68	3317.98	42.10
d_d_28	Y ~ s(mean_temp) + s(mean_ASum) + Season + s(Ind, bs = "re")	3194.26	3260.47	43.44
d_d_29	Y ~ s(mean_temp) + s(mean_JD) + s(mean_moon) + s(Ind, bs = "re")	3119.67	3224.50	48.02
d_d_30	Y ~ s(mean_temp) + s(mean_JD) + Season + s(Ind, bs = "re")	3109.91	3220.76	48.61
d_d_31	Y ~ s(mean_temp) + s(mean_moon) + Season + s(Ind, bs = "re")	3199.27	3248.61	42.81
d_d_32	Y ~ s(mean_flow) + s(mean_ASum) + s(mean_JD) + s(Ind, bs = "re")	3190.86	3301.03	44.55
d_d_33	Y ~ s(mean_flow) + s(mean_ASum) + s(mean_moon) + s(Ind, bs = "re")	3414.75	3490.53	30.81
d_d_34	Y ~ s(mean_flow) + s(mean_ASum) + Season + s(Ind, bs = "re")	3352.07	3434.55	34.89
d_d_35	Y ~ s(mean_flow) + s(mean_JD) + s(mean_moon) + s(Ind, bs = "re")	3208.56	3299.31	43.21
d_d_36	Y ~ s(mean_flow) + s(mean_JD) + Season + s(Ind, bs = "re")	3173.38	3273.22	45.24
d_d_37	Y ~ s(mean_flow) + s(mean_moon) + Season + s(Ind, bs = "re")	3370.81	3432.35	33.22
d_d_38	Y ~ s(mean_ASum) + s(mean_JD) + s(mean_moon) + s(Ind, bs = "re")	3225.21	3321.86	42.45
d_d_39	Y ~ s(mean_ASum) + s(mean_JD) + Season + s(Ind, bs = "re")	3200.59	3305.48	43.93
d_d_40	Y ~ s(mean_ASum) + s(mean_moon) + Season + s(Ind, bs = "re")	3387.75	3453.14	32.26
d_d_41	Y ~ s(mean_JD) + s(mean_moon) + Season + s(Ind, bs = "re")	3207.76	3295.73	43.19
d_d_42	Y ~ s(mean_temp) + s(mean_flow) + s(mean_ASum) + s(mean_JD) + s(Ind, bs = "re")	3101.67	3247.71	49.68
d_d_43	Y ~ s(mean_temp) + s(mean_flow) + s(mean_ASum) + s(mean_moon) + s(Ind, bs = "re")	3212.89	3320.84	43.35
d_d_44	Y ~ s(mean_temp) + s(mean_flow) + s(mean_ASum) + Season + s(Ind, bs = "re")	3182.69	3270.57	44.50
d_d_45	Y ~ s(mean_temp) + s(mean_flow) + s(mean_JD) + s(mean_moon) + s(Ind, bs = "re")	3108.43	3235.47	48.99
d_d_46	Y ~ s(mean_temp) + s(mean_flow) + s(mean_JD) + Season + s(Ind, bs = "re")	3099.12	3228.57	49.48

d_d_47	Y ~ s(mean_temp) + s(mean_flow) + s(mean_moon) + Season + s(Ind, bs = "re")	3192.15	3258.91	43.56
d_d_48	Y ~ s(mean_temp) + s(mean_ASum) + s(mean_JD) + s(mean_moon) + s(Ind, bs = "re")	3111.28	3240.51	48.90
d_d_49	Y ~ s(mean_temp) + s(mean_ASum) + s(mean_JD) + Season + s(Ind, bs = "re")	3108.80	3221.01	48.69
d_d_50	Y ~ s(mean_temp) + s(mean_ASum) + s(mean_moon) + Season + s(Ind, bs = "re")	3192.04	3264.12	43.68
d_d_51	Y ~ s(mean_temp) + s(mean_JD) + s(mean_moon) + Season + s(Ind, bs = "re")	3113.61	3206.47	48.07
d_d_52	Y ~ s(mean_flow) + s(mean_ASum) + s(mean_JD) + s(mean_moon) + s(Ind, bs = "re")	3191.13	3306.42	44.65
d_d_53	Y ~ s(mean_flow) + s(mean_ASum) + s(mean_JD) + Season + s(Ind, bs = "re")	3161.83	3284.69	46.29
d_d_54	Y ~ s(mean_flow) + s(mean_ASum) + s(mean_moon) + Season + s(Ind, bs = "re")	3351.48	3438.51	35.03
d_d_55	Y ~ s(mean_flow) + s(mean_JD) + s(mean_moon) + Season + s(Ind, bs = "re")	3173.52	3278.11	45.33
d_d_56	Y ~ s(mean_ASum) + s(mean_JD) + s(mean_moon) + Season + s(Ind, bs = "re")	3196.63	3307.10	44.26
d_d_57	Y ~ s(mean_temp) + s(mean_flow) + s(mean_ASum) + s(mean_JD) + s(mean_moon) + s(Ind, bs = "re")	3100.30	3251.28	49.84
d_d_58	Y ~ s(mean_temp) + s(mean_flow) + s(mean_ASum) + s(mean_JD) + Season + s(Ind, bs = "re")	3093.81	3227.68	49.82
d_d_59	Y ~ s(mean_temp) + s(mean_flow) + s(mean_ASum) + s(mean_moon) + Season + s(Ind, bs = "re")	3180.92	3273.96	44.70
d_d_60	Y ~ s(mean_temp) + s(mean_flow) + s(mean_JD) + s(mean_moon) + Season + s(Ind, bs = "re")	3101.22	3215.85	49.09
d_d_61	Y ~ s(mean_temp) + s(mean_ASum) + s(mean_JD) + s(mean_moon) + Season + s(Ind, bs = "re")	3103.86	3221.70	49.03
d_d_62	Y ~ s(mean_flow) + s(mean_ASum) + s(mean_JD) + s(mean_moon) + Season + s(Ind, bs = "re")	3161.37	3289.31	46.42
d_d_63	Y ~ s(mean_temp) + s(mean_flow) + s(mean_ASum) + s(mean_JD) + s(mean_moon) + Season + s(Ind, bs = "re")	3091.30	3230.11	50.03

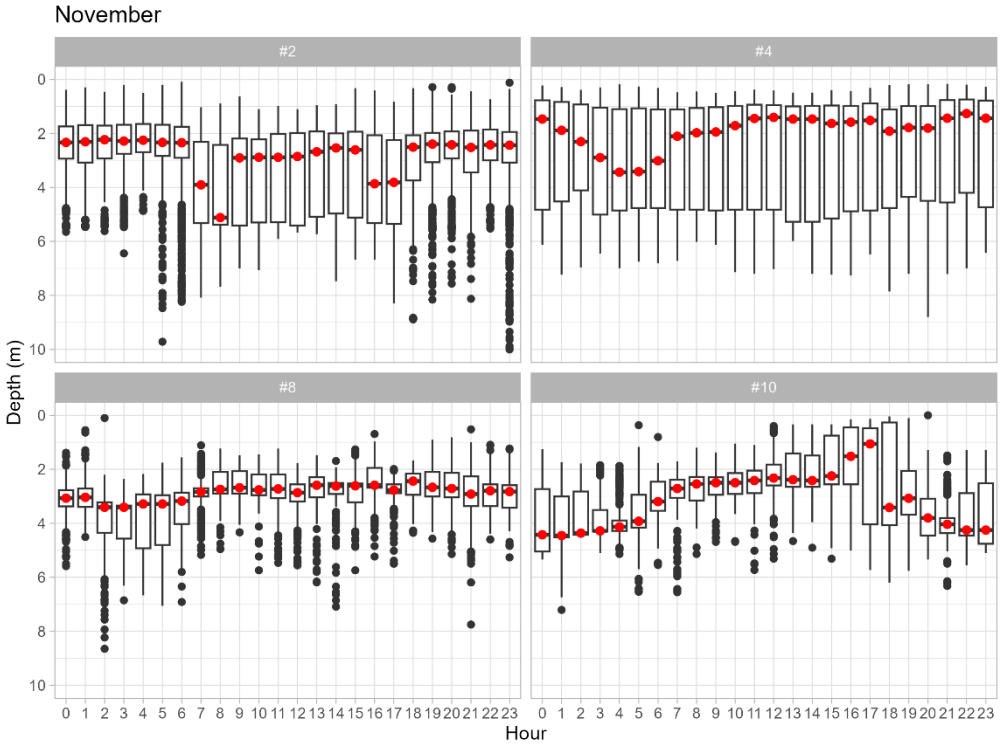

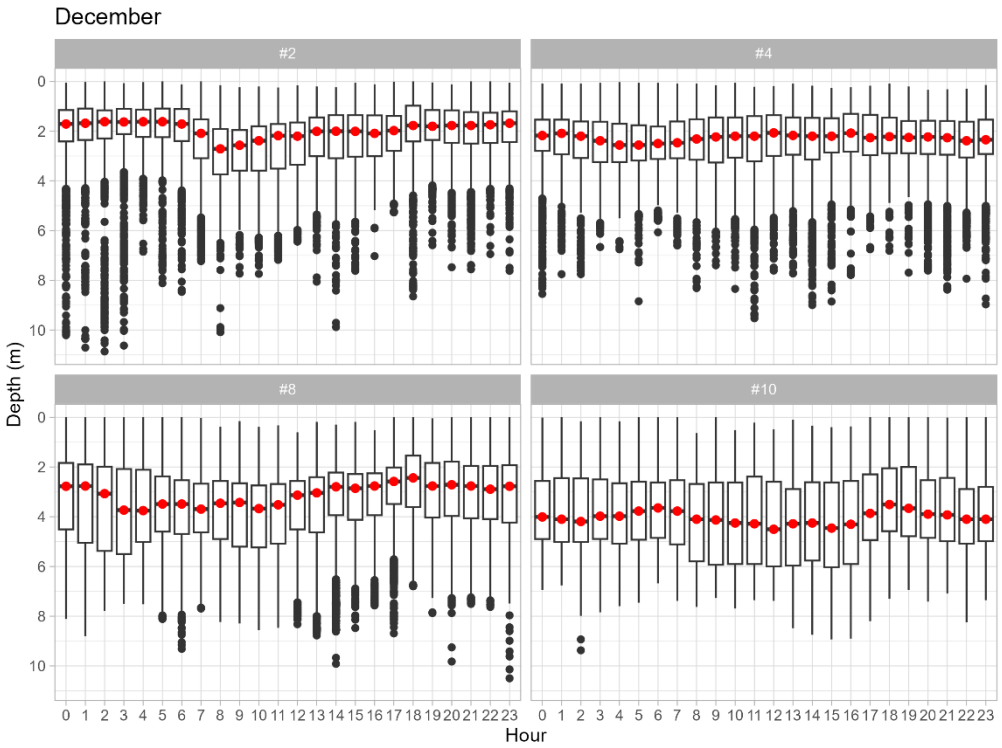

(Figure continues in the next page)

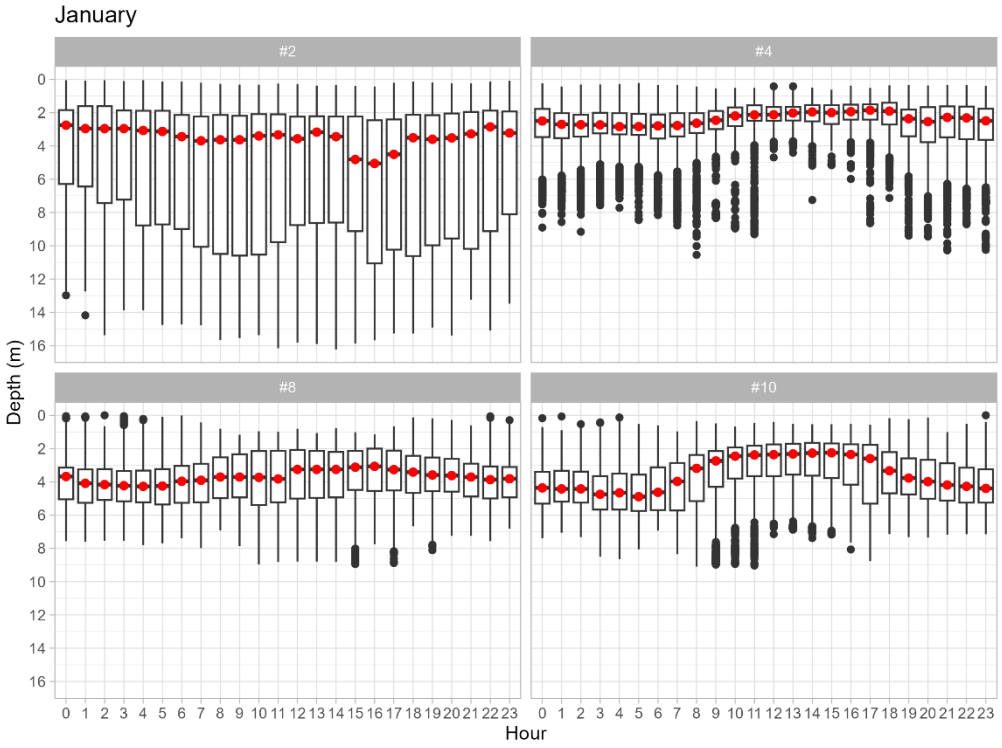

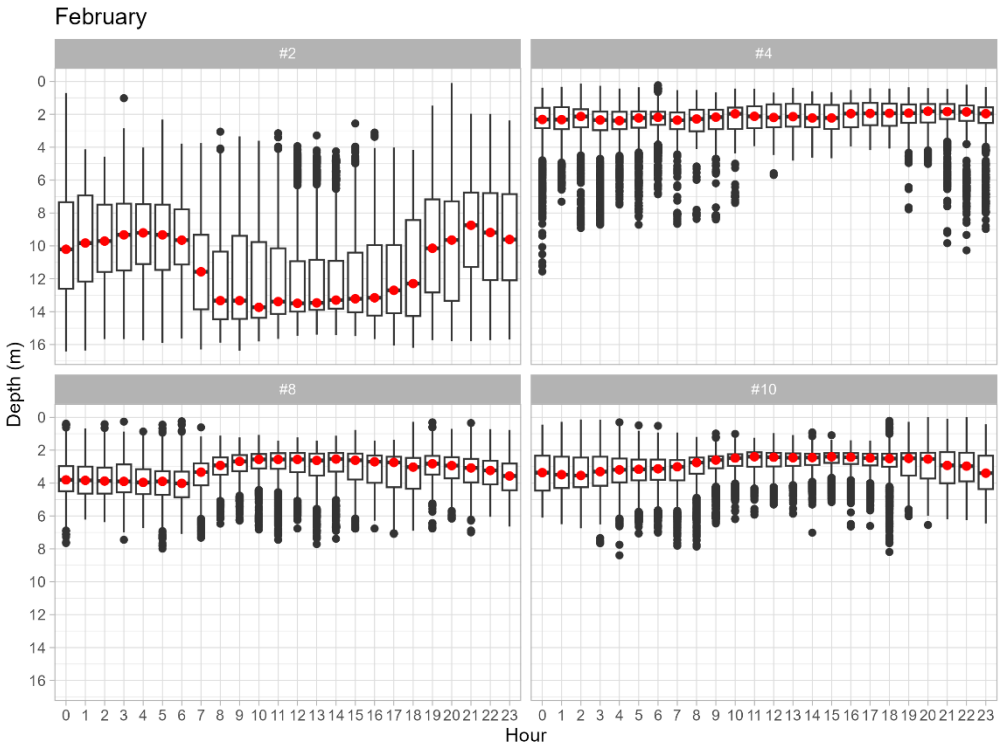

(Figure continues in the next page)

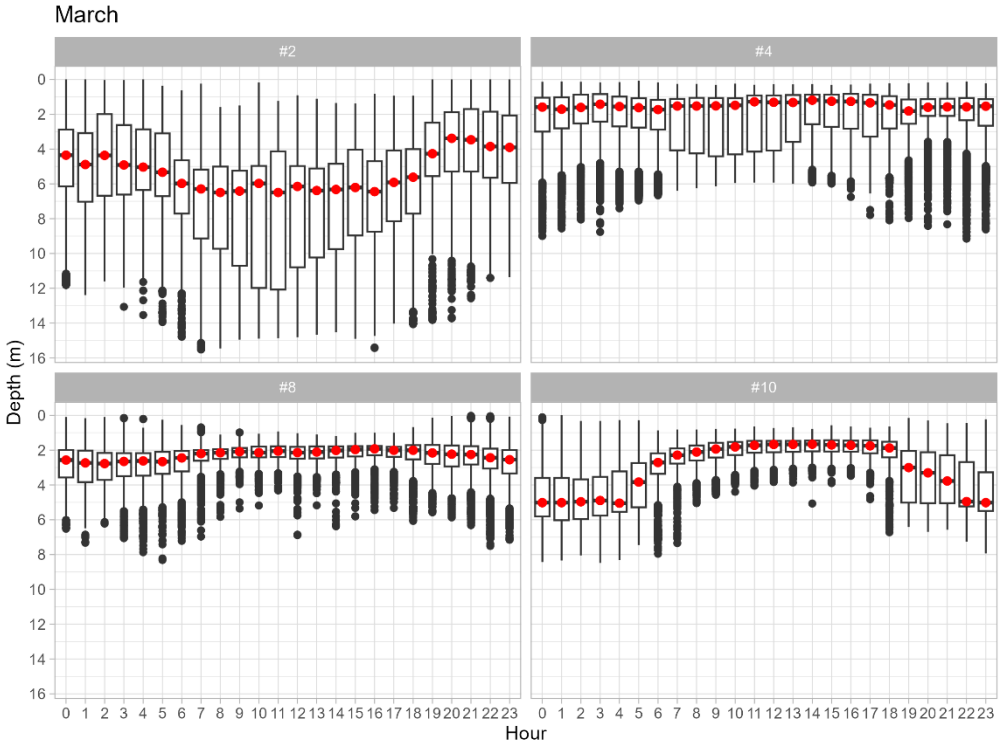

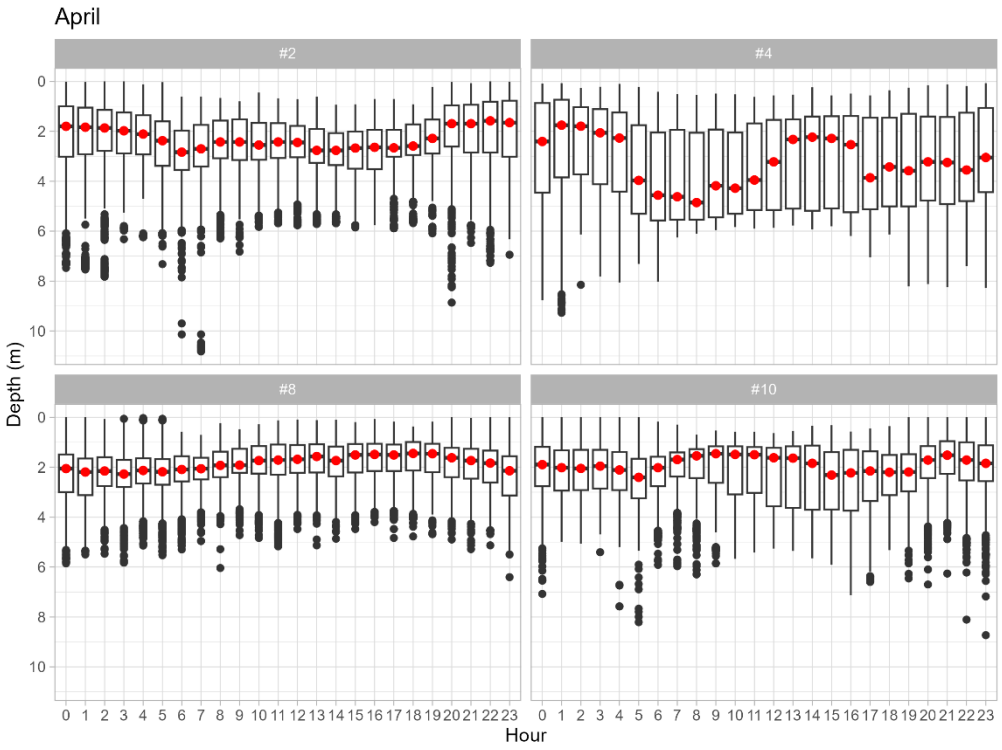

(Figure continues in the next page)

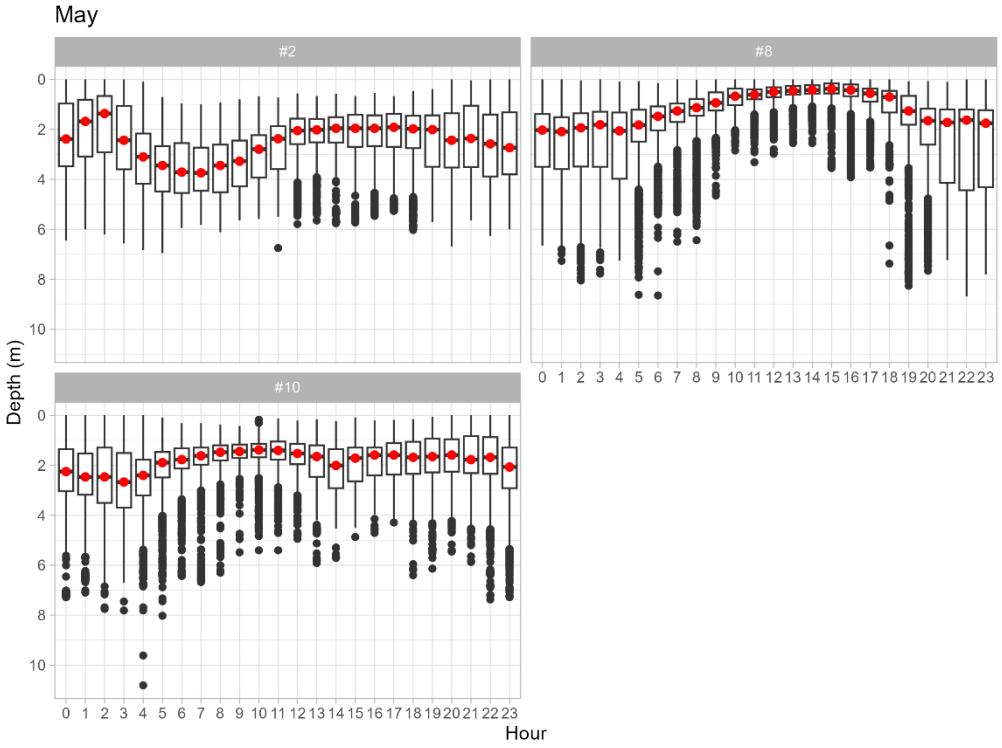

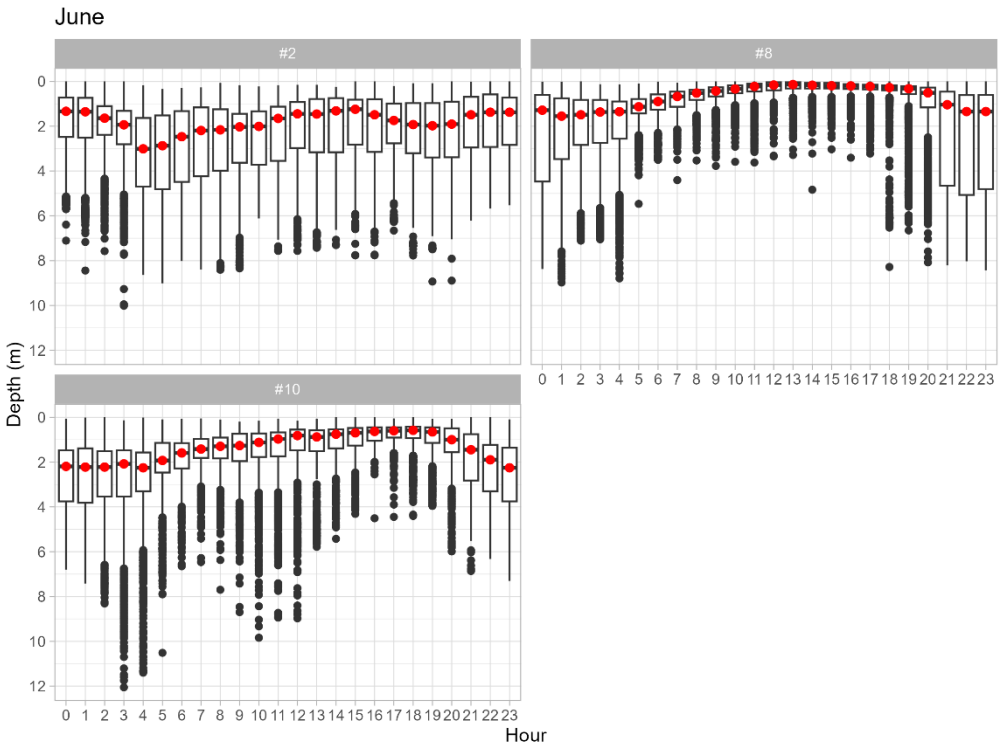

(Figure continues in the next page)

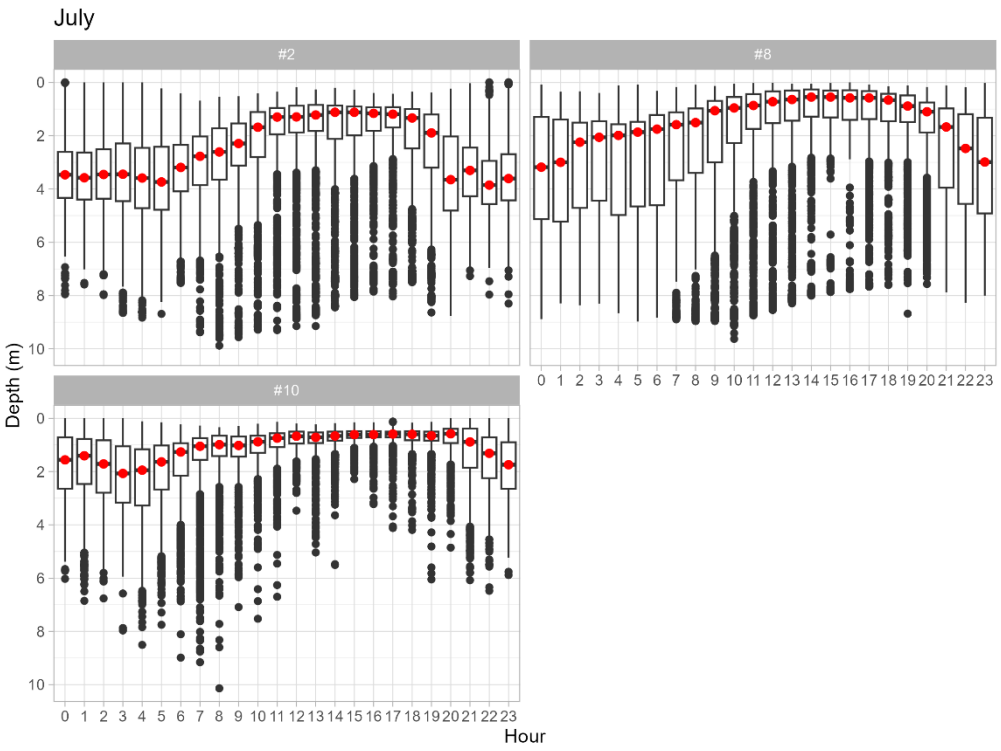

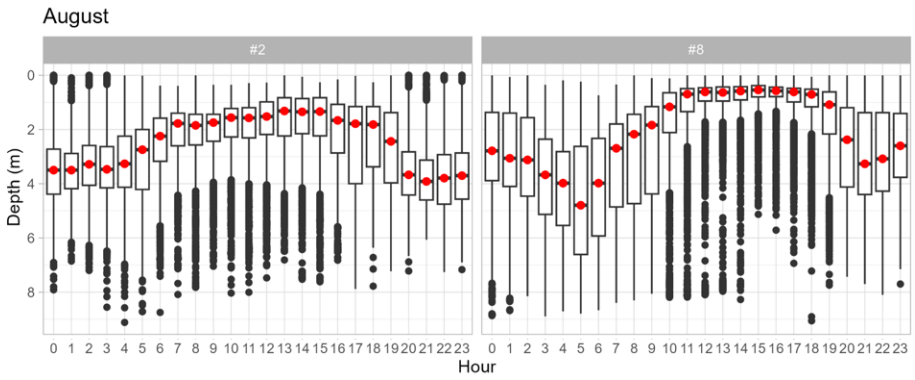

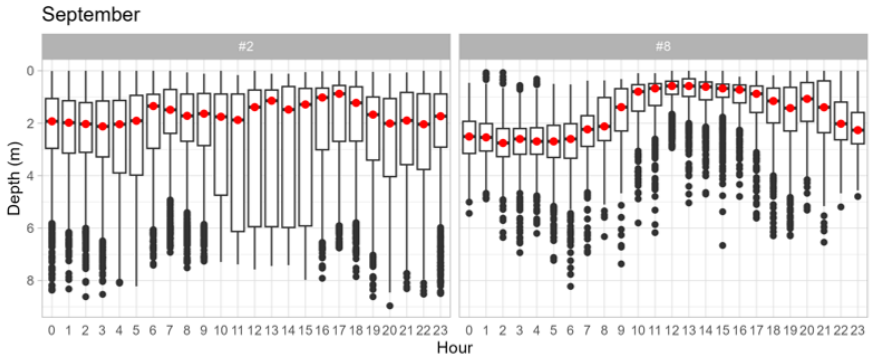

(Figure continues in the next page)

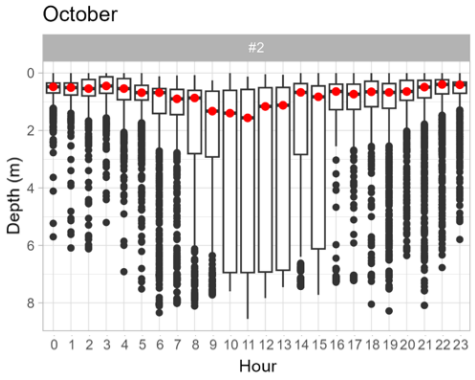

Figure II.1 – Monthly individual circadian vertical habitat use (i.e., depth) considering the data collected from the four recaptured European catfish. Represented by boxplots for each monitored month with medians accentuated by the red dots.

Table II.2 – Summary table of the selection process of the predictors on individual Generalized Additive Models (GAMs) of the daily mean depth of catfish as the response variable. The Akaike Information Criterion (AIC), the Bayesian Information Criterion (BIC) and the deviance explained are presented for each fitted model.

Fish ID	Model ID	Depth Model Formula	AIC	BIC	Deviance explained (%)
2	d_d_9	Y ~ s(mean_temp) + s(mean_JD)	1046.66	1115.22	74.69
4	d_d_49	Y ~ s(mean_temp) + s(mean_ASum) + s(mean_JD) + Season	324.14	377.67	70.30
8	d_d_58	Y ~ s(mean_temp) + s(mean_flow) s(mean_ASum) + s(mean_JD) + Season	531.99	611.38	75.38
10	d_d_62	Y ~ s(mean_flow) s(mean_ASum) + s(mean_JD) + s(mean_moon) + Season	333.79	410.05	82.10

#2

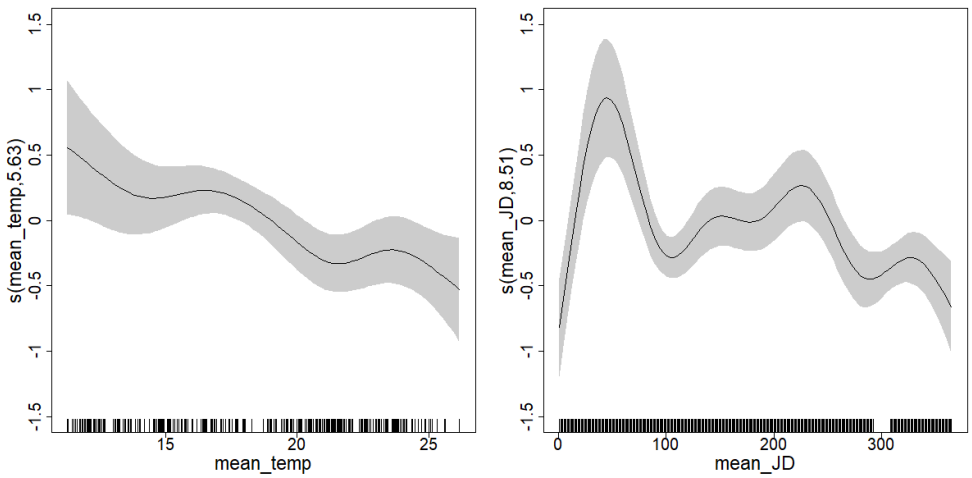

(Figure continues in the next page)

#4

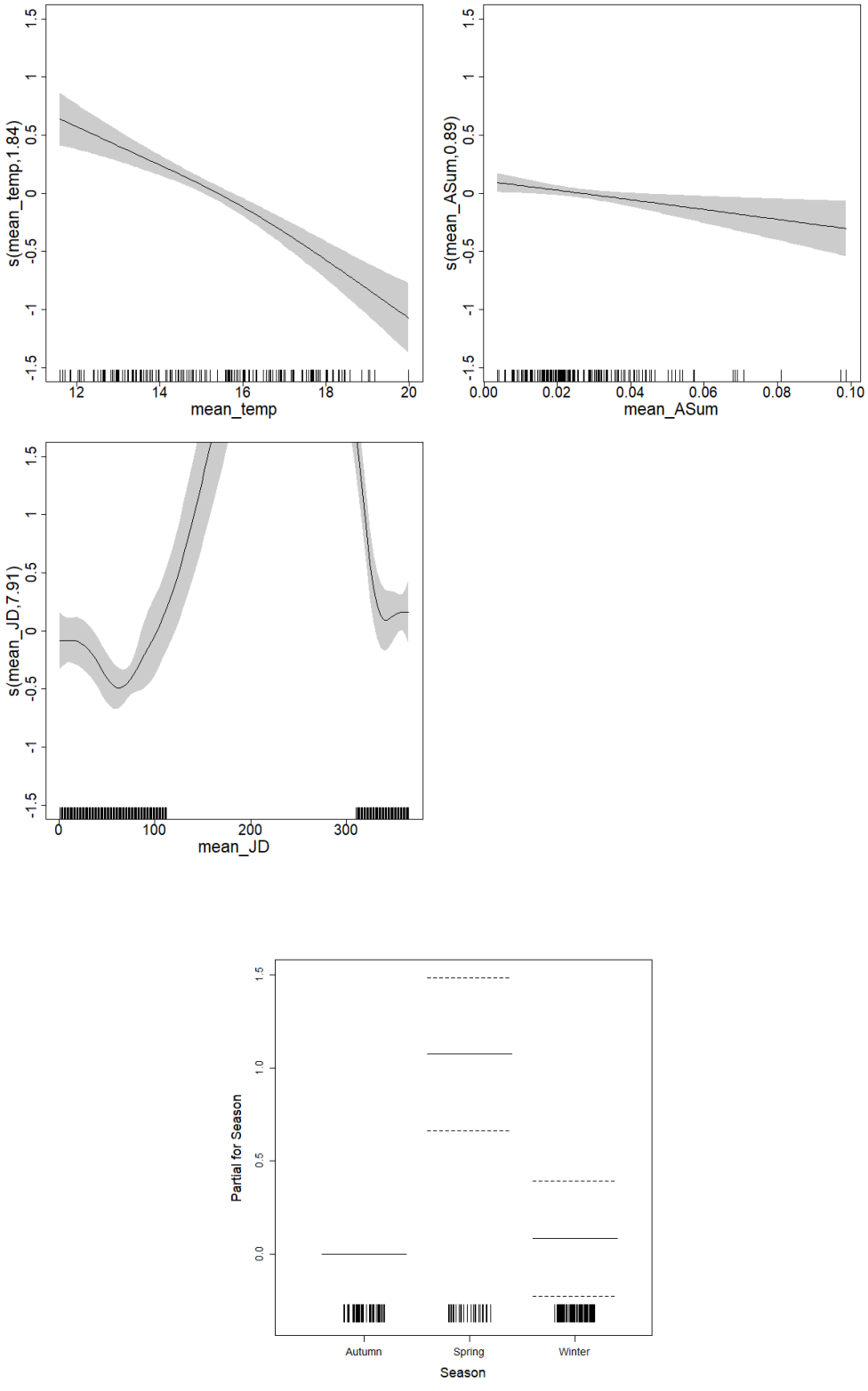

(Figure continues in the next page)

#8

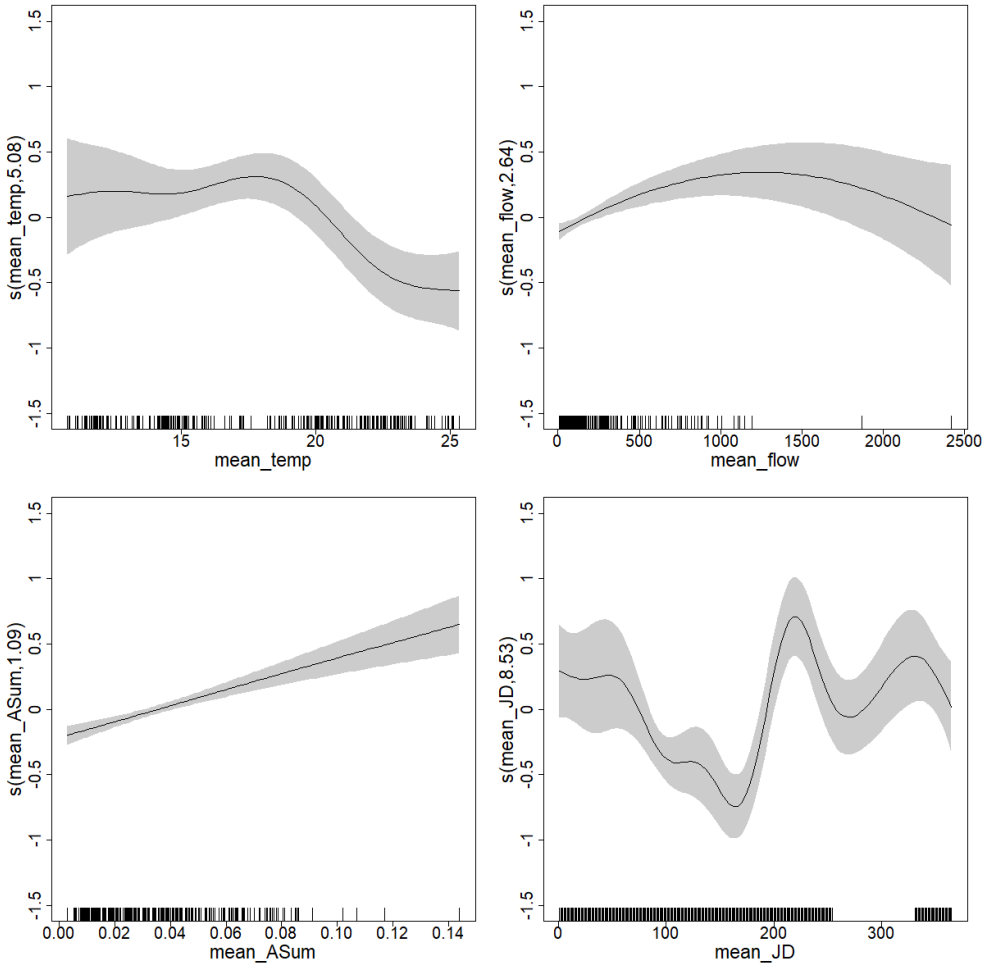

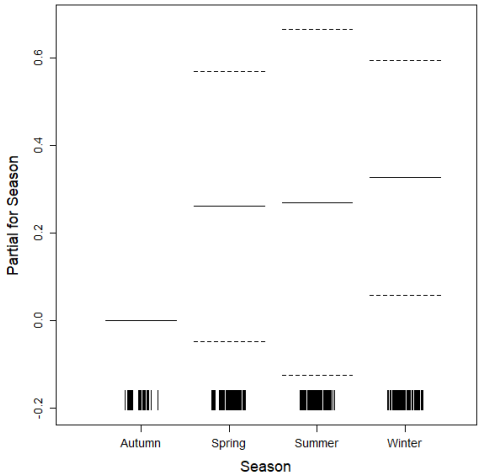

(Figure continues in the next page)

#10

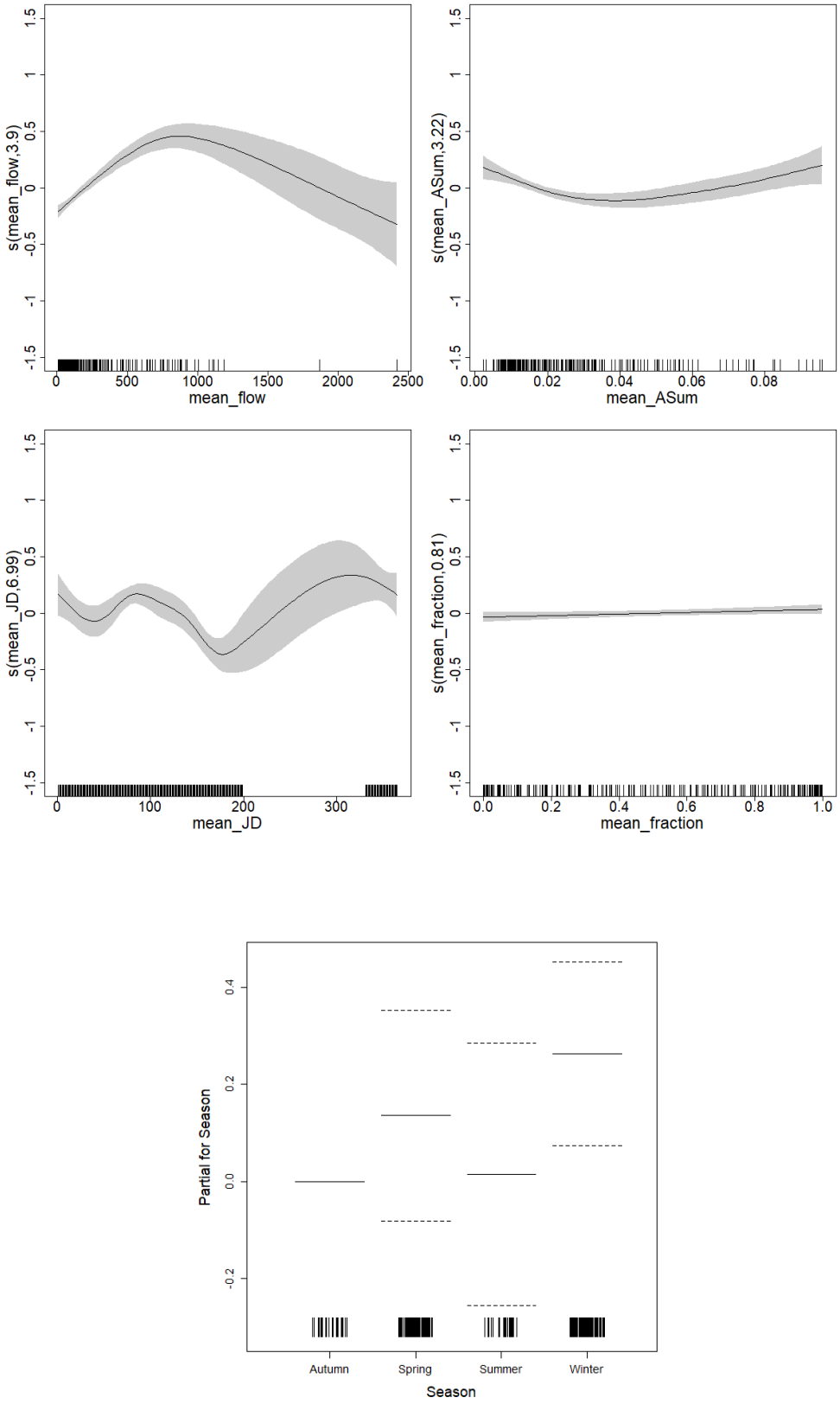

Figure II. 2 – Partial effect plots of the chosen depth use individual GAMs revealing the correlations between the predictors and the mean daily depth use as response variable, for each individual fish. All plots for the parametric variable season of the year as a different scale as well as all plots for individual #4.

Table II.3 – Full table on the selection process of the predictors on Generalized Additive Models (GAMs) of the daily mean activity of catfish as the response variable. The Akaike Information Criterion (AIC), the Bayesian Information Criterion (BIC) and the deviance explained are presented for each fitted model.

Model ID	Activity Model Formula	AIC	BIC	Deviance explained (%)
a_d_1	Y ~ s(mean_temp) + s(Ind, bs = "re")	-5926.19	-5875.29	42.64
a_d_2	Y ~ s(mean_flow) + s(Ind, bs = "re")	-5514.78	-5471.13	16.20
a_d_3	Y ~ s(mean_ASum) + s(Ind, bs = "re")	-5532.24	-5469.87	18.08
a_d_4	Y ~ s(mean_JD) + s(Ind, bs = "re")	-6095.89	-6027.20	51.30
a_d_5	Y ~ s(mean_moon) + s(Ind, bs = "re")	-5385.78	-5356.34	5.35
a_d_6	Y ~ Season + s(Ind, bs = "re")	-6005.03	-5965.75	46.44
a_d_7	Y ~ s(mean_temp) + s(mean_flow) + s(Ind, bs = "re")	-5926.41	-5868.83	42.79
a_d_8	Y ~ s(mean_temp) + s(mean_ASum) + s(Ind, bs = "re")	-5976.19	-5880.31	46.15
a_d_9	Y ~ s(mean_temp) + s(mean_JD) + s(Ind, bs = "re")	-6098.19	-6002.41	51.90
a_d_10	Y ~ s(mean_temp) + s(mean_moon) + s(Ind, bs = "re")	-5925.19	-5869.11	42.70
a_d_11	Y ~ s(mean_temp) + Season + s(Ind, bs = "re")	-6052.48	-5989.95	49.18
a_d_12	Y ~ s(mean_flow) + s(mean_ASum) + s(Ind, bs = "re")	-5579.77	-5522.52	21.40
a_d_13	Y ~ s(mean_flow) + s(mean_JD) + s(Ind, bs = "re")	-6099.03	-6025.22	51.54
a_d_14	Y ~ s(mean_flow) + s(mean_moon) + s(Ind, bs = "re")	-5512.90	-5464.29	16.21
a_d_15	Y ~ s(mean_flow) + Season + s(Ind, bs = "re")	-6019.28	-5974.97	47.24
a_d_16	Y ~ s(mean_ASum) + s(mean_JD) + s(Ind, bs = "re")	-6126.39	-6018.26	53.36
a_d_17	Y ~ s(mean_ASum) + s(mean_moon) + s(Ind, bs = "re")	-5530.27	-5462.91	18.09
a_d_18	Y ~ s(mean_ASum) + Season + s(Ind, bs = "re")	-6047.72	-5972.96	49.19
a_d_19	Y ~ s(mean_JD) + s(mean_moon) + s(Ind, bs = "re")	-6093.94	-6020.26	51.31
a_d_20	Y ~ s(mean_JD) + Season + s(Ind, bs = "re")	-6118.58	-6035.61	52.57
a_d_21	Y ~ s(mean_moon) + Season + s(Ind, bs = "re")	-6003.51	-5959.27	46.46
a_d_22	Y ~ s(mean_temp) + s(mean_flow) + s(mean_ASum) + s(Ind, bs = "re")	-5981.07	-5868.13	46.73
a_d_23	Y ~ s(mean_temp) + s(mean_flow) + s(mean_JD) + s(Ind, bs = "re")	-6103.90	-6002.07	52.26
a_d_24	Y ~ s(mean_temp) + s(mean_flow) + s(mean_moon) + s(Ind, bs = "re")	-5925.15	-5862.54	42.84

a_d_25	Y ~ s(mean_temp) + s(mean_flow) + Season + s(Ind, bs = "re")	-6074.08	-6010.78	50.21
a_d_26	Y ~ s(mean_temp) + s(mean_ASum) + s(mean_JD) + s(Ind, bs = "re")	-6137.63	-5996.11	54.43
a_d_27	Y ~ s(mean_temp) + s(mean_ASum) + s(mean_moon) + s(Ind, bs = "re")	-5975.11	-5874.36	46.19
a_d_28	Y ~ s(mean_temp) + s(mean_ASum) + Season + s(Ind, bs = "re")	-6085.69	-5990.06	51.34
a_d_29	Y ~ s(mean_temp) + s(mean_JD) + s(mean_moon) + s(Ind, bs = "re")	-6096.60	-5995.46	51.93
a_d_30	Y ~ s(mean_temp) + s(mean_JD) + Season + s(Ind, bs = "re")	-6119.90	-6019.15	52.95
a_d_31	Y ~ s(mean_temp) + s(mean_moon) + Season + s(Ind, bs = "re")	-6052.63	-5984.46	49.30
a_d_32	Y ~ s(mean_flow) + s(mean_ASum) + s(mean_JD) + s(Ind, bs = "re")	-6132.20	-6003.81	53.97
a_d_33	Y ~ s(mean_flow) + s(mean_ASum) + s(mean_moon) + s(Ind, bs = "re")	-5578.02	-5515.79	21.42
a_d_34	Y ~ s(mean_flow) + s(mean_ASum) + Season + s(Ind, bs = "re")	-6063.48	-5983.20	50.03
a_d_35	Y ~ s(mean_flow) + s(mean_JD) + s(mean_moon) + s(Ind, bs = "re")	-6097.07	-6018.44	51.54
a_d_36	Y ~ s(mean_flow) + s(mean_JD) + Season + s(Ind, bs = "re")	-6119.43	-6031.46	52.70
a_d_37	Y ~ s(mean_flow) + s(mean_moon) + Season + s(Ind, bs = "re")	-6017.47	-5968.21	47.25
a_d_38	Y ~ s(mean_ASum) + s(mean_JD) + s(mean_moon) + s(Ind, bs = "re")	-6124.53	-6011.58	53.37
a_d_39	Y ~ s(mean_ASum) + s(mean_JD) + Season + s(Ind, bs = "re")	-6152.49	-6031.50	54.70
a_d_40	Y ~ s(mean_ASum) + s(mean_moon) + Season + s(Ind, bs = "re")	-6046.49	-5966.97	49.23
a_d_41	Y ~ s(mean_JD) + s(mean_moon) + Season + s(Ind, bs = "re")	-6116.57	-6028.63	52.57
a_d_42	Y ~ s(mean_temp) + s(mean_flow) + s(mean_ASum) + s(mean_JD) + s(Ind, bs = "re")	-6146.20	-5982.30	55.17
a_d_43	Y ~ s(mean_temp) + s(mean_flow) + s(mean_ASum) + s(mean_moon) + s(Ind, bs = "re")	-5978.39	-5870.65	46.49
a_d_44	Y ~ s(mean_temp) + s(mean_flow) + s(mean_ASum) + Season + s(Ind, bs = "re")	-6119.16	-6000.28	53.24
a_d_45	Y ~ s(mean_temp) + s(mean_flow) + s(mean_JD) + s(mean_moon) + s(Ind, bs = "re")	-6102.01	-5995.08	52.27
a_d_46	Y ~ s(mean_temp) + s(mean_flow) + s(mean_JD) + Season + s(Ind, bs = "re")	-6122.29	-6015.59	53.16
a_d_47	Y ~ s(mean_temp) + s(mean_flow) + s(mean_moon) + Season + s(Ind, bs = "re")	-6073.25	-6004.83	50.26

a_d_48	Y ~ s(mean_temp) + s(mean_ASum) + s(mean_JD) + s(mean_moon) + s(Ind, bs = "re")	-6135.91	-5989.60	54.44
a_d_49	Y ~ s(mean_temp) + s(mean_ASum) + s(mean_JD) + Season + s(Ind, bs = "re")	-6155.06	-6015.28	55.13
a_d_50	Y ~ s(mean_temp) + s(mean_ASum) + s(mean_moon) + Season + s(Ind, bs = "re")	-6085.76	-5985.24	51.43
a_d_51	Y ~ s(mean_temp) + s(mean_JD) + s(mean_moon) + Season + s(Ind, bs = "re")	-6118.38	-6011.87	52.98
a_d_52	Y ~ s(mean_flow) + s(mean_ASum) + s(mean_JD) + s(mean_moon) + s(Ind, bs = "re")	-6130.17	-5997.05	53.96
a_d_53	Y ~ s(mean_flow) + s(mean_ASum) + s(mean_JD) + Season + s(Ind, bs = "re")	-6152.63	-6026.85	54.79
a_d_54	Y ~ s(mean_flow) + s(mean_ASum) + s(mean_moon) + Season + s(Ind, bs = "re")	-6061.90	-5976.83	50.05
a_d_55	Y ~ s(mean_flow) + s(mean_JD) + s(mean_moon) + Season + s(Ind, bs = "re")	-6117.42	-6024.56	52.70
a_d_56	Y ~ s(mean_ASum) + s(mean_JD) + s(mean_moon) + Season + s(Ind, bs = "re")	-6150.60	-6024.87	54.70
a_d_57	Y ~ s(mean_temp) + s(mean_flow) + s(mean_ASum) + s(mean_JD) + s(mean_moon) + s(Ind, bs = "re")	-6144.17	-5975.58	55.17
a_d_58	Y ~ s(mean_temp) + s(mean_flow) + s(mean_ASum) + s(mean_JD) + Season + s(Ind, bs = "re")	-6160.37	-6000.43	55.69
a_d_59	Y ~ s(mean_temp) + s(mean_flow) + s(mean_ASum) + s(mean_moon) + Season + s(Ind, bs = "re")	-6117.08	-5993.43	53.23
a_d_60	Y ~ s(mean_temp) + s(mean_flow) + s(mean_JD) + s(mean_moon) + Season + s(Ind, bs = "re")	-6120.49	-6008.42	53.17
a_d_61	Y ~ s(mean_temp) + s(mean_ASum) + s(mean_JD) + s(mean_moon) + Season + s(Ind, bs = "re")	-6153.67	-6008.35	55.16
a_d_62	Y ~ s(mean_flow) + s(mean_ASum) + s(mean_JD) + s(mean_moon) + Season + s(Ind, bs = "re")	-6150.65	-6020.07	54.79
a_d_63	Y ~ s(mean_temp) + s(mean_flow) + s(mean_ASum) + s(mean_JD) + s(mean_moon) + Season + s(Ind, bs = "re")	-6158.23	-5994.00	55.67

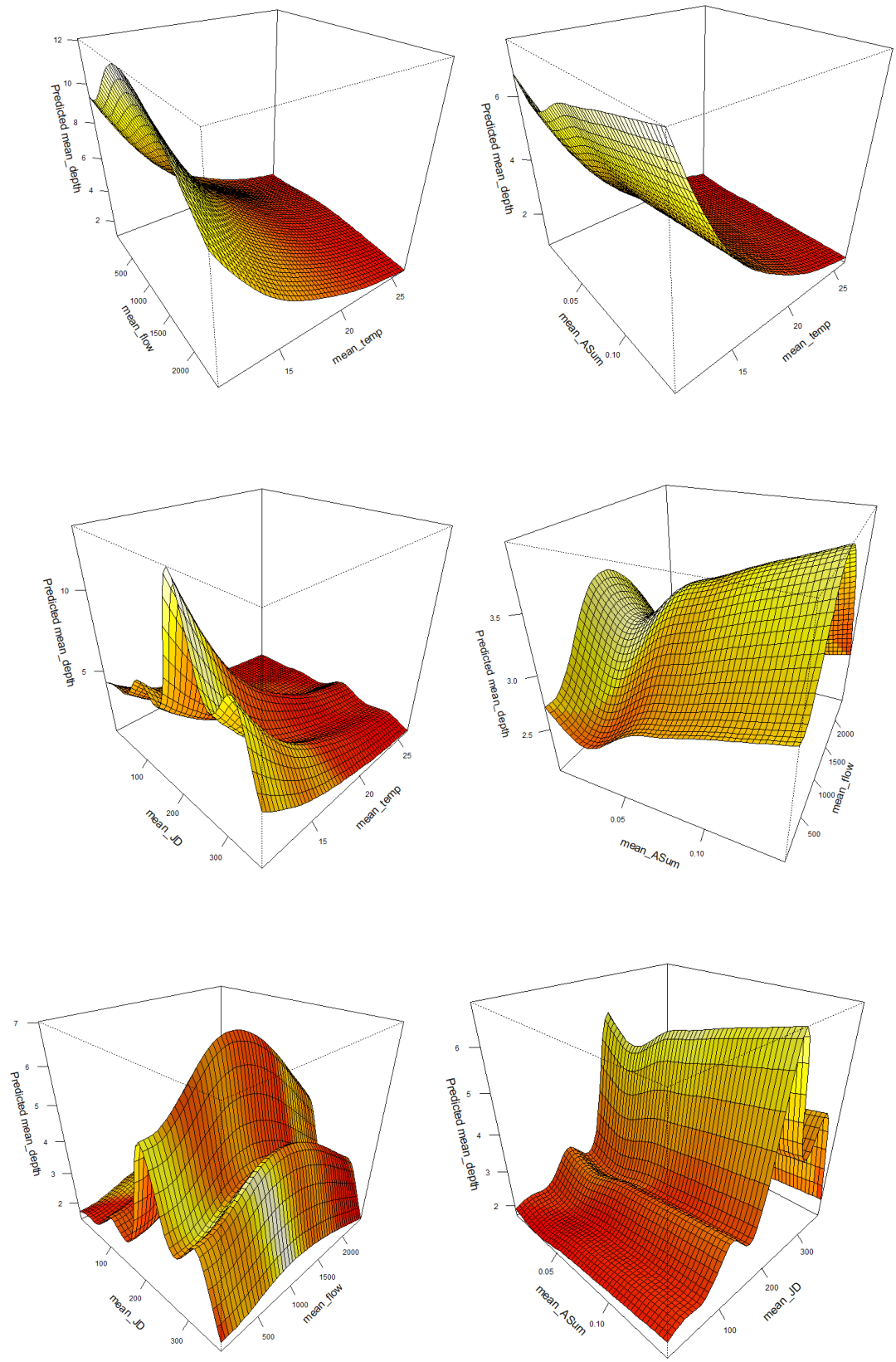

Figure II. 3 – **Perspective plots of the depth use (m) GAM predictions (model d_d_58) for the combination of the 4 main independent variables on the model: mean_temp - Temperature (ºC), mean_flow -Flow (m3/s), mean_ASum – Activity (g) and mean_JD – Julian Day of the year**. The remaining variables ommited in each graph have their value fixed to the closest observed value to the median. The red color indicates minimum predicted values and white color maximum predicted values.

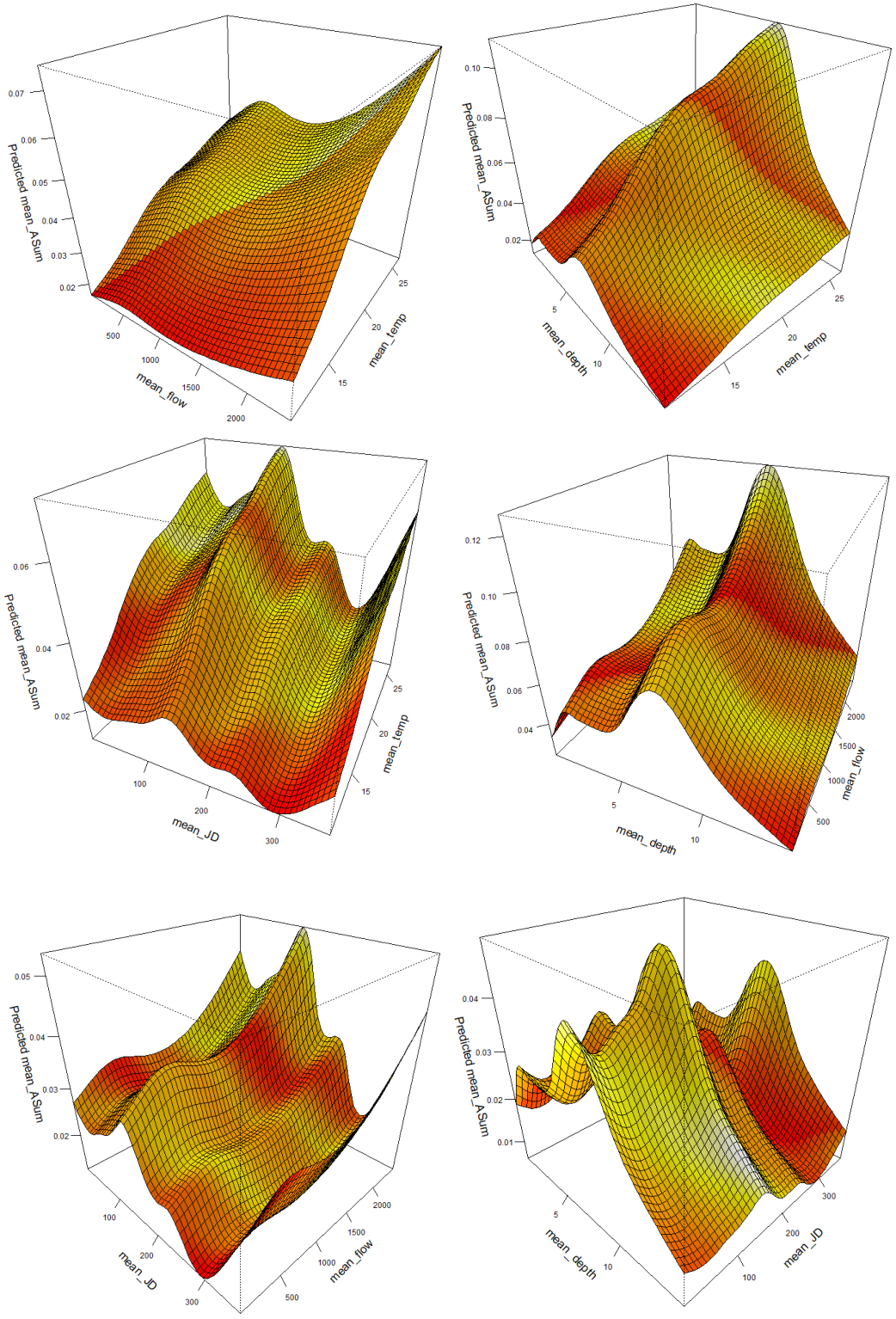

Figure II. 4 – **Perspective plots of the activity levels (g) GAM predictions (model a_d_58) for the combination of the 4 main independent variables on the model: mean_temp - Temperature (ºC), mean_flow -Flow (m3/s), mean_depth – Depth (m) and mean_JD – Julian Day of the year**. The remaining variables ommited in each graph have their value fixed to the closest observed value to the median. The red color indicates minimum predicted values and white color maximum predicted values.

Table II.4 – Full table on the selection process of the predictors of the Hurdle model of the rate of European catfish burst movements (Y). Predictors tested for both count and zero Hurdle (binomial) parts of the Hurdle model are presented, as well as the distribution used for the count part – Negative Binomial (NB) and Poisson. The Akaike Information Criterion (AIC) and the Bayesian Information Criterion (BIC) each fitted model are also presented for each of the fitted models.

Model ID		Burst Movement Hurdle Model Formula		Distribution	AIC	BIC
		Zero Hurdle	Count			
1	Y ~	mean_temp	mean_temp	NB	22624.76	22659.86
2	Y ~	mean_flow	mean_flow	NB	22897.68	22932.78
3	Y ~	mean_depth	mean_depth	NB	22874.23	22909.32
4	Y ~	Period	Period	NB	22744.69	22807.87
5	Y ~	Season	Season	NB	22053.94	22117.11
6	Y ~	mean_temp + mean_flow	mean_temp + mean_flow	NB	22612.01	22661.15
7	Y ~	mean_temp + mean_depth	mean_temp + mean_depth	NB	22624.60	22673.74
8	Y ~	mean_temp + Period	mean_temp + Period	NB	22420.92	22498.14
9	Y ~	mean_temp + Season	mean_temp + Season	NB	22047.50	22124.72
10	Y ~	mean_flow + mean_depth	mean_flow + mean_depth	NB	22874.38	22923.52
11	Y ~	mean_flow + Period	mean_flow + Period	NB	22721.15	22798.37
12	Y ~	mean_flow + Season	mean_flow + Season	NB	21995.73	22072.95
13	Y ~	mean_depth + Period	mean_depth + Period	NB	22695.76	22772.98
14	Y ~	mean_depth + Season	mean_depth + Season	NB	22054.58	22131.80
15	Y ~	Period + Season	Period + Season	NB	21779.80	21885.10
16	Y ~	mean_temp + mean_flow + mean_depth	mean_temp + mean_flow + mean_depth	NB	22613.05	22676.23

17	Y ~	mean_temp + mean_flow + Period	mean_temp + mean_flow + Period	NB	22420.72	22511.98
18	Y ~	mean_temp + mean_flow + Season	mean_temp + mean_flow + Season	NB	21982.44	22073.70
19	Y ~	mean_temp + mean_depth + Period	mean_temp + mean_depth + Period	NB	22423.40	22514.66
20	Y ~	mean_temp + mean_depth + Season	mean_temp + mean_depth + Season	NB	22044.91	22136.16
21	Y ~	mean_temp + Period + Season	mean_temp + Period + Season	NB	21766.95	21886.28
22	Y ~	mean_flow + mean_depth + Period	mean_flow + mean_depth + Period	NB	22686.54	22777.79
23	Y ~	mean_flow + mean_depth + Season	mean_flow + mean_depth + Season	NB	21997.73	22088.99
24	Y ~	mean_flow + Period + Season	mean_flow + Period + Season	NB	21753.25	21872.58
25	Y ~	mean_depth + Period + Season	mean_depth + Period + Season	NB	21782.72	21902.06
26	Y ~	mean_temp + mean_flow + mean_depth + Period	mean_temp + mean_flow + mean_depth + Period	NB	22423.30	22528.59
27	Y ~	mean_temp + mean_flow + mean_depth + Season	mean_temp + mean_flow + mean_depth + Season	NB	21982.10	22087.40
28	**Y ~**	**mean_temp + mean_flow + Period + Season**	**mean_temp + mean_flow + Period + Season**	**NB**	**21735.26**	**21868.64**
29	Y ~	mean_temp + mean_depth + Period + Season	mean_temp + mean_depth + Period + Season	NB	21768.41	21901.79
30	Y ~	mean_flow + mean_depth + Period + Season	mean_flow + mean_depth + Period + Season	NB	21754.93	21888.31

31	Y ~	mean_temp + mean_flow + mean_depth + Period + Season	mean_temp + mean_flow + mean_depth + Period + Season	NB	21736.92	21884.34
32	Y ~	mean_temp	mean_temp	Poisson	22807.93	22836.01
33	Y ~	mean_flow	mean_flow	Poisson	23079.77	23107.85
34	Y ~	mean_depth	mean_depth	Poisson	23056.71	23084.79
35	Y ~	Period	Period	Poisson	22920.87	22977.03
36	Y ~	Season	Season	Poisson	22227.34	22283.50
37	Y ~	mean_temp + mean_flow	mean_temp + mean_flow	Poisson	22793.63	22835.75
38	Y ~	mean_temp + mean_depth	mean_temp + mean_depth	Poisson	22807.55	22849.67
39	Y ~	mean_temp + Period	mean_temp + Period	Poisson	22597.93	22668.13
40	Y ~	mean_temp + Season	mean_temp + Season	Poisson	22213.22	22283.42
41	Y ~	mean_flow + mean_depth	mean_flow + mean_depth	Poisson	23056.61	23098.73
42	Y ~	mean_flow + Period	mean_flow + Period	Poisson	22897.98	22968.18
43	Y ~	mean_flow + Season	mean_flow + Season	Poisson	22166.46	22236.65
44	Y ~	mean_depth + Period	mean_depth + Period	Poisson	22873.04	22943.24
45	Y ~	mean_depth + Season	mean_depth + Season	Poisson	22225.34	22295.54
46	Y ~	Period + Season	Period + Season	Poisson	21948.10	22046.38
47	Y ~	mean_temp + mean_flow + mean_depth	mean_temp + mean_flow + mean_depth	Poisson	22794.64	22850.79
48	Y ~	mean_temp + mean_flow + Period	mean_temp + mean_flow + Period	Poisson	22596.63	22680.87
49	Y ~	mean_temp + mean_flow + Season	mean_temp + mean_flow + Season	Poisson	22143.82	22228.05

50	Y ~	mean_temp + mean_depth + Period	mean_temp + mean_depth + Period	Poisson	22600.58	22684.82
51	Y ~	mean_temp + mean_depth + Season	mean_temp + mean_depth + Season	Poisson	22206.42	22290.66
52	Y ~	mean_temp + Period + Season	mean_temp + Period + Season	Poisson	21924.25	22036.56
53	Y ~	mean_flow + mean_depth + Period	mean_flow + mean_depth + Period	Poisson	22864.15	22948.39
54	Y ~	mean_flow + mean_depth + Season	mean_flow + mean_depth + Season	Poisson	22166.75	22250.99
55	Y ~	mean_flow + Period + Season	mean_flow + Period + Season	Poisson	21919.68	22032.00
56	Y ~	mean_depth + Period + Season	mean_depth + Period + Season	Poisson	21949.55	22061.86
57	Y ~	mean_temp + mean_flow + mean_depth + Period	mean_temp + mean_flow + mean_depth + Period	Poisson	22599.29	22697.57
58	Y ~	mean_temp + mean_flow + mean_depth + Season	mean_temp + mean_flow + mean_depth + Season	Poisson	22140.73	22239.01
59	Y ~	mean_temp + mean_flow + Period + Season	mean_temp + mean_flow + Period + Season	Poisson	21889.20	22015.55
60	Y ~	mean_temp + mean_depth + Period + Season	mean_temp + mean_depth + Period + Season	Poisson	21923.07	22049.43
61	Y ~	mean_flow + mean_depth + Period + Season	mean_flow + mean_depth + Period + Season	Poisson	21920.42	22046.78
62	Y ~	mean_temp + mean_flow + mean_depth + Period + Season	mean_temp + mean_flow + mean_depth + Period + Season	Poisson	21889.13	22029.53

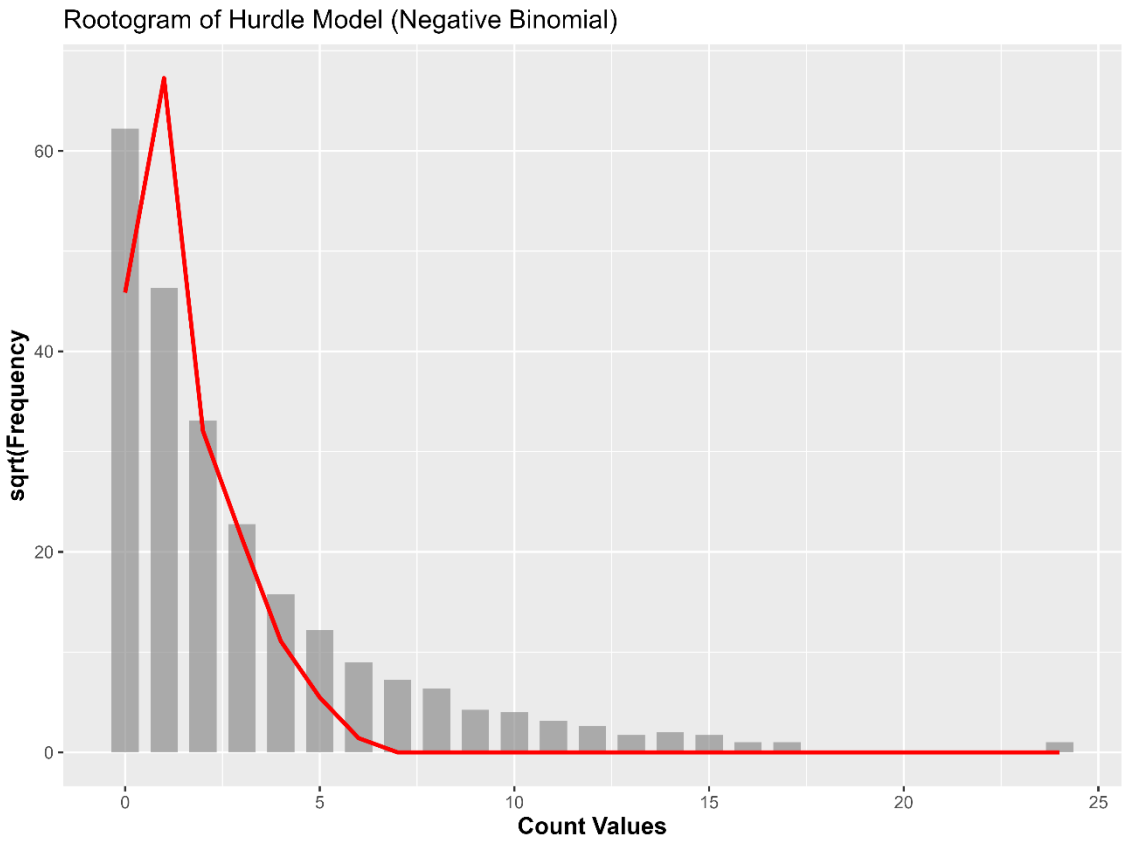

Figure II.5 – Rootogram showing the square-rooted frequencies of the number of outliers with the superimposed curve of the fitted Hurdle model (model 28).